DEUTSCHES ELEKTRONEN-SYNCHROTRON DESY

DESY 84-123
MPI-PAE/PTh 76/84
December 1984



# TESTS AND PRESENT STATUS OF GAUGE THEORIES

by

R.D. Peccei

*Max-Planck-Institut f. Physik und Astrophysik, München*

ISSN 0418-9833

NOTKESTRASSE 85 · 2 HAMBURG 52

To be sure that your preprints are promptly included in the
HIGH ENERGY PHYSICS INDEX ,
send them to the following address ( if possible by air mail ) :

DESY
Bibliothek
Notkestrasse 85
2 Hamburg 52
Germany

DESY 84-123
MPI-PAE/PTh 76/84
December 1984

ISSN 0418-9833

# Tests and Present Status of Gauge Theories

R.D. Peccei *

Max-Planck-Institut für Physik und Astrophysik, Munich,
Federal Republic of Germany

Lectures delivered at the Advanced Study Institute on Techniques and Concepts of High Energy Physics, Aug. 2 - 13, 1984, St. Croix, Virgin Island. To appear in the ASI proceedings.

* Permanent address after Sept. 15th, 1984, DESY, Hamburg, Federal Republic of Germany



TESTS AND PRESENT STATUS OF GAUGE THEORIES

R.D. Peccei

Max-Planck-Institut für Physik und Astrophysik

Munich, Federal Republic of Germany

## PROLOGUE

In these lectures I want to discuss in a pedagogical way the predictions of the, so called, standard model for the strong, weak and electromagnetic interactions. For the benefit of the diligent student, I have included at the end of the lectures a set of exercises which I hope can be helpful for understanding better the material covered.

In the standard model the strong interactions are described by Quantum Chromodynamics (QCD) /1/ and the weak and electromagnetic interactions are given by the unified electroweak model of Glashow, Salam and Weinberg (GSW) /2/. The standard model is based on the gauge group:

$$G = SU(3) \times SU(2) \times U(1)$$

Here SU(3) is the exact gauge symmetry of QCD, in which the associated gauge bosons (gluons) are massless. In the electroweak case, the gauge group SU(2) x U(1) is spontaneously broken to $U(1)_{em}$:

$$SU(2) \times U(1) \longrightarrow U(1)_{em}$$

As a result of this phenomena, three out of the four gauge bosons of SU(2) x U(1) acquire mass ($W^{\pm}$ and $Z^{0}$) while one, associated with the photon ($\gamma$), remains massless.

Although the above features of the standard model are by now well known, it is useful, before embarking in a detailed examination of the standard model, to illustrate the crucial concepts with a simple example.

## GAUGE THEORIES AT WORK: U(1) ABELIAN MODEL

Imagine two non interacting scalar particles of masses $m_1$ and $m_2$. Using the particle-field correspondence, we may describe this system by the Lagrangian

$$\mathcal{L} = -\frac{1}{2}\partial^\mu\phi_1(x)\,\partial_\mu\phi_1(x) - \frac{1}{2}m_1^2\,\phi_1^2(x) - \frac{1}{2}\partial^\mu\phi_2(x)\,\partial_\mu\phi_2(x) - \frac{1}{2}m_2^2\,\phi_2^2(x) \quad (1)$$

The fields $\phi_i(x)$, i = 1,2 are real fields since they each describe only one degree of freedom. From the Euler-Lagrange equations:

$$\partial_\mu \frac{\partial \mathcal{L}}{\partial\,\partial_\mu\phi_i(x)} - \frac{\partial \mathcal{L}}{\partial\,\phi_i(x)} = 0 \quad (2)$$

one obtains the equations of motion

$$(-\partial^2 + m_i^2)\,\phi_i(x) = 0 \quad (3)$$

for the fields $\phi_i$. These equations are what one would expect for uncoupled excitations of masses $m_i$, i = 1,2.

If $m_1 = m_2$ the Lagrangian in (1) has an $O(2) \sim U(1)$ symmetry. That is, the Lagrangian remains invariant ($\mathcal{L} \to \mathcal{L}$) under the transformation:

$$\begin{pmatrix}\phi_1\\ \phi_2\end{pmatrix} \to \begin{pmatrix}\phi_1'\\ \phi_2'\end{pmatrix} = \begin{pmatrix}\cos\theta & \sin\theta\\ -\sin\theta & \cos\theta\end{pmatrix}\begin{pmatrix}\phi_1\\ \phi_2\end{pmatrix} \quad (4)$$

It is useful to write the real fields $\phi_1$ and $\phi_2$ in terms of a complex field

$$\phi = \frac{1}{\sqrt{2}}(\phi_1 + i\phi_2)$$
$$\phi^\dagger = \frac{1}{\sqrt{2}}(\phi_1 - i\phi_2) \quad (5)$$

In terms of this notation, the Lagrangian of Eq. (1) for $m_1 = m_2 = m$ becomes simply

$$\mathcal{L} = -\partial^\mu\phi^\dagger(x)\,\partial_\mu\phi(x) - m^2\,\phi^\dagger(x)\,\phi(x) \quad (6)$$

The U(1) invariance of this Lagrangian, under the transformation

$$\phi(x) \to \phi'(x) = e^{i\theta}\,\phi(x) \quad (7)$$

is obvious. For future use, I record here also the infinitesimal version of this transformation:



$$\phi'(x) = \phi(x) + \delta\phi(x)$$
$$\delta\phi(x) = i\,\delta\theta\,[1]\,\phi(x) \quad (8)$$

The transformation in Eq. (7), or Eq. (8), is a <u>global</u> transformation since the parameter $\theta$, or $\delta\theta$, are independent of the space-time point x. Although the Lagrangian (6) is globally U(1) invariant, it is not invariant under <u>local</u> U(1) transformations, where $\theta = \theta(x)$ This is clear, since the derivatives in the kinetic energy terms contain an additional term when transformed:

$$\partial_\mu\phi(x) \to \partial_\mu\phi'(x) = \partial_\mu\left(e^{i\theta(x)}\,\phi(x)\right)$$
$$= e^{i\theta(x)}\left(\partial_\mu\phi(x) + i(\partial_\mu\theta(x))\,\phi(x)\right) \quad (9)$$

It is possible to construct a locally U(1) invariant Lagrangian, from that of Eq. (6), by introducing into the theory compensating <u>gauge fields</u>. This, in fact, is a general result: a globally symmetric Lagrangian can always be made locally symmetric by introducing into the theory a gauge field for each of the local symmetries.

Consider the local transformation

$$\phi(x) \to \phi'(x) = e^{i\theta(x)}\,\phi(x)$$
$$A_\mu(x) \to A_\mu'(x) = A_\mu(x) + \frac{1}{g}\partial_\mu\theta(x) \quad (10)$$

Here $A_\mu(x)$ is a real gauge field - a Lorentz vector - and g is an arbitrary parameter which will eventually play the role of a coupling constant. Note that $A_\mu(x)$ transforms inhomogeneously under the U(1) transformation. It is easy to check that, precisely because of this inhomogeneous behaviour, the <u>covariant derivative</u> of the field $\phi(x)$:

$$D_\mu\phi(x) \equiv (\partial_\mu - ig\,A_\mu(x))\,\phi(x) \quad (11)$$

transforms homogeneously under local U(1) transformations:

$$D_\mu\phi(x) \to D_\mu'\phi'(x) = e^{i\theta(x)}\,D_\mu\phi(x) \quad (12)$$

In view of Eq. (12), it is clear that the Lagrangian

$$\mathcal{L} = -(D^\mu \phi(x))^\dagger (D_\mu \phi(x)) - m^2 \phi^\dagger(x)\phi(x) \tag{13a}$$

is locally U(1) invariant. Note that local invariance is achieved only by introducing interactions. Writing Eq.(13a) out in detail one has

$$\mathcal{L} = -\partial^\mu \phi^\dagger \partial_\mu \phi - m^2 \phi^\dagger \phi + \{ g A^\mu [ i(\partial_\mu \phi^\dagger)\phi - i\phi^\dagger(\partial_\mu \phi)] - g^2 A^\mu A_\mu \phi^\dagger \phi \} \tag{13b}$$

The terms in the curly bracket above, which are the necessary additions to the Lagrangian of Eq. (6) to guarantee local U(1) invariance, represent interactions of the scalar fields $\phi$ and $\phi^\dagger$ with the gauge field $A_\mu$. These interactions are depicted schematically in Fig. 1.

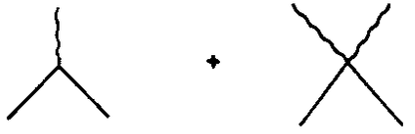

current-gauge field  sea gull

Fig. 1: Interactions which follow from the demand of local U(1) invariance

The "sea-gull" term above is necessary for scalar particles, because of their quadratic kinetic energy. For fermions only the "current-gauge field" term arises, from the demand of local invariance.

The Lagrangian (13) is not complete because the gauge field $A_\mu$ is only dynamical when kinetic terms for it are added. This is easily done, although the local U(1) invariance of Eq. (10) (gauge invariance) imposes certain restrictions. The field strength

$$F^{\mu\nu} = \partial^\mu A^\nu - \partial^\nu A^\mu \tag{14}$$

because of its curl-form is clearly invariant under local U(1) transformations:

$$F^{\mu\nu}(x) \to F'^{\mu\nu}(x) = F^{\mu\nu}(x) \tag{15}$$



Thus a sensible gauge field kinetic energy term is provided by

$$\mathcal{L}_{kin} = -\frac{1}{4} F^{\mu\nu} F_{\mu\nu} \tag{16}$$

However, no mass term for the gauge field $A_\mu$ is allowed by the local U(1) invariance.

To summarize, the Lagrangian

$$\mathcal{L} = -\frac{1}{4} F^{\mu\nu} F_{\mu\nu} - (D^\mu \phi)^\dagger (D_\mu \phi) - m^2 \phi^\dagger \phi \tag{17}$$

is invariant under the local U(1) transformations of Eq. (10). It describes a doublet of scalar fields which are degenerate in mass interacting (in a specific way) with a massless gauge field $A_\mu$.

Quantum Chromodynamics (QCD) is an SU(3) generalization of the above procedure, with various important (but no in principle) differences. The fundamental matter fields in QCD, instead of the scalars above, are spin 1/2 colored quarks of various different types (flavors). A convenient notation for these fields is $q_a^f$, where f is a flavor index distinguishing the various type of quarks

$$q_a^f = \{ u_a, d_a, c_a, s_a, t_a, b_a, \ldots \}$$

and a = 1,2,3 is an SU(3)-color-index. In what follows, unless it is needed for clarity, I shall suppress the flavor index. The quarks, $q_a$, transform as a $\underline{3}$ under the SU(3) group. Specifically, under infinitesimal SU(3) transformations one has

$$q_a \to q_a' = q_a + \delta q_a \tag{18a}$$

with

$$\delta q_a = i\,\delta\omega_i \left(\frac{\lambda_i}{2}\right)_{ab} q_b \tag{18b}$$

Here the $\delta\omega_i$, i = 1,2,..8 are the eight independent infinitesimal parameters characterizing SU(3) transformations (the analogs of $\delta\theta$ in Eq. (8)) and the matrices $\frac{1}{2}\lambda_i$ provide a 3 dimensional representation of the SU(3) generators $G_i$ (the analog of 1, for the Abelian case of Eq. (8)). That is, the $\frac{1}{2}\lambda_i$ satisfy the SU(3) commutation relations:

$$\left[\frac{1}{2}\lambda_i, \frac{1}{2}\lambda_j\right] = i f_{ijk} \frac{1}{2}\lambda_k \tag{19}$$

where the $f_{ijk}$ are the (totally antisymmetric) SU(3) structure constants.

To guarantee that the QCD Lagrangian constructed out of the quarks fields $q_a$ is locally SU(3) invariant (invariant under transformations

where $\delta\omega_i = \delta\omega_i(x)$ ) one must introduce a compensating gauge field (gluon field) for each of the eight parameters $\delta\omega_i$ . These gauge fields $A_i^\mu(x)$ transform as the 8, or adjoint, representation of SU(3). Under infinitesimal local SU(3) transformations one has

$$A_j^\mu(x) \to A_j'^\mu(x) = A_j^\mu(x) + \delta A_j^\mu(x) \tag{20a}$$

where

$$\delta A_j^\mu(x) = i\,\delta\omega_i(x)(g_i)_{jk} A_k^\mu(x) + \frac{1}{g_3}\partial^\mu(\delta\omega_j(x)) \tag{20b}$$

The second term above is precisely the analog of the inhomogeneous term appearing in Eq. (10). The first term in Eq. (20b), which has no counterpart in the Abelian case, arises because the gluon fields transform non trivially under SU(3). Indeed the 8-dimensional matrices $g_i$ are precisely those appropriate for the adjoint representation of SU(3):

$$(g_i)_{jk} = -i f_{ijk} \tag{21}$$

where the $f_{ijk}$ are the SU(3) structure constants.

In analogy to what was done in the U(1) example, to construct the QCD Lagrangian one needs to know the quark fields covariant derivatives, $D_\mu q_a$, and a generalization of the gauge fields field strength, $F_i^{\mu\nu}$ . The covariant derivative for the quark fields is easily found. It is easy to check that

$$D_\mu q_a(x) = \left(\partial_\mu \delta_{ab} - i g_3 \tfrac{1}{2}(\lambda_i)_{ab} A_{\mu i}(x)\right) q_b(x) \tag{22}$$

under local SU(3) transformations transforms in the same way as quarks field do (Eq. 18b):

$$\delta(D_\mu q_a(x)) = i\,\delta\omega_i(x)\left(\frac{\lambda_i}{2}\right)_{ab}\left(D_\mu q_b(x)\right) \tag{23}$$

The generalized field strengths $F_i^{\mu\nu}$ are also not difficult to find by the requirement that they transform homogeneously under local SU(3) transformations: That is, for infinitesimal transformations:

$$\begin{aligned}\delta F_j^{\mu\nu}(x) &= i\,\delta\omega_i(x)\,(g_i)_{jk} F_k^{\mu\nu}(x) \\ &= \delta\omega_i(x)\, f_{ijk} F_k^{\mu\nu}(x)\end{aligned} \tag{24}$$



A simple calculation gives the expression

$$F_i^{\mu\nu} = \partial^\mu A_i^\nu - \partial^\nu A_i^\mu + g_3 f_{ijk} A_j^\mu A_k^\nu \tag{25}$$

where the appearance of the last term is due precisely to the non Abelian nature of SU(3).

Putting all these ingredients together - and restoring the flavor index - gives the QCD Lagrangian

$$\mathcal{L}_{QCD} = -\bar{q}_a^f \gamma^\mu \tfrac{1}{i} D_\mu q_a^f - m_f \bar{q}_a^f q_a^f - \frac{1}{4} F_i^{\mu\nu} F_{i\mu\nu} \tag{26}$$

The principal structural difference of Eq. (26) from the U(1) example previously discussed resides in the interactions among the gauge fields, implicit in the $-1/4\,F^2$ term. Because of the quadratic term in Eq. (25), the gluon "kinetic energy" term contains both trilinear and quadrilinear interactions among the gluon fields, as depicted pictorially in Fig. 2.

Fig. 2: Additional interactions among gauge fields due to the non Abelian nature ($f_{ijk} \neq 0$) of SU(3)

In QCD the SU(3) local symmetry is realized in, what is called commonly, the Wigner-Weil way. That is, for each flavor of quark f one has a degenerate triplet of massive quark states, of mass $m_f$, interacting in the precise way specified by Eq. (26) with massless gluons, whose selfinteractions are also totally fixed. This, however, is not the only way in which symmetries can be realized in nature. Symmetries can also be realized in the, so called, Nambu-Goldstone way, in which the symmetry is a symmetry of the Lagrangian but not of the particle spectrum, because the vacuum state is not invariant under the symmetry. The GSW SU(2) x U(1) model is a theory in which the gauge symmetry is realized in the Nambu Goldstone way. The vacuum state is not SU(2)xU(1) invariant but only $U(1)_{em}$ invariant, so SU(2) x U(1) is spontaneously broken to $U(1)_{em}$. It is this phenomenon of spontaneous breakdown which provides the $W^\pm$ and $Z^0$ gauge bosons with a mass. To understand better what happens in the GSW model, it behoves us to study anew the

simple U(1) model of before - with a modification which allows for the occurrence of spontaneous symmetry breakdown.

A slight generalization of the U(1) model of Eq. (17) is provided by the Lagrangian

$$\mathcal{L} = -\frac{1}{4} F^{\mu\nu} F_{\mu\nu} - (D^{\mu}\phi)^{\dagger}(D_{\mu}\phi) - V(\phi^{\dagger}\phi) \qquad (27)$$

that is, the mass term for the scalar fields is replaced by a general function of $\phi^{\dagger}\phi$ , which can include terms of self interaction. Renormalizability restricts the "potential" $V(\phi^{\dagger}\phi)$ to contain terms with at most four fields. The physics of the model in Eq. (27) is considerably different depending on whether the minimum of the potential V occurs for $\phi^{\dagger}\phi = 0$ or not. In the first case, the features of the model are essentially like those of the simple U(1) model of Eq. (17), except for some additional scalar self interactions. If $\phi^{\dagger}\phi \neq 0$ at the minimum, however, the physics is completely different.

Classically, if the minimum of V occurs at $\phi^{\dagger}\phi = 0$ one has a unique minimum value, $\phi_{min} = 0$ . On the other hand, if the minimum of V occurs at $\phi^{\dagger}\phi \neq 0$ one has an infinite set of equivalent parametrization for $\phi_{min}$, namely

$$\phi_{min}(\alpha) = |\phi_{min}| e^{i\alpha} \qquad (28)$$

Quantum mechanically, the first case corresponds to having a field $\phi$ whose vacuum expectation value $\langle \phi \rangle$ vanishes, while in the second case $\langle \phi \rangle \neq 0$ . Such a non vanishing vacuum expectation value can only obtain if the vacuum itself is not invariant under U(1) transformations.

The physics of what is going on can be illustrated by picking V to have the specific form

$$V = \lambda \left( \phi^{\dagger}\phi - \frac{1}{2} v^2 \right)^2 \qquad (29)$$

shown in Fig. 3. The potential V above breaks the U(1) symmetry spontaneously. Although the Lagrangian (27) is locally U(1) invariant, the vacuum state of the theory is not.




Fig. 3: The potential V of Eq. (29)

One can label the infinite set of vacua, corresponding to the classical configuration of Eq. (28), by the value of the angle $\alpha$ : $|\alpha\rangle$ . Thus

$$\langle \alpha | \phi(x) | \alpha \rangle = \phi_{min}(\alpha) = e^{i\alpha} \frac{1}{\sqrt{2}} v \qquad (30)$$

Clearly the U(1) transformation

$$\phi(x) \rightarrow \phi'(x) = U_{\theta}\, \phi(x)\, U_{\theta}^{-1} = e^{i\theta}\, \phi(x) \qquad (31)$$

does not leave the vacuum invariant. In view of Eq. (30) one easily deduces that

$$U_{\theta} |\alpha\rangle = |\alpha - \theta\rangle \qquad (32)$$

The spontaneous breakdown of the U(1) symmetry caused by the presence of the potential V, with its asymmetric minimum, has two effects:

(1) The U(1) degeneracy in the scalar sector of the theory is lifted.
(2) The U(1) gauge field acquires a mass (Higgs Mechanism).

The first phenomenon above occurs irrespective of whether the symmetry is a local or global symmetry of the Lagrangian. If the symmetry is global, as a result of the breakdown a zero mass excitation (or zero mass excitations, if more than one symmetry is spontaneously broken) appears in the theory (Goldstone boson). This Goldstone boson disappears if the Lagrangian symmetry is local. However, in this case, point 2) above obtains, in which the erstwhile massless gauge field gets a mass. Roughly speaking, one can think of the Goldstone excitation of the global symmetry as being the longitudinal component of the massive vector field.

These phenomena can be deduced by a somewhat more careful inspection of the Lagrangian (27). If the potential $V(\phi^{\dagger}\phi)$ is as in Eq. (29), to do physics one must compute the excitations of the field

around $\phi_{min}$ and not zero. Therefore, the Lagrangian in (27) ought to be reparametrized to take this fact into account. In effect, instead of dealing with a complex field $\phi$, with non zero vacuum expectation value $\langle \phi \rangle \neq 0$, one should deal with the two real scalar fields, which characterize the excitations about $\phi_{min}$. Although the physical phenomena described above obtain independently of how one parametrizes $\phi$, a very convenient parametrization is provided by

$$\phi(x) = e^{i\xi(x)/v} \frac{1}{\sqrt{2}} (v + \rho(x)) \tag{33}$$

The real scalar fields $\xi(x)$ and $\rho(x)$, obviously, have zero vacuum expectation value.

A number of results are now easy to check:
(a) The potential $V(\phi^\dagger \phi)$ is obviously independent of $\xi$. If there were no gauge interactions, $\xi$ would therefore be interpreted as the massless Goldstone boson.

(b) The "sea-gull" term $-g^2 A^\mu A_\mu \phi^\dagger \phi$, present in the scalar field "kinetic energy" term $-(D^\mu \phi)^\dagger (D_\mu \phi)$, generates a mass for the gauge field $A_\mu$, when $\phi^\dagger \phi$ is replaced by its value at the minimum: $(1/2)v^2$,

$$\mathcal{L}_{mass} = -\frac{1}{2}(gv)^2 A^\mu A_\mu \tag{34}$$

This is the famous Higgs mechanism /3/.

(c) The covariant derivative $D_\mu \phi$, after a gauge transformation of the field $A_\mu$, has a trivial $\xi$ dependence. To wit, one has

$$\begin{aligned} D_\mu \phi &= (\partial_\mu - ig A_\mu) \frac{1}{\sqrt{2}} (v + \rho) e^{i\xi/v} \\ &= e^{i\xi/v} (\partial_\mu - ig B_\mu) \frac{1}{\sqrt{2}} (v + \rho) \end{aligned} \tag{35}$$

where

$$B_\mu = A_\mu - \frac{1}{gv} \partial_\mu \xi \tag{36}$$

From these observations one concludes that the Lagrangian of the theory is in fact independent of the field $\xi$. This Lagrangian describes the interaction of a massive vector field $B_\mu$ with a real scalar field $\rho$. No vestiges of the U(1) local symmetry remain, except for certain



coupling relationships. (The derivation of the shifted Lagrangian is left as an exercise, Ex. 7.) It is worthwhile contrasting the particle spectrum in the two different possible realizations of the U(1) symmetry. In the Wigner-Weyl case one has a degenerate massive scalar doublet and a massless gauge field, in total four degrees of freedom. In the Nambu-Goldstone case these degrees of freedom are redistributed and one has a massive real scalar field along with a massive gauge field.

The Glashow-Salam-Weinberg SU(2) x U(1) model of electroweak interactions is a generalization of the above procedure. Although SU(2) x U(1) is a symmetry of the Lagrangian, it is not a symmetry of the spectrum of the theory. There is a breakdown of SU(2) x U(1) to $U(1)_{em}$, so that the only manifest multiplets of the theory are charge multiplets (the $e^+$ and $e^-$ have the same mass, so do $W^+$ and $W^-$, etc.). The breakdown of SU(2) x U(1) $\rightarrow U(1)_{em}$ causes three of the gauge fields ($W^\pm$ and $Z^0$) to become massive, but the photon is massless, reflecting the unbroken $U(1)_{em}$ local symmetry.

The GSW Lagrangian contains three distinct pieces

$$\mathcal{L}_{GSW} = \mathcal{L}_{\substack{fermion \\ gauge}} + \mathcal{L}_{\substack{Higgs \\ gauge}} + \mathcal{L}_{\substack{Higgs \\ fermion}} \tag{37}$$

The first term above contains all the weak and electromagnetic interactions of quarks and leptons and it is phenomenologically checked to high accuracy. The tests of the standard model, which I will describe in some detail in what follows, are really tests of this part of the GSW Lagrangian. The Higgs-gauge Lagrangian in Eq. (37) is put in essentially to precipitate the spontaneous breakdown of SU(2) x U(1) to $U(1)_{em}$. None of its detailed structure is really checked, except for the, so-called, $\Delta I_W = 1/2$ rule - which I will explain below. Finally, the last term in Eq. (37) is even more arbitrary. It is put in to allow for the appearance of quark and lepton masses, but it is really not checked at all otherwise. I discuss each of these terms in turn.

To construct $\mathcal{L}_{\substack{fermion \\ gauge}}$ one needs to know the quantum number assignments of quarks and leptons under SU(2) x U(1). These assignments are dictated by phenomenology. For instance, the fact that the currents that participate in the weak interactions have a (V-A) form implies that only the left-handed quarks and leptons have non trivial SU(2) transformations. To be more precise the fermion structure of the GSW model is as follows:

(i) There is a repetive generation structure, with each generation having the same SU(2) x U(1) properties. At the moment we know of the existence of three families of quarks and leptons: the electron family $(\nu_e, e; u, d)$; the muon family $(\nu_\mu, \mu; c, s)$; the tau family $(\nu_\tau, \tau; t, b)$. There could be, however, more families yet to be discovered.

(ii) The quarks and leptons of each family have the SU(2) x U(1) assignments shown in Table I

| states | $\begin{pmatrix} u \\ d \end{pmatrix}_L$ | $u_R$ | $d_R$ | $\begin{pmatrix} \nu_e \\ e \end{pmatrix}_L$ | $e_R$ |
|---|---|---|---|---|---|
| SU(2) | 2 | 1 | 1 | 2 | 1 |
| U(1) | 1/6 | 2/3 | -1/3 | -1/2 | -1 |

Table I: SU(2) x U(1) quantum numbers of quarks and leptons. $\psi_L$, $\psi_R$ are the helicity projections: $\psi_L = \frac{1}{2}(1-\gamma_5)\psi$ ; $\psi_R = \frac{1}{2}(1+\gamma_5)\psi$

No right-handed neutrinos are introduced into the model. If these states existed they would be totally SU(2) x U(1) singlets. The U(1) assignments of Table I follow from the formula for the electromagnetic charge in the model

$$Q = T_3 + Y \tag{38}$$

with Y being the U(1) quantum number

Armed with the SU(2) x U(1) transformation laws for the fermions of Table I, it is now straightforward to write down the appropriate covariant derivatives for these fields (cf Eq. (11) and (22) for an Abelian and a non Abelian symmetry, respectively). If $W_i^\mu$ are the three SU(2) gauge fields and $Y^\mu$ is the U(1) gauge field and if g and g' are their appropriate coupling constants one has for the covariant derivatives:

$$D_\mu \begin{pmatrix} u \\ d \end{pmatrix}_L = \left(\partial_\mu - i g' \tfrac{1}{6} Y_\mu - i g \tfrac{\tau_i}{2} W_{\mu i}\right) \begin{pmatrix} u \\ d \end{pmatrix}_L \tag{39a}$$

$$D_\mu u_R = \left(\partial_\mu - i g' \tfrac{2}{3} Y_\mu\right) u_R \tag{39b}$$

$$D_\mu d_R = \left(\partial_\mu + i g' \tfrac{1}{3} Y_\mu\right) d_R \tag{39c}$$

$$D_\mu \begin{pmatrix} \nu_e \\ e \end{pmatrix}_L = \left(\partial_\mu + i g' \tfrac{1}{2} Y_\mu - i g \tfrac{\tau_i}{2} W_{\mu i}\right) \begin{pmatrix} \nu_e \\ e \end{pmatrix}_L \tag{39d}$$

$$D_\mu e_R = \left(\partial_\mu + i g' Y_\mu\right) e_R \tag{39e}$$

The $\mathcal{L}_{\substack{\text{fermion} \\ \text{gauge}}}$ piece of $\mathcal{L}_{GSW}$ follows now immediately, exactly as in the U(1) example:



$$\mathcal{L}_{\substack{\text{fermion} \\ \text{gauge}}} = -(\bar{u}\bar{d})_L \gamma^\mu \tfrac{1}{i} D_\mu \begin{pmatrix} u \\ d \end{pmatrix}_L - \bar{u}_R \gamma^\mu \tfrac{1}{i} D_\mu u_R$$

$$- \bar{d}_R \gamma^\mu \tfrac{1}{i} D_\mu d_R - (\bar{\nu}_e \bar{e})_L \gamma^\mu \tfrac{1}{i} D_\mu \begin{pmatrix} \nu_e \\ e \end{pmatrix}_L$$

$$- \bar{e}_R \gamma^\mu \tfrac{1}{i} D_\mu e_R - \frac{1}{4} Y^{\mu\nu} Y_{\mu\nu} - \frac{1}{4} W_i^{\mu\nu} W_{i\mu\nu} \tag{40}$$

In the above the field strengths $Y^{\mu\nu}$ and $W_i^{\mu\nu}$ are given by

$$Y^{\mu\nu} = \partial^\mu Y^\nu - \partial^\nu Y^\mu \tag{41a}$$

$$W_i^{\mu\nu} = \partial^\mu W_i^\nu - \partial^\nu W_i^\mu + g\, \varepsilon_{ijk}\, W_j^\mu W_k^\nu \tag{41b}$$

I have written the above only for one family - for three families one just repeats the same structure three times. Also in writing Eqs. (39) and (40) I have suppressed the color indices of the quarks. These should be understood and summed over in Eq. (40).

There are a number of remarks that should be made at this point:

(1) No mass terms for leptons or quarks are allowed by the SU(2) symmetry and such terms are not included therefore in Eq. (40). A mass term involves a L-R transition

$$\mathcal{L}_{mass} = -m \bar{\psi}\psi = -m(\bar{\psi}_L \psi_R + \bar{\psi}_R \psi_L) \tag{42}$$

Since left-handed fields are doublets under SU(2) and right-handed fields are singlets, mass terms violate SU(2). Masses for the quarks and leptons will eventually be generated through a coupling to scalar fields, after SU(2) x U(1) is broken. Thus, for example, the masses $m_f$ present in the QCD Lagrangian (26) have a non trivial weak interaction origin. I will return to this point again below.

(2) The Lagrangian of Eq. (40) contains explicit fermion-gauge field interactions which take the form

$$\mathcal{L}_{int} = g' J_Y^\mu Y_\mu + g J_i^\mu W_{i\mu} \tag{43}$$

where $J_Y^\mu$ is the "weak hypercharge" current and $J_i^\mu$ is the "weak isospin" current. A simple calculation - again written only for one family - yields the formulas

$$J^\mu_i = (\bar{u}\,\bar{d})_L\,\gamma^\mu\,\frac{\tau_i}{2}\begin{pmatrix} u \\ d \end{pmatrix}_L + (\bar{\nu}_e\,\bar{e})_L\,\gamma^\mu\,\frac{\tau_i}{2}\begin{pmatrix} \nu_e \\ e \end{pmatrix}_L \qquad (44a)$$

$$J^\mu_Y = \frac{1}{6}(\bar{u}\,\bar{d})_L\,\gamma^\mu\begin{pmatrix} u \\ d \end{pmatrix}_L + \frac{2}{3}\bar{u}_R\,\gamma^\mu u_R - \frac{1}{3}\bar{d}_R\,\gamma^\mu d_R$$

$$- \frac{1}{2}(\bar{\nu}_e\,\bar{e})_L\,\gamma^\mu\begin{pmatrix} \nu_e \\ e \end{pmatrix}_L - \bar{e}_R\,\gamma^\mu e_R \qquad (44b)$$

3) It is anticipated that, because of the SU(2) x U(1) $\rightarrow$ $U(1)_{em}$ breakdown and the fact that the charge operator is a linear combination of $T_3$ and Y (cf Eq. (38)), some linear combination of $Y_\mu$ and $W_{3\mu}$ will describe the massive $Z^0_\mu$ field, while the orthogonal combination will be the photon field, $A_\mu$. Conventionally, one writes

$$W_3^\mu = \cos\theta_W\,Z^\mu + \sin\theta_W\,A^\mu \qquad (45)$$

$$Y^\mu = -\sin\theta_W\,Z^\mu + \cos\theta_W\,A^\mu$$

where $\theta_W$ is the, so called, Weinberg angle.

It is useful therefore to rewrite the interaction Lagrangian (43) in terms of the mass eigenstates $A_\mu$ and $Z_\mu$, and to replace the hypercharge current $J^\mu_Y$ by

$$J^\mu_Y = J^\mu_3 - J^\mu_{em} \qquad (46)$$

A simple calculation then gives the formula

$$\mathcal{L}_{int} = \frac{1}{2\sqrt{2}}\,g\,(W^\mu_+ J_{-\mu} + W^\mu_- J_{+\mu})$$

$$+ \{(g\cos\theta_W + g'\sin\theta_W)J^\mu_3 - g'\sin\theta_W J^\mu_{em}\}Z_\mu \qquad (47)$$

$$+ \{g'\cos\theta_W J^\mu_{em} + (g'\cos\theta_W - g\sin\theta_W)J^\mu_3\}A_\mu$$

In the above we have made use of the definitions:



$$W^\mu_\pm = \frac{1}{\sqrt{2}}(W^\mu_1 \mp i W^\mu_2) \qquad (48a)$$

$$J^\mu_\pm = 2\,(J^\mu_1 \mp i J^\mu_2) \qquad (48b)$$

where the factor of 2 for the charged currents in Eq. (48b) is just a convention. Eq. (47) can be simplified by noting that if $A^\mu$ is indeed the photon field it <u>must</u> couple only to $J^\mu_{em}$ and this coupling must have the strength e, of the electromagnetic charge. This physical requirement gives the relation

$$g'\cos\theta_W = g\sin\theta_W = e \qquad (49)$$

Eliminating g and g' in favour of e and the Weinberg angle yields for the interaction Lagrangian the, by now, standard form:

$$\mathcal{L}_{int} = e\,J^\mu_{em}A_\mu + \frac{e}{2\sqrt{2}\sin\theta_W}\{J^\mu_+ W_{-\mu} + J^\mu_- W_{+\mu}\}$$

$$+ \frac{e}{2\cos\theta_W\sin\theta_W}J^\mu_{NC}Z_\mu \qquad (50)$$

where the neutral current, $J^\mu_{NC}$, is given by

$$J^\mu_{NC} = 2\,[J^\mu_3 - \sin^2\theta_W J^\mu_{em}] \qquad (51)$$

Although Eq. (50) describes the electroweak interactions in the GSW model, for many purposes it suffices to work with a low energy approximation to this Lagrangian. Most weak interaction experiments deal with processes where the relevant momentum transfers are tiny compared to the values of the W and Z masses (which - as will be seen soon - are of the order of 100 GeV). For $q^2 \ll M_W^2, M_Z^2$, it suffices to replace the W and Z propagators by

$$\langle T(W^\mu_+(q)\,W^\nu_-(0))\rangle \simeq \frac{1}{i}\frac{\delta^{\mu\nu}}{M_W^2} \qquad (52a)$$

$$\langle T(Z^\mu(q)\,Z^\nu(0))\rangle \simeq \frac{1}{i}\frac{\delta^{\mu\nu}}{M_Z^2} \qquad (52b)$$

where $\eta^{\mu\nu} = \begin{pmatrix} -1 & & & \\ & 1 & & \\ & & 1 & \\ & & & 1 \end{pmatrix}$ is the metric tensor. Using the approximation (52), the interaction Lagrangian (50) yields in second order perturbation theory an effective Lagrangian for the weak interactions of a current-current form:

$$\mathcal{L}_{eff}^{Weak} = \left(\frac{e}{2\sqrt{2}\sin\theta_W}\right)^2 \frac{1}{M_W^2} \; J_+^\mu J_{-\mu} + \frac{1}{2}\left(\frac{e}{2\cos\theta_W \sin\theta_W}\right)^2 \frac{1}{M_Z^2} \; J_{NC}^\mu J_{NC\mu} \tag{53}$$

For the charged current interactions this Lagrangian must agree with the Fermi theory

$$\mathcal{L}_{Fermi} = \frac{G_F}{\sqrt{2}} \; J_+^\mu J_{-\mu} \tag{54}$$

This then identifies the Fermi constant $G_F$ as

$$\frac{G_F}{\sqrt{2}} = \frac{e^2}{8 \sin^2\theta_W M_W^2} \tag{55}$$

It proves convenient to define the parameter $\rho$ as

$$\rho = \frac{M_W^2}{M_Z^2 \cos^2\theta_W} \tag{56}$$

Then the effective interaction (53) takes the simple form

$$\mathcal{L}_{eff}^{Weak} = \frac{G_F}{\sqrt{2}} \left\{ J_+^\mu J_{-\mu} + \rho \; J_{NC}^\mu J_{NC\mu} \right\} \tag{57}$$

One sees from the above that the only free parameters to describe the (low energy) neutral current interactions in the GSW model are $\rho$ and the Weinberg angle $\theta_W$, which enters in the definition of $J_{NC\mu}$ of



Eq. (51). As I will discuss in much more detail later, experiments indicate that $\sin^2\theta_W \simeq 1/4$ and $\rho \simeq 1$. Using Eqs. (55) and (56) and the experimental value of the Fermi constant one can check that the W and Z boson masses are indeed of O (100 GeV). Thus the approximations that led to Eq. (57) are certainly justified for most "low energy" weak interaction experiments. The value $\rho \simeq 1$ is particularly noteworthy, since it gives some direct insight on how SU(2) x U(1) is broken down.

To examine this point it is necessary to consider how SU(2) x U(1) is broken down in the GSW model. This is the job of the Higgs-gauge piece of $\mathcal{L}_{GSW}$ in Eq. (37). Conventionally one introduces into the model some elementary scalar fields, whose self interaction causes (some of) them to have SU(2) x U(1) violating vacuum expectation values. Remarkably the result $\rho = 1$ ensues if the breakdown of SU(2) x U(1) $\rightarrow$ U(1)$_{em}$ is generated by scalar fields which are doublets under SU(2) x U(1). This result - which is also known as the $\Delta I_W = 1/2$ rule - will be demonstrated in detail by considering the simplest case of only one SU(2) doublet Higgs field.

Consider a complex SU(2) doublet scalar field

$$\Phi = \begin{pmatrix} \phi^0 \\ \phi^- \end{pmatrix} \tag{58}$$

With the charges as above indicated $\Phi$ has Y = - 1/2. Note that $\Phi^+ \neq \Phi$ so that $\Phi$ really describes four degrees of freedom. An SU(2) x U(1) locally invariant Lagrangian for $\Phi$ is immediate to write down:

$$\mathcal{L}_{\substack{Higgs \\ gauge}} = -(D^\mu \Phi)^+ (D_\mu \Phi) - V(\Phi^+ \Phi) \tag{59}$$

where

$$D_\mu \Phi = \left(\partial_\mu + i\frac{g'}{2} Y_\mu - ig \frac{\tau_i}{2} W_{\mu i}\right)\Phi \tag{60}$$

is the appropriate covariant derivative. If the potential V is chosen of the form

$$V = \lambda\left(\Phi^+\Phi - \tfrac{1}{2}v^2\right)^2 \tag{61}$$

SU(2) x U(1) will clearly break down. The choice for the vacuum expectation value of $\Phi$ :

$$\langle \Phi \rangle = \begin{pmatrix} \frac{1}{\sqrt{2}} v \\ 0 \end{pmatrix} \tag{62}$$

assures that the unbroken U(1) agrees precisely with $U(1)_{em}$, * for

$$Q\langle\Phi\rangle = \begin{pmatrix} 0 & 0 \\ 0 & -1 \end{pmatrix}\begin{pmatrix} \frac{1}{\sqrt{2}}v \\ 0 \end{pmatrix} = 0 \tag{63}$$

The masses for the gauge fields are obtained, as in the U(1) example, by replacing in the "seagull" terms the scalar field $\Phi$ by its vacuum expectation value $\langle\Phi\rangle$. This yields

$$\mathcal{L}_{mass} = -\left[\left(g\frac{\tau_i}{2}W_i^\mu - g'\frac{1}{2}Y^\mu\right)\langle\Phi\rangle\right]^\dagger\left[\left(g\frac{\tau_j}{2}W_\mu^j - g'\frac{1}{2}Y_\mu\right)\langle\Phi\rangle\right]$$

$$= -\frac{1}{2}v^2(1,0)\left[\left(g\frac{\tau_i}{2}W_i^\mu - g'\frac{1}{2}Y^\mu\right)\left(g\frac{\tau_j}{2}W_\mu^j - g'\frac{1}{2}Y_\mu\right)\right]\begin{pmatrix}1\\0\end{pmatrix} \tag{64}$$

$$= -\left(\frac{gv}{2}\right)^2 W_+^\mu W_{-\mu} - \frac{1}{2}\left(W_3^\mu\, Y^\mu\right)\begin{bmatrix} \frac{1}{4}g^2v^2 & -\frac{1}{4}gg'v^2 \\ -\frac{1}{4}gg'v^2 & \frac{1}{4}g'^2v^2 \end{bmatrix}\begin{pmatrix} W_{3\mu} \\ Y_\mu \end{pmatrix}$$

Clearly one sees that

$$M = \frac{1}{2}gv \tag{65a}$$

and that $W_3^\mu$ and $Y^\mu$ are not mass eigenstates. The 2x2 mass matrix in Eq. (64) is diagonalized by the transformation of Eq. (45) provided that the Weinberg angle $\theta_W$ obeys

$$\tan\theta_W = g'/g \tag{66}$$

This result agrees with that obtained earlier in Eq. (49), as it must. The eigenvalues of the 2x2 matrix are $0$ and $\frac{1}{4}(g^2+g'^2)v^2$ corresponding to the mass squared of the photon and of the $Z^0$. Hence

$$M_Z = \frac{1}{2}\sqrt{g^2+g'^2}\,v \tag{65b}$$

Using Eqs. (65) and (66) it follows that the parameter $\rho$, defined in Eq. (56), is unity.

---

* This can always be chosen to happen for just one Higgs doublet by appropriate redefinitions. With more than one Higgs doublet one has to impose the preservation of $U(1)_{em}$ by the Higgs potential minimum.



In the case of the minimal Higgs model, with just one doublet $\Phi$, after symmetry breakdown only one physical excitation remains. Three of the four degrees of freedom in $\Phi$ disappear physically, becoming the longitudinal component of the $W^\pm$ and $Z^0$ bosons. The presence of a scalar particle - the Higgs boson - is an unavoidably consequence of the symmetry breakdown. One may parametrize $\Phi$ in the model, in an analogous way to that done for the U(1) model (c.f. Eq. (33)), so that $\mathcal{L}_{\text{Higgs-gauge}}$ just describes the interaction of this Higgs scalar with massive gauge fields. Consider

$$\Phi = e^{i\vec{\tau}\cdot\vec{\xi}/v}\begin{pmatrix}\frac{1}{\sqrt{2}}(v+H)\\0\end{pmatrix} \tag{67}$$

Clearly the potential term $V(\Phi^\dagger\Phi)$ is independent of $\vec{\xi}$. The dependence of $D_\mu\Phi$ on $\vec{\xi}$ is also trivial, after a gauge transformation:

$$D_\mu\Phi = \left(\partial_\mu - ig\frac{\tau_i}{2}W_{\mu i} + ig'\frac{1}{2}Y_\mu\right)e^{i\vec{\tau}\cdot\vec{\xi}/v}\begin{pmatrix}\frac{1}{\sqrt{2}}(v+H)\\0\end{pmatrix}$$

$$= e^{i\vec{\tau}\cdot\vec{\xi}/v}\left[\partial_\mu - ig\left\{e^{-i\vec{\tau}\cdot\vec{\xi}/v}\frac{\tau_i}{2}W_{\mu i}\,e^{i\vec{\tau}\cdot\vec{\xi}/v} - \frac{1}{ig}e^{-i\vec{\tau}\cdot\vec{\xi}/v}\left(\partial_\mu e^{i\vec{\tau}\cdot\vec{\xi}/v}\right)\right\} + ig'\frac{1}{2}Y_\mu\right]\begin{pmatrix}\frac{1}{\sqrt{2}}(v+H)\\0\end{pmatrix} \tag{68}$$

Since the term in the curly brackets in Eq. (68) is just a gauge transformed field

$$e^{-i\vec{\tau}\cdot\vec{\xi}/v}\frac{\tau_i}{2}W_{\mu i}\,e^{i\vec{\tau}\cdot\vec{\xi}/v} - \frac{1}{ig}e^{-i\vec{\tau}\cdot\vec{\xi}/v}\left(\partial_\mu e^{i\vec{\tau}\cdot\vec{\xi}/v}\right) = \frac{\tau_i}{2}W'_{\mu i} \tag{69}$$

all $\vec{\xi}$ dependence in $D_\mu\Phi$ resides in the phase factor in front in Eq. (68). Thus only H enters in $\mathcal{L}_{\text{Higgs-gauge}}$ and one finds *

---

* In (70) we have, for simplicity, denoted the gauge transformed fields by the same symbol used before the gauge transformation

$$\mathcal{L}_{\substack{\text{Higgs}\\ \text{gauge}}} = -\frac{1}{2}\partial^\mu H \partial_\mu H - \lambda\left(vH + \frac{1}{2}H^2\right)^2$$

$$-\frac{1}{4}g^2(v+H)^2 W_+^\mu W_{-\mu} - \frac{1}{8}(g^2+g'^2)(v+H)^2 Z^\mu Z_\mu \qquad (70)$$

I note two properties of the Higgs field :

(1) The vacuum expectation value v has a magnitude fixed by the Fermi constant. Using Eq. (55) and (65a) one has

$$v = (\sqrt{2}\,G_F)^{-1/2} \simeq 250\ GeV \qquad (71)$$

The Higgs mass, although proportional to v, is arbitrary since it depends on the unknown quartic Higgs coupling $\lambda$ :

$$m_H^2 = 2\lambda v^2 \qquad (72)$$

(2) The coupling of the Higgs meson to the W and Z, which can be read off Eq. (70), is proportional to the mass of the gauge bosons. Namely one finds

$$\mathcal{L}_{HZZ} = -\frac{1}{2}(g^2+g'^2)^{1/2} M_Z Z^\mu Z_\mu H \qquad (73)$$

$$\mathcal{L}_{HWW} = -g M_W W_+^\mu W_{-\mu} H$$

I discuss now briefly the final ingredient in the GSW Lagrangian, the $\mathcal{L}_{\text{Fermion-Higgs}}$ term. Even though this sector is not checked at all, from its general structure an important property of the theory emerges. The existence of a doublet field $\Phi$, transforming as (2,-1/2) with respect to SU(2) x U(1), and of its charge conjugate

$$\tilde{\Phi} = i\tau_2 \Phi^* \sim (2, 1/2) \qquad (74)$$

allows one to write SU(2) x U(1) invariant interactions which connect left and right quark and lepton fields. For instance, one can write the following SU(2) x U(1) invariant coupling involving u quarks

$$\mathcal{L}_{Yukawa} = -h\left\{(\bar{u}\bar{d})_L \begin{pmatrix}\phi^0\\ \phi^-\end{pmatrix} u_R + \bar{u}_R (\phi_0^* \ \phi^+) \begin{pmatrix}u\\ d\end{pmatrix}_L\right\} \qquad (75)$$



Such a Yukawa interaction has the very nice property that it generates a mass for the u quark after SU(2) x U(1) breakdown. That is, the term in (75) when $\Phi \to \langle\Phi\rangle = \frac{1}{\sqrt{2}}v$ corresponds to a mass term

$$\mathcal{L}_{mass} = -\frac{hv}{\sqrt{2}}(\bar{u}_L u_R + \bar{u}_R u_L) \qquad (76)$$

so

$$m_u = \frac{hv}{\sqrt{2}} \qquad (77)$$

As in the Higgs case also here the mass for the fermions - in this case the u quark - is arbitrary, because the parameter h is. Using the parametrization (67) for the doublet Higgs field, and redefining the $\begin{pmatrix}u\\ d\end{pmatrix}_L$ field via an SU(2) rotation

$$\begin{pmatrix}u\\ d\end{pmatrix}_L \to e^{i\vec{\xi}\cdot\vec{\tau}/v}\begin{pmatrix}u\\ d\end{pmatrix}_L \qquad (78)$$

gives

$$\mathcal{L}_{Yukawa} = -m_u \bar{u}u - \frac{m_u}{v}\bar{u}uH \qquad (79)$$

One sees that the Higgs coupling is also here proportional to mass.

The analysis just discussed can be repeated for the d quark and the electron - using couplings involving - and can be extended to families of quarks and leptons. In so doing the notion of mixing naturally emerges. Because this has important phenomenological consequences I want to explain clearly its origins. For the case of various families of quarks and leptons let us adopt the convenient notation:

$$Q_{iL} = \left\{\begin{pmatrix}u\\ d\end{pmatrix}_L, \begin{pmatrix}c\\ s\end{pmatrix}_L, \begin{pmatrix}t\\ b\end{pmatrix}_L, \dots\right\};$$

$$L_{iL} = \left\{\begin{pmatrix}\nu_e\\ e\end{pmatrix}_L, \begin{pmatrix}\nu_\mu\\ \mu\end{pmatrix}_L, \begin{pmatrix}\nu_\tau\\ \tau\end{pmatrix}_L, \dots\right\}; \qquad (80)$$

$$u_{iR} = \{u_R, c_R, t_R, \dots\}; \quad d_{iR} = \{d_R, s_R, b_R, \dots\}$$

$$l_{iR} = \{e_R, \mu_R, \tau_R, \dots\}$$

Then the most general SU(2) x U(1) invariant Yukawa interaction reads

$$\mathcal{L}_{Yukawa} = \Big\{ -h^u_{ij}\,[\bar{Q}_{iL}\,\Phi\,u_{jR}] + h^d_{ij}\,[\bar{Q}_{iL}\,\tilde{\Phi}\,d_{jR}] + h^\ell_{ij}\,[\bar{L}_{iL}\,\tilde{\Phi}\,\ell_{jR}] + h.c. \Big\} \tag{81}$$

Note that in general there is no reason to suppose that there is vanishing intrageneration couplings. So $h_{ii} \neq 0$ also for $i \neq j$. When $\Phi$ and $\tilde{\Phi}$ are replaced by their vacuum expectation values, mass matrices

$$M^f_{ij} = h^f_{ij}\,\frac{v}{\sqrt{2}} \qquad \{f = u, d, \ell\} \tag{82}$$

are generated which are arbitrary and non diagonal, since so are the $h^f_{ij}$.

Obviously, if the matrices $M^f_{ij}$ are not diagonal one must make a basis change to deal with states of definite mass. This implies that the weak interaction eigenstates are in general not the mass eigenstates. Changing basis to mass eigenstates causes for the weak currents mixing between generations. This is the origin of the famous Cabibbo mixing angle! To be more precise, the basis change to mass eigenstates:

(i) Has no effect on leptonic currents, because $m_\nu = 0$.
(ii) Has no effect on neutral currents, because these are flavor diagonal. This is the well known GIM mechanism /4/.
(iii) Affects hadronic charged currents.

I will leave the proof of the first two assertions as a problem but will illustrate point (iii) explicitly. Consider specifically $J^r_-$, which is given by

$$J^r_- = 2\,[\,\bar{u}_L \gamma^r d_L + \bar{c}_L \gamma^r s_L + \bar{t}_L \gamma^r b_L + \dots\,] = 2\,(\bar{u}_L\,\bar{c}_L\,\bar{t}_L \dots)\,\gamma^r\,1 \begin{pmatrix} d_L \\ s_L \\ b_L \\ \vdots \end{pmatrix} \equiv 2\,(\bar{\psi}_u)_L\,\gamma^r\,1\,(\psi_d)_L \tag{83}$$

A basis change to render $M^f$ diagonal implies the replacements

$$(\psi_u)_L \to U^u_L\,(\psi_u)_L \quad ; \quad (\psi_d)_L \to U^d_L\,(\psi_d)_L \tag{84}$$



For $J^r_-$ this change gives

$$J^r_- = 2\,(\bar{\psi}_u)_L\,\gamma^r\,(U^{u*}_L)^+\,(U^d_L)\,(\psi_d)_L = 2(\bar{\psi}_u)_L\,\gamma^r\,\tilde{C}\,(\psi_d)_L \tag{85}$$

For n families the matrix $\tilde{C}$ is a unitary n x n matrix which has $\frac{1}{2}n(n-1)$ real angles and $\frac{n(n+1)}{2}$ phases. However, not all of these phases are physical since one can rotate (2 n-1) phases away, by redefinitions of the quarks fields $\psi \to e^{i\alpha}\psi$ which do not affect $M^f_{diag}$.* After this redefinition the matrix $\tilde{C} \to C$, which is known as the Cabibbo matrix. The Cabibbo matrix thus has $\frac{1}{2}n(n-1)$ real angles and $\frac{1}{2}(n-1)(n-2)$ physical phases. All of these angles and phases are undetermined in the model, since they originate from the unknown Yukawa couplings $h^f_{ij}$. Nevertheless, the model does predict that in general there should be a non trivial mixing matrix.

I end this section with three remarks on the mixing matrix C.
1) For the case of two generations there is only one angle and no phase:

$$C = \begin{pmatrix} \cos\theta_c & \sin\theta_c \\ -\sin\theta_c & \cos\theta_c \end{pmatrix} \tag{86}$$

where $\theta_c$ is the Cabibbo angle. The current $J^r_-$ reads

$$J^r_- = 2\,\{\,\bar{u}_L \gamma^r d_L \cos\theta_c + \bar{u}_L \gamma^r s_L \sin\theta_c - \bar{c}_L \gamma^r d_L \sin\theta_c + \bar{c}_L \gamma^r s_L \cos\theta_c\,\} \tag{87}$$

The first two terms above are the Cabibbo piece /5/ of the charged current, known already in the early 60's. The last two terms were added by Glashow, Iliopoulos and Maiani /4/ to guarantee that the "neutral current" $J^r_3$, arising from the commutation algebra of $J^r_-$ and $J^r_+$, be flavor diagonal. In the SU(2) x U(1) model the full (Cabibbo plus GIM) form of the current arises naturally, when changing to a basis in which the mass matrix of quarks is diagonal.

2) For three generations of quarks and leptons - as we apparently have - C is the Kobayashi Maskawa matrix /6/. This matrix has three real angles and one phase. The Kobayashi Maskawa phase allows for CP violation in the standard model. I will return to this point at the end of these lectures.

3) Even in the case of many families one can check that the coupling of the physical Higgs particle to the fermions is flavor diagonal and proportional to the fermion's mass:

---

* 2n-1 not 2n because one overall phase has no meaning.

$$\mathcal{L}_{Hff} = -\frac{m_f}{v}\,\bar{f}\,f\,H \qquad (88)$$

DYNAMICS OF NAGT: ASYMPTOTIC FREEDOM, CONFINEMENT AND PARTON MODELS

Up to now I discussed only the symmetry properties of the standard model, without worrying too much about the dynamics. The dynamical issues in the electroweak theory, except for what really causes the SU(2) x U(1) breakdown, are not so difficult to tackle. Because the coupling constants g and g' are small, a perturbation treatment is warranted. For QCD, on the other hand, the dynamics is complex and needs to be discussed. In particular, the QCD Lagrangian is described in terms of quarks and gluons and yet, in the real world, we see only hadrons.

The important concept that allows one to make progress in QCD, even though its dynamics is complex, is the idea of the running coupling constant. To appreciate this concept it is particularly useful to refer back to a well known phenomenon in QED, that of vacuum polarization. Because of the possibility of virtual pair creation, the QED vacuum acts as a polarizable medium. This causes the effective charge of an electron to be screened at large distance. Because of this vacuum polarization effect the Coulomb potential is modified from its usual $\alpha/r$ form to:

$$V_{Coulomb}(r) = \frac{\alpha(r)}{r} \qquad (89)$$

The function $\alpha(r)$, which plays the role of an effective coupling constant squared, because of the screening of the electron charge becomes smaller as r increases. This effect can be computed by considering the modification to the photon propagator due to the possibility of pair creation (see Fig. 4).

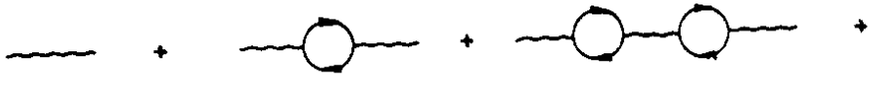

Fig. 4: Corrections to the photon propagator due to vacuum polarization

The result of this calculation, done first almost 50 years ago by Uehling /7/, reads for $q^2 \gg m^2$ and in momentum space:



$$\alpha(q^2) = \frac{\alpha}{1 - \frac{3\alpha}{\pi}\ln q^2/m^2} \qquad (90)$$

The running coupling constant $\alpha(q^2)$ in QED increases as $q^2$ becomes large, reflecting the fact that the electron's charge is screened by the virtual $e^+e^-$ pairs in the vacuum. Knowing $\alpha(q^2)$ as a function of $q^2$ one may compute the, so called, $\beta$-function, which is defined by:

$$\beta(q^2) = \frac{d\,\alpha(q^2)}{d\ln q^2} \simeq \frac{1}{3\pi}\left(\alpha(q^2)\right)^2 \qquad (91)$$

The last result above, follows from Eq. (90) and is the lowest order approximation for $\beta$. This function is an intrinsic property of QED and it can be determined in a power series expansion in $\alpha$.

$$\beta(\alpha) = b\alpha^2 + b'\alpha^4 + \ldots \qquad (92)$$

From the Uehling calculation one knows that $b = 1/3\pi$ and is therefore positive. The positivity of b, coupled with the definition (91), is enough to tell one immediately that there is screening in QED. That is, $\alpha(q^2)$ goes up as $q^2$ increases.

One can define an analogous $\beta$-function for QCD, which now depends on $\alpha_s = g_s^2/4\pi$, and calculate this function in perturbation theory. The result, up to terms of $O(\alpha_s^4)$, is

$$\beta(\alpha_s) = -\frac{(33-2n_f)}{12\pi}\,\alpha_s^2\left\{1 + \frac{(153-19n_f)}{2\pi(33-2n_f)}\,\alpha_s + \ldots\right\} \qquad (93)$$

In the above $n_f$ stands for the number of flavors of quarks in QCD. The most remarkable feature of Eq. (93) is the negative sign in front of the $\alpha_s^2$ term. This means that in QCD, in contrast to what happens in QED, there is antiscreening. This property was apparently known to 't Hooft, but the calculation of $\beta$ to $O(\alpha_s^2)$ was carried out independently and first published by Politzer and Gross and Wilczek /8/. The terms of $O(\alpha_s^4)$ in Eq. (93) were calculated by Caswell and Jones /9/.

From the $\beta$-function of Eq. (93), provided that these are less than 17 flavors, one deduces that in QCD the effective coupling constant (running coupling constant) has the behaviour shown in Fig. 5.

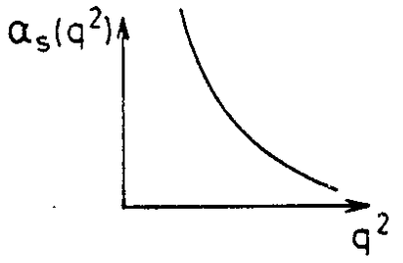


Fig. 5: Running coupling constant in QCD

The fact that $\alpha_s(q^2)$ decreases for large $q^2$ is due to the negative sign of the $\alpha_s^2$ term in (93), whose cause can be traced to the gluons. These terms, which are absent in the Abelian QED case, contribute the factor of $-33/12\pi$. This number is due (in part) to the additional gluonic contributions to the gluon propagator, shown in Fig. 6.

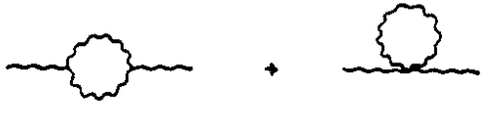

Fig. 6: Gluonic contributions to gluon propagator

The behavior of $\alpha_s(q^2)$ of Fig. 5 allows one to arrive at the following qualitative picture for the interactions of quarks and gluons. At small $q^2$ (large distances) the effective coupling constant $\alpha_s(q^2)$ becomes very large and colored objects bind strongly into color singlet states, the hadrons. This is the confinement property of QCD. For large $q^2$ (short distances), on the other hand, the effective coupling constant becomes very small and quarks and gluons act as quasi free objects. This is the famous asymptotic freedom of QCD. Confinement and asymptotic freedom explain two features of hadrons which were contradictory in the 1960's and early 1970's: Hadrons appear to be made up of quarks which are strongly bound together since they never seem to materialize in collisions (confinement) and yet when hadrons are probed at short distances they appear to be essentially composed of free quarks and gluons (Asymptotic freedom).

There are clearly two aspects of QCD dynamics which can be studied and probed. Either one examines the long distance behaviour of the theory, in which quark and gluons bind to make hadrons. This is the realm of hadronic spectroscopy and, theoretically, of lattice QCD or, one studies the short distance properties of the theory by examining "hard" collisions in which one is essentially dealing with scattering at the quark and gluon level. I shall, in the remainder of these lectures, only concentrate on this latter aspect of QCD, where one can proceed perturbatively.



For processes where hadrons scatter with large momentum transfer (hard scattering) one may make use of asymptotic freedom to compute the relevant cross sections. Because for large $q^2$ the effective coupling $\alpha_s(q^2)$ is small, hadronic hard scattering can be computed perturbatively at the quark and gluon level. To be more precise, three elements enter into these parton model hard scattering calculations:

1) Hadronic structure functions: These functions describe the distribution of quarks and gluons (partons) within the initial state hadrons.

2) Parton cross sections: These cross sections are calculable in QCD provided $q^2$ is large enough, so that a perturbation expansion in $\alpha_s(q^2)$ is tenable. It is this restriction that circumscribes parton model calculations of hadronic scattering processes to those involving large $q^2$. Only in this case can one compute - albeit approximately - the parton cross sections.

3) Hadronic fragmentation functions: These functions describe the distribution of hadrons expected from a given parton.

The calculation of a hadronic hard scattering process involves, in general, the convolution of the above three elements. Only the parton cross sections are calculable, so that only the overall structure but not the detailed form of the hadronic hard scattering reaction can be determined. Although the structure and fragmentation functions are, at present, uncalculable, because they involve the "soft processes" of transmutation of hadrons into quarks and vice versa, their universality makes the above procedure relevant. Because the distribution of quarks within a hadron, or the probability of creating a certain hadron from a quark, is process independent, once these distributions are known from some hadronic hard scattering process they allow one to predict what is to be expected in another hard scattering process.

These points are best illustrated by a practical example. Imagine trying to compute the deep inelastic production of pions in muon-proton scattering, for large momentum transfer, $q^2$. The process $\mu p \to \mu \pi X$ can be computed by convoluting three separate elements, as shown graphically in Fig. 6. The cross section involves the probability $f_q(\xi;q^2)$ (Box 1 in Fig. 6) of finding a quark with fractional momentum $\xi$ within the proton, convoluted with the (parton) cross sections for the elastic scattering of this quark with the incoming muon (Box 2 in Fig. 6), convoluted with the probability $D_q^\pi(\xi';q^2)$ that the outgoing quark becomes a pion with fractional momentum $\xi'$ (Box 3 in Fig. 6)*

* This is a slight simplification. I will discuss later the role of gluons in deep inelastic processes.

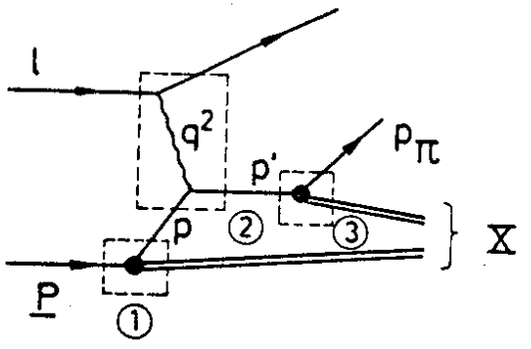


Fig. 6: Parton model breakup of deep inelastic pion production in $\mu$ – proton scattering

Let me be more specific. If $P^\mu$ and $\ell^\mu$ are the initial momenta of the proton and muon, $P_\pi{}^\mu$ is the final momentum of the produced pion, and $q^\mu$ is the momentum transfer, it is usual to define the following kinematical variables:

$$x = -\frac{q^2}{2P\cdot q} \quad ; \quad y = \frac{P\cdot q}{P\cdot \ell} \quad ; \quad z = \frac{P\cdot P_\pi}{P\cdot q} \tag{94}$$

The quarks in Fig. 6 carry momenta $p^\mu$ and $p'^\mu$ and the fractions $\xi$ and $\xi'$ are defined by

$$p^\mu = \xi P^\mu \quad ; \quad P_\pi^\mu = \xi' p'^\mu \tag{95}$$

Thus at the parton level the kinematical variables $x_p$ and $z_p$ defined analogously to (94) are given by

$$x_p = \frac{-q^2}{2p\cdot q} = \frac{-q^2}{2\frac{P\cdot q}{\xi}} = \frac{x}{\xi} \tag{96a}$$

$$z_p = \frac{P\cdot p'}{P\cdot q} = \frac{P\cdot(\quad)}{P\cdot q} = \frac{z}{\xi'} \tag{96b}$$



The inclusive cross section for the process $\mu P \to \mu \pi X$ computed from Fig. 6, assuming that the scattering proceeds as the sum of incoherent scatterings from each parton, is given explicitly by the formula

$$\frac{d\sigma^\pi}{dx\,dy\,dz} = \sum_q \int_x^1 \frac{d\xi}{\xi} \int_z^1 \frac{d\xi'}{\xi'} f_q(\xi;q^2)\left[\frac{d\sigma_{part}(q^2)}{dx_p\,dy\,dz_p}\right] D_q^\pi(\xi';q^2) \tag{97}$$

That is, the cross section is the sum of the convolutions of the probability $f_q(\xi;q^2)$ of having a quark of given fractional momentum within the proton scatter with the incoming muon, producing a final quark which has a probability $D_q^\pi(\xi';\xi')$ of producing the observed pion. The $q^2$ dependence of the structure and fragmentation functions, as well as that of the parton cross sections, is an effect of QCD, which I will discuss later in more detail. If one supposed that quarks were really free inside the proton at short distance ($\alpha_s(q^2) \to 0$), as was assumed in the oldfashioned parton model of pre QCD days /10/, then this $q^2$ dependence would be omitted. The limits in Eq. (97) follow since $x_p$ and $z_p$ kinematically can reach only unity – neglecting mass effects – and the fractions $\xi$ and $\xi'$ can be at most one. The factors of $\xi$ and $\xi'$, are needed, furthermore, to transform x and z into $x_p$ and $z_p$.

To lowest order in the electroweak interaction and in QCD ($\alpha_s^0$) the parton cross section is given by the tree graph $\mu$-quark scattering of Fig. 7. Except for very large $q^2$, where the $Z^0$ contribution is also important, the exchanged boson is just the photon and the cross section is proportional to $(q^2)^{-2}$.

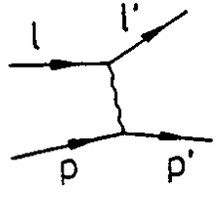


Fig. 7: Lowest order contribution to muon-quark scattering

Because one is dealing with a 2-2 scattering process it is easy to convince oneself, neglecting all masses relative to $q^2$ and P.q, that

$$\frac{d\sigma_{part}}{dx_p\,dy\,dz_p} \sim \delta(1-x_p)\,\delta(1-z_p) \tag{98}$$

Hence, in this approximation, the hadronic scattering process is just proportional to the product of the structure and fragmentation functions:

$$\frac{d\sigma^{\pi}}{dx\,dy\,dz} \sim \sum_{q} f_q(x)\, D_q^{\pi}(z) \tag{99}$$

It is useful to summarize the structure of the hadronic hard scattering cross sections by the symbolic formula:

$$d\sigma^{H} \sim f_{parton} \otimes d\sigma_{parton} \otimes D^{H}_{parton} \tag{100}$$

where $f_{parton}$ and $D^{H}_{parton}$ are process independent but uncalculable, while $d\sigma_{parton}$ is process dependent but calculable in a power series in $\alpha_s$. Eq. (100) suggests already a general test of QCD, in the perturbative regime. Having found $f_{parton}$ and $D^{H}_{parton}$ from some process one may use them to compute another process. This procedure works rather well in practice. For instance, large $p_\perp$ jet production at the collider can be computed knowing the structure functions in deep inelastic scattering. There are, however, some subtleties and complications - like the K factor in Drell-Yan - which I will explain later on in these lectures.

In special circumstances, when one studies processes which are inclusive enough, one can altogether eliminate the fragmentation functions $D^{H}_{parton}$. The two best known examples are deep inelastic scattering processes (like $\mu p \to \mu X$ ) and $e^+e^-$ annihilation into hadrons ($e^+e^- \to X$). Physically it is quite clear why no D-functions appear in these processes, since one is summing over all possible hadrons. In QCD this circumstance allows one to compute the process in a quark-gluon basis, because the probability of hadronization is unity. More formally, the fragmentation functions are eliminated by using the energy-momentum sum rule

$$\sum_{H} \int_0^1 d\xi'\, \xi'\, D_q^{H}(\xi'; q^2) = 1 \tag{101}$$

It is not hard to convince oneself that, for the processes at hand, precisely this weighted sum of the fragmentation functions enters.

Jet production, in which one is asking again for gross properties of a reaction, is also independent of the fragmentation functions, provided one is prepared to neglect effects due to the soft hadronization of quarks and gluons into hadrons *. To neglect the fragmentation functions one needs to assume that the jet direction coincides with the parton direction. This then provides additional QCD tests, which are spectacularly successful qualitatively but less so quantitatively. I refer here to the presence of 3 jets at PETRA and at PEP and of large $p_\perp$ jets at the collider, whose really detailed comparisons with QCD, as I will explain, must still rely on some sensible hadronization model.

* More technically, as I will explain in a later section, one must also deal with processes which are infrared insensitive.



Before embarking in a more detailed analysis of QCD effects in hard scattering, it will prove useful to devote the next section to a discussion of deep inelastic scattering, calculated at zeroth order in QCD. This will allow me to interrelate a variety of processes and test thereby some of the predictions of the GSW model. In subsequent sections I will return to the QCD corrections to these results and see how these fare experimentally. Of course, this separate testing of aspects of the GSW model and of QCD is done here only for pedagogical purposes. In practice, one deals with both phenomena simultaneously.

## DEEP INELASTIC PHENOMENA: $0^{th}$ ORDER QCD TESTING THE GSW THEORY

I want to discuss in some detail the related deep inelastic processes

$$\ell^{\pm} p \to \ell^{\pm} X \tag{102a}$$

$$\begin{pmatrix} \nu_\ell \\ \bar{\nu}_\ell \end{pmatrix} p \to \begin{pmatrix} e^- \\ e^+ \end{pmatrix} X \tag{102b}$$

$$\begin{pmatrix} \nu_\ell \\ \bar{\nu}_\ell \end{pmatrix} p \to \begin{pmatrix} \nu_\ell \\ \bar{\nu}_\ell \end{pmatrix} X \tag{102c}$$

For the first process above both the electromagnetic and the weak neutral current contribute. The reaction (102b) is a purely weak charged current process, while (102c) occurs only because of the existence of weak neutral currents. Because all three of these processes are totally inclusive, the expression for the differential scattering cross section will not contain fragmentation functions. The differential cross section for these processes, therefore, takes the form (cf. Eq. (97))

$$\frac{d\sigma}{dx\,dy} = \sum_{parton} \int_x^1 \frac{d\xi}{\xi} f_{parton}(\xi; q^2)\, \frac{d\sigma^{(q^2)}_{parton}}{dx_p\,dy} \tag{103}$$

As indicated above, I will compute Eq. (103) in this section only to lowest order in QCD. This means that all $q^2$-dependence in $f_{parton}$ will be ignored and that the parton cross section corresponds to the simple quark lepton scattering process shown in Fig. 8.

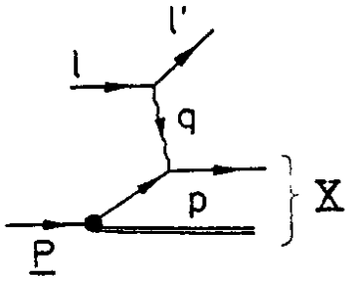


Fig. 8: Lowest order QCD contribution for deep inelastic scattering

To be a little more explicit, $d\sigma_{parton}$ will be calculated as the appropriate quark-lepton scattering processes, neglecting all fermion masses and spin averaging over the fermions. (Averaging over initial spins and summing over final spins). Simple kinematics gives for the 2-2 scattering process involved:

$$\frac{d\sigma_{parton}}{dx_p\, dy} = \frac{y}{16\pi q^2}\,\delta(1-x_p)\,\langle|T|^2\rangle \qquad (104)$$

Here $\langle|T|^2\rangle$ is the spin-averaged T-matrix element squared for lepton-quark scattering

$$\frac{1}{2}\sum_{s_q s_{q'}} \cdot \begin{pmatrix} 1/2 \\ 1 \end{pmatrix} \sum_{s_\ell s_{\ell'}} |T|^2 \equiv \langle|T|^2\rangle \qquad (105)$$

In the above the factor of 1/2 applies for initial state charged leptons, corresponding to the averaging over their initial polarizations. For neutrino initiated scattering, however, the corresponding factor is 1, since neutrinos, or antineutrinos, come in only one helicity.

For the reactions in Eqs. (102), the T matrix element can be calculated from the graph of Fig. 9. For moderate values of $q^2$, for reaction

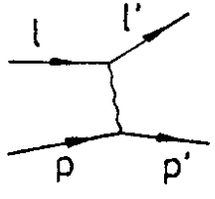


Fig. 9: Contribution to quark-lepton scattering



(102a) it suffices to consider only the photon exchange contribution. Similarly, for the charged current and neutral current reactions of Eqs. (102b) and (102c) one may replace the propagator by a contact interaction and therefore use the interaction Lagrangian of Eq. (57) to compute the T-matrix. One finds in this way the following parton T-matrices, for the corresponding processes of Eqs. (102):

$$T = -i\,\frac{e^2 e_q}{q^2}\left(J^\mu_{em}\cdot J_{\mu\,em}\right) \qquad (106a)\quad \text{EM}$$

$$T = i\,\frac{G_F}{\sqrt{2}}\left(J^\mu_{+}\cdot J_{-\mu}\right) \qquad (106b)\quad \text{CC}$$

$$T = i\,\frac{G_F}{\sqrt{2}}\,\rho\left(J^\mu_{NC}\cdot J_{\mu\,NC}\right) \qquad (106c)\quad \text{NC}$$

Here $e_q$ is the quark charge in units of the positron charge. Hence it follows that

$$\langle|T|^2\rangle = \frac{16\pi^2\alpha^2 e_q^2}{(q^2)^2}\,L^{em}_{\mu\nu}\,Q^{\mu\nu}_{em} \qquad (107a)\quad \text{EM}$$

$$\langle|T|^2\rangle = \frac{G_F^2}{2}\,L^{cc}_{\mu\nu}\,Q^{\mu\nu}_{cc} \qquad (107b)\quad \text{CC}$$

$$\langle|T|^2\rangle = \frac{G_F^2}{2}\,\rho^2\,L^{NC}_{\mu\nu}\,Q^{\mu\nu}_{NC} \qquad (107c)\quad \text{NC}$$

The tensor structures $L_{\mu\nu}$ and $Q_{\mu\nu}$ are straightforward to compute, for all processes, using the explicit form of the currents in the standard GSW model.

I will give an example of this computation for the charged current process $\nu_e d \to \ldots u$. The T-matrix element is just

$$T = i\,\frac{G_F}{\sqrt{2}}\left[\bar{u}_\ell(\ell')\,\gamma^\mu(1-\gamma_5)\,u_{\nu_e}(\ell)\right]\cdot\left[\bar{u}_u(p')\,\gamma_\mu(1-\gamma_5)\,u_d(p)\right] \qquad (108)$$

The tensors $L^{cc}_{\mu\nu}$ and $Q^{cc}_{\mu\nu}$ come from the spin average of the factors in bracket above, corresponding to leptons and quarks, respectively. Thus

$$L^{cc}_{\mu\nu} = \sum_{s_\ell s_\nu} [\bar{u}_\ell(\ell')\gamma_\mu(1-\gamma_5)u_{\nu_\ell}(\ell)]\cdot[\bar{u}_\ell(\ell')\gamma_\nu(1-\gamma_5)u_{\nu_\ell}(\ell)]^*$$

$$= \mathrm{Tr}\ \gamma_\mu(1-\gamma_5)(-\gamma\cdot\ell)\gamma_\nu(1-\gamma_5)(-\gamma\cdot\ell')$$

$$= 2\,\mathrm{Tr}\,\gamma_\mu\gamma\cdot\ell\,\gamma_\nu\gamma\cdot\ell'(1-\gamma_5)$$

$$= 8[\ell_\mu\ell'_\nu + \ell'_\mu\ell_\nu - \ell\cdot\ell' g_{\mu\nu} - i\epsilon_{\mu\nu\alpha\beta}\ell^\alpha\ell'^\beta]$$

$$\equiv 8[\ell^S_{\mu\nu} - \ell^A_{\mu\nu}] \qquad (109)$$

Note that the spin averaging in $L^{cc}_{\mu\nu}$ has no factor of 1/2 because one deals with initial neutrino (c.f. the discussion after Eq. 105). Also the functions $\ell^S_{\mu\nu}$ and $\ell^A_{\mu\nu}$ are obviously defined as the symmetric and antisymmetric terms in $\ell$ and $\ell'$ appearing in the next to last line in Eq. (109). Similarly one calculates

$$Q^{cc}_{\mu\nu} = \frac{1}{2}\sum_{s_d s_u}[\bar{u}_u(p')\gamma_\mu(1-\gamma_5)u_d(p)]\cdot[\bar{u}_u(p')\gamma_\nu(1-\gamma_5)u_d(p')]^*$$

$$= \frac{1}{2}\,\mathrm{Tr}\ \gamma_\mu(1-\gamma_5)(-\gamma\cdot p)\gamma_\nu(1-\gamma_5)(-\gamma\cdot p')$$

$$= \mathrm{Tr}\ \gamma_\mu\gamma\cdot p\ \gamma_\nu\gamma\cdot p'(1-\gamma_5)$$

$$= 4[p_\mu p'_\nu + p'_\mu p_\nu - p\cdot p' g_{\mu\nu} - i\epsilon_{\mu\nu\alpha\beta}p^\alpha p'^\beta]$$

$$\equiv 4[q^S_{\mu\nu} - q^A_{\mu\nu}] \qquad (110)$$

where $q^S_{\mu\nu}$ and $q^A_{\mu\nu}$ are defined in an analogous way to $\ell^S_{\mu\nu}$ and $\ell^A_{\mu\nu}$.



Performing similar calculations for all the parton subprocesses, involving lepton scattering off both quarks and antiquarks, one secures the following list of formulas:

$$(L_{\mu\nu})^{\ell\to\ell}_{em} = (L_{\mu\nu})^{\bar{\ell}\to\bar{\ell}}_{em} = 2[\ell^S_{\mu\nu}] \qquad (111a)$$

$$(L_{\mu\nu})^{\nu_\ell\to\ell}_{cc} = (L_{\mu\nu})^{\nu_\ell\to\nu_\ell}_{NC} = 8[\ell^S_{\mu\nu} - \ell^A_{\mu\nu}] \qquad (111b)$$

$$(L_{\mu\nu})^{\bar{\nu}_\ell\to\bar{\ell}}_{cc} = (L_{\mu\nu})^{\bar{\nu}_\ell\to\bar{\nu}_\ell}_{NC} = 8[\ell^S_{\mu\nu} + \ell^A_{\mu\nu}] \qquad (111c)$$

$$(Q_{\mu\nu})^{q\to q}_{em} = (Q_{\mu\nu})^{\bar{q}\to\bar{q}}_{em} = 2[q^S_{\mu\nu}] \qquad (111d)$$

$$(Q_{\mu\nu})^{q\to q'}_{cc} = 4[q^S_{\mu\nu} - q^A_{\mu\nu}] \qquad (111e)$$

$$(Q_{\mu\nu})^{\bar{q}\to\bar{q}'}_{cc} = 4[q^S_{\mu\nu} + q^A_{\mu\nu}] \qquad (111f)$$

$$(Q_{\mu\nu})^{q\to q}_{NC} = 4(Q^{NC}_{qL})^2[q^S_{\mu\nu} - q^A_{\mu\nu}] + 4(Q^{NC}_{qR})^2[q^S_{\mu\nu} + q^A_{\mu\nu}] \qquad (111g)$$

$$(Q_{\mu\nu})^{\bar{q}\to\bar{q}}_{NC} = 4(Q^{NC}_{qL})^2[q^S_{\mu\nu} + q^A_{\mu\nu}] + 4(Q^{NC}_{qR})^2[q^S_{\mu\nu} - q^A_{\mu\nu}] \qquad (111h)$$

In the above the "charges" $Q^{NC}_{qL}$ and $Q^{NC}_{qR}$ which characterize the strength of the neutral current coupling to left- and right-handed quarks, are given in the GSW model by

$$Q^{NC}_{qL} = \left(\frac{\tau_3}{2}\right)_q - e_q \sin^2\theta_W \qquad (112a)$$

$$Q^{NC}_{qR} = -e_q \sin^2\theta_W \qquad (112b)$$

We note that in the above formulas going from particles to antiparticles corresponds to the changes of S $\leftrightarrow$ S and A $\leftrightarrow$ -A. This follows since this change corresponds precisely to the interchange of the roles of $\ell \leftrightarrow \ell'$ and/or $p \leftrightarrow p'$. Note that these same changes also occur in flipping (V-A) into (V+A) interactions. That is, going to the antiparticle is akin to flipping helicity.

To compute the parton cross sections it remains to evaluate the contraction of $L_{\mu\nu}$ with $Q^{\mu\nu}$, for each of the cases in question. Simple kinematics yields the formulas

$$\ell^S_{\mu\nu}\, q^{\mu\nu}_A = \ell^A_{\mu\nu}\, q^{\mu\nu}_S = 0 \tag{113a}$$

$$\ell^S_{\mu\nu}\, q^{\mu\nu}_S = \frac{(q^2)^2}{2y^2}\left[1 + (1-y)^2\right] \tag{113b}$$

$$\ell^A_{\mu\nu}\, q^{\mu\nu}_A = \frac{(q^2)^2}{2y^2}\left[1 - (1-y)^2\right] \tag{113c}$$

It follows therefore that the y-dependence for the parton subprocesses is simple. To wit:

1) For electromagnetic processes, since only S-terms enter one has

$$\left(\frac{d\sigma}{dy}\right)^{em} \sim \left[1 + (1-y)^2\right] \tag{114}$$

2) for scattering of a left-handed quark with a left-handed lepton (or right-handed quark with a right-handed lepton) one has

$$\frac{d\sigma_{LL}}{dy} \sim \frac{d\sigma_{RR}}{dy} \sim \left[\ell^S_{\mu\nu} \mp \ell^A_{\mu\nu}\right]\cdot\left[q^{S\mu\nu} \mp q^{A\mu\nu}\right] \sim 1 \tag{115}$$

3) Mixed scattering, on the other hand, gives

$$\frac{d\sigma_{LR}}{dy} \sim \frac{d\sigma_{RL}}{dy} \sim \left[\ell^S_{\mu\nu} \mp \ell^A_{\mu\nu}\right]\cdot\left[q^{S\mu\nu} \pm q^{A\mu\nu}\right] \sim (1-y)^2 \tag{116}$$

4) Scattering leptons off antiquarks is equivalent to the scattering of leptons off quarks of the opposite helicity.



These results can be understood qualitatively in a simpler way /11/. In all the parton processes considered one is dealing with vector interactions which conserve helicity at each vertex. Consider then scattering of two left handed objects in the CM system, as shown in Fig. 10a. The initial state has J = o and so one expects that $(d\sigma/d\Omega)_{CM}$ be isotropic. This implies directly Eq. (115). If a right- and a left-handed state scatter, as in Fig. 10b, then J = 1 and backward scattering is forbidden, since it corresponds to $\Delta J = 2$. So $\left(\frac{d\sigma}{d\Omega}\right)_{CM} \sim (1+\cos\theta)^2$ which is equivalent to Eq. (116).


Fig. 10: Scattering of LL(a) and LR(b) fermions in the CM, with vector interactions.

Armed with Eqs. (103) and (104), and the explicit forms for $\langle|T|^2\rangle$ which follow from Eqs. (107), (111) and (113), it is now straightforward to derive the parton model (Oth order QCD) expressions for the reactions (102). In the laboratory system one finds:

$$\left(\frac{d\sigma}{dx\,dy}\right)^{EM} = \frac{8\pi\alpha^2 M E_\ell}{(q^2)^2}\left[\frac{1+(1-y)^2}{2}\right]\cdot\left\{\sum_q e_q^2 \times\left(f_q(x) + f_{\bar q}(x)\right)\right\} \tag{117}$$

$$\left(\frac{d\sigma}{dx\,dy}\right)^{cc.}_{\nu\ \text{induced}} = \frac{G_F^2 M E_\nu}{\pi}\cdot\left\{\sum_i 2x\, f_{d_i}(x)\,[1] + \sum_i 2x\, f_{\bar u_i}(x)\,[1-y]^2\right\} \tag{118a}$$

$$\left(\frac{d\sigma}{dx\,dy}\right)^{cc}_{\bar\nu\ \text{induced}} = \frac{G_F^2 M E_\nu}{\pi}\cdot\left\{\sum_i 2x\, f_{\bar d_i}(x)\,[1] + \sum_i 2x\, f_{u_i}(x)\,[1-y]^2\right\} \tag{118b}$$

$$\left(\frac{d\sigma}{dx\,dy}\right)^{NC}_{\nu\ \text{induced}} = \frac{G_F^2 M E_\nu}{\pi}\rho^2 \cdot \left\{ \sum_i z\, x f_{q_i}(x)\left[(Q^{NC}_{q_i L})^2 + (Q^{NC}_{q_i R})^2 (1-y)^2\right] + \sum_i z\, x f_{\bar{q}_i}(x)\left[(Q^{NC}_{q_i R})^2 + (Q^{NC}_{q_i L})(1-y)^2\right]\right\} \tag{119a}$$

$$\left(\frac{d\sigma}{dx\,dy}\right)^{NC}_{\bar{\nu}\ \text{induced}} = \frac{G_F^2 M E_\nu}{\pi}\rho^2 \cdot \left\{ \sum_i z\, x f_{q_i}(x)\left[(Q^{NC}_{q_i R})^2 + (Q^{NC}_{q_i L})^2 (1-y)^2\right] + \sum_i z\, x f_{\bar{q}_i}(x)\left[(Q^{NC}_{q_i L})^2 + (Q^{NC}_{q_i R})^2 (1-y)^2\right]\right\} \tag{119b}$$

These equations simplify in the, so called, valence quark approximation in which one neglects altogether the contributions of antiquarks in the nucleon. For lepton proton scattering, in this case, the curly brackets in Eqs. (117) - (118) become

$$\left\{\ \right\}^{EM}_{ep} \xrightarrow[\text{Valence}]{} \frac{4}{9}\, x u_v(x) + \frac{1}{9}\, x d_v(x) \tag{120}$$

$$\left\{\ \right\}^{CC}_{\nu p} \xrightarrow[\text{Valence}]{} z\, x d_v(x) \tag{121a}$$

$$\left\{\ \right\}^{CC}_{\bar{\nu} p} \xrightarrow[\text{Valence}]{} z\, x u_v(x)\,(1-y)^2 \tag{121b}$$

Here $u_v(x)$ and $d_v(x)$ are the distribution functions of up and down (valence) quarks in a proton. By charge symmetry they describe, respectively, also the distribution of down and up quarks in a neutron. Hence for lepton neutron scattering the curly brackets in Eqs. (117) and (118), in the valence approximation, become



$$\left\{\ \right\}^{EM}_{eN} \xrightarrow[\text{Valence}]{} \frac{4}{9}\, x d_v(x) + \frac{1}{9}\, x u_v(x) \tag{122}$$

$$\left\{\ \right\}^{CC}_{\nu N} \xrightarrow[\text{Valence}]{} z\, x u_v(x) \tag{123a}$$

$$\left\{\ \right\}^{CC}_{\bar{\nu} N} \xrightarrow[\text{Valence}]{} z\, x d_v(x)\,(1-y)^2 \tag{123b}$$

For an isoscalar target $N = \frac{1}{2}(n+p)$ the relevant formulas are simply:

$$\left\{\ \right\}^{EM}_{eN} \xrightarrow[\text{Valence}]{} \frac{5}{18}\left[x u_v(x) + x d_v(x)\right] \tag{124}$$

$$\left\{\ \right\}^{CC}_{\nu N} \xrightarrow{} \left[x u_v(x) + x d_v(x)\right] \tag{125a}$$

$$\left\{\ \right\}^{CC}_{\bar{\nu} N} \xrightarrow[\text{Valence}]{} \left[x u_v(x) + x d_v(x)\right](1-y)^2 \tag{125b}$$

Data from the CHARM experiment at CERN /12/, shown in Fig. 11, for neutrino and antineutrino scattering on an isoscalar target shows that the characteristic y-dependence predicted in the valence approximation ( $d\sigma_{\nu N}/dy \sim 1$ ; $d\sigma_{\bar{\nu}N}/dy \sim (1-y)^2$ ) is satisfied to within perhaps 10 % - 15 %. Furthermore, charged current and electromagnetic deep inelastic processes are interrelated in this approximation. From Eqs. (124) and (125a) one predicts that

$$\frac{\left\{\ \right\}^{CC}_{\nu N}}{\left\{\ \right\}^{EM}_{eN}} \equiv \frac{F_2^{\nu N}(x)}{F_2^{eN}(x)} = \frac{18}{5} \tag{126}$$

This behaviour is also well reproduced by the data, as Fig. 12 shows.

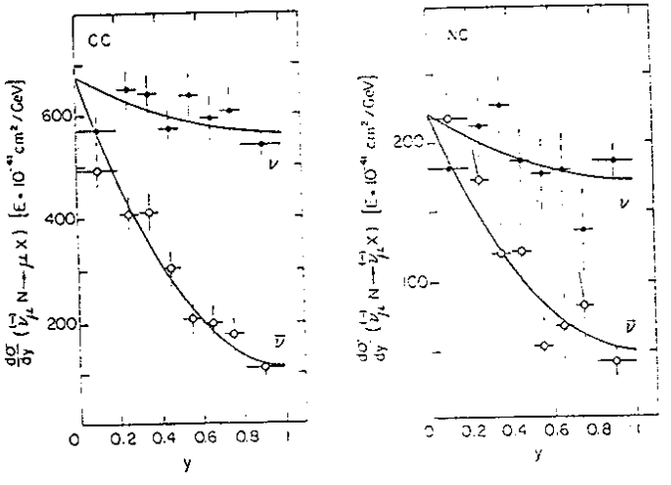


Fig. 11: $\nu_\mu$ and $\bar{\nu}_\mu$ scattering on isoscalar targets. Data from Ref. 12

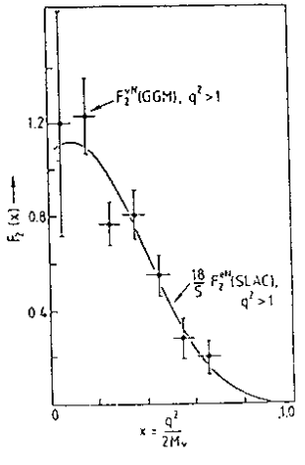


Fig. 12: Test of Eq. (126) using Gargamelle and SLAC data, from Ref. 13



In the valence quark approximation neutrino and antineutrino neutral current scattering off isoscalar targets also simplify. From Eqs. (119a) and (119b) one obtains

$$\left\{ \right\}^{NC}_{\nu N} = \left[ (Q^{NC}_{dL})^2 + (Q^{NC}_{uL})^2 + (1-y)^2 \left( (Q^{NC}_{dR})^2 + (Q^{NC}_{uR})^2 \right) \right] \times \left( d_v(x) + U_v(x) \right)$$

$$= \left[ \left( \tfrac{1}{2} - \sin^2\theta_W + \tfrac{5}{9}\sin^4\theta_W \right) + (1-y)^2 \tfrac{5}{9}\sin^4\theta_W \right] \cdot \left\{ \right\}^{CC}_{\nu N} \qquad (127a)$$

$$\left\{ \right\}^{NC}_{\bar{\nu} N} = \left[ (Q^{NC}_{dR})^2 + (Q^{NC}_{uR})^2 + (1-y)^2 \left( (Q^{NC}_{dL})^2 + (Q^{NC}_{uL})^2 \right) \right] \times \left( d_v(x) + U_v(x) \right)$$

$$= \left[ \tfrac{5}{9}\sin^4\theta_W \cdot \frac{1}{(1-y)^2} + \left( \tfrac{1}{2} - \sin^2\theta_W + \tfrac{5}{9}\sin^4\theta_W \right) \right] \cdot \left\{ \right\}^{CC}_{\bar{\nu} N} \qquad (127b)$$

These formulas allow one to compute the ratio of NC to CC processes, independently of the structure functions. Consider the ratio

$$R_\nu = \frac{\sigma_{NC}(\nu N)}{\sigma_{CC}(\nu N)} = \frac{\int_0^1 dx\, dy \left( \frac{d\sigma}{dx\, dy} \right)^{NC}_{\nu N}}{\int_0^1 dx\, dy \left( \frac{d\sigma}{dx\, dy} \right)^{CC}_{\nu N}} \qquad (128)$$

Using Eq. (127a), and remembering that the NC cross section has an extra factor of $\rho^2$, yields:

$$R_\nu = \rho^2 \left[ \tfrac{1}{2} - \sin^2\theta_W + \tfrac{20}{27}\sin^4\theta_W \right] \qquad (129a)$$

A similar calculation for the antineutrino processes gives instead

$$R_{\bar{\nu}} = \rho^2 \left[ \tfrac{1}{2} - \sin^2\theta_W + \tfrac{20}{9}\sin^4\theta_W \right] \qquad (129b)$$

Recent experimental values from the CDHS /14/ and CHARM /15/ experiments at CERN give the values

$$R_{\nu} = 0.300 \pm 0.007 \qquad R_{\bar{\nu}} = 0.357 \pm 0.015 \qquad \text{(CDHS)} \tag{130a}$$

$$R_{\nu} = 0.320 \pm 0.010 \qquad R_{\bar{\nu}} = 0.377 \pm 0.025 \qquad \text{(CHARM)} \tag{130b}$$

Using our formulas and taking $\rho = 1$ and a value of $\sin^2\theta_W = 0.23$ implies

$$R_{\nu} = 0.31 \qquad R_{\bar{\nu}} = 0.39 \tag{131}$$

which are in nice agreement with Eqs. (130). A more careful analysis, which includes the contribution of the quark sea, carried out by Kim et al. /16/ yields

$$\sin^2\theta_W = 0.234 \pm 0.011 \tag{132}$$

for $\rho = 1$. Letting $\rho$ vary also, the authors of Ref. 16 obtain

$$\sin^2\theta_W = 0.232 \pm 0.027 \qquad \rho = 0.999 \pm 0.025 \tag{133}$$

As I will show in the next section, a variety of other experiments involving neutral currents give values of $\sin^2\theta_W$ and $\rho$ in agreement with the above. All these experiments taken together provide strong evidence for the validity of the GSW model - at least in its fermion-gauge sector.

It is conventional to describe deep inelastic experiments in terms of structure functions. For processes involving parity violation one can write on general grounds /17/, for $m_\ell = 0$ and $E_\ell \gg M$, the differential cross section in terms of three independent structure functions:

$$\left(\frac{d\sigma}{dx\,dy}\right)^{CC/NC}_{\nu,\bar{\nu}} = \frac{G_F^2 M E_\ell}{\pi}\left\{\tfrac{1}{2}\left(2xF_1 \pm xF_3\right) + \tfrac{1}{2}(1-y)^2\left(2xF_1 \mp xF_3\right) + (1-y)\left(F_2 - 2xF_1\right)\right\} \tag{134}$$

For the electromagnetic processes the $F_3$ structure function does not contribute and one has



$$\left(\frac{d\sigma}{dx\,dy}\right)^{EM}_{\ell} = \frac{8\pi\alpha^2 M E_\ell}{(q^2)^2}\left[\left(1+\frac{(1-y)^2}{2}\right)2xF_1 + (1-y)\left(F_2 - 2xF_1\right)\right] \tag{135}$$

In general the structure functions $F_i$ are functions of both x and $q^2$. However, in the parton model (0th order QCD) approximation employed to derive Eqs. (117) - (119), the structure functions depend only on x. Furthermore, as can be seen from these equations, there is a relation between $F_1$ and $F_2$, since no terms proportional to (1-y) enter. This relation, first derived by Callan and Gross /18/, is a result of having spin 1/2 partons and reads

$$F_2 = 2xF_1 \tag{136}$$

The structure functions $F_2$ and $F_3$ are easily extracted from Eqs. (117) - (119). One has

$$F_2^{EM}(x) = x\sum_q e_q^2\left(f_q(x) + f_{\bar{q}}(x)\right) \tag{137a}$$

$$\left(F_2^{NC}(x)\right)_{\nu} = \left(F_2^{NC}(x)\right)_{\bar{\nu}} = 2\rho^2 x\sum_q\left[\left(Q^{NC}_{qL}\right)^2 + \left(Q^{NC}_{qR}\right)^2\right]\left(f_q(x) + f_{\bar{q}}(x)\right) \tag{137b}$$

$$\left(F_3^{NC}(x)\right)_{\nu} = \left(F_3^{NC}(x)\right)_{\bar{\nu}} = 2\rho^2\sum_q\left[\left(Q^{NC}_{qL}\right)^2 - \left(Q^{NC}_{qR}\right)^2\right]\left(f_q(x) - f_{\bar{q}}(x)\right) \tag{137c}$$

$$\left(F_2^{CC}(x)\right)_{\nu} = 2x\sum_i\left(f_{d_i}(x) + f_{\bar{u}_i}(x)\right) \tag{137d}$$

$$\left(F_2^{CC}(x)\right)_{\bar{\nu}} = 2x\sum_i\left(f_{u_i}(x) + f_{\bar{d}_i}(x)\right) \tag{137e}$$

$$\left(F_3^{CC}(x)\right)_{\nu} = 2\sum_i\left(f_{d_i}(x) - f_{\bar{u}_i}(x)\right) \tag{137f}$$

$$\left(F_3^{CC}(x)\right)_{\bar{\nu}} = 2\sum_i\left(f_{u_i}(x) - f_{\bar{d}_i}(x)\right) \tag{137g}$$

Note that the structure function $F_3$ contains differences between quark and antiquark distributions, so that in principle it is sensitive to the valence content in the nucleon. This, non singlet, property is made apparent by considering, for charged current scattering, the case

of 4 flavors, for deep inelastic scattering off an isoscalar target. One finds, using the fact that the distribution of charmed and strange quarks in proton and neutrons are the same and equal to the distribution of their antiparticles,

$$\left(F_3^{cc}(x)\right)_{\nu N} = \left[d(x) + u(x) - \bar{d}(x) - \bar{u}(x)\right] + 2\left[s(x) - c(x)\right] \quad (138a)$$

$$\left(F_3^{cc}(x)\right)_{\bar{\nu} N} = \left[d(x) + u(x) - \bar{d}(x) - \bar{u}(x)\right] + 2\left[c(x) - s(x)\right] \quad (138b)$$

The first bracket in Eqs. (138) measures just the distribution of valence d and u quarks. The small sea contribution in the last term can be eliminated by averaging the result of (138a) and (138b). Hence, indeed,

$$\bar{F}_3^{cc}(x) = \frac{1}{2}\left[\left(F_3^{cc}(x)\right)_{\nu N} + \left(F_3^{cc}(x)\right)_{\bar{\nu} N}\right] = d_v(x) + u_v(x) \quad (139)$$

measures only the valence quark distribution.

Because $\bar{F}_3^{cc}$ measures the distribution of valence quarks, clearly its integral gives the total number of valence quarks in a nucleon and so one expects

$$\int_0^1 dx\ \bar{F}_3^{cc}(x) = \int_0^1 dx\ \left(d_v(x) + u_v(x)\right) = 3 \quad (140)$$

This result is the Gross-Llewellyn Smith sum rule /19/. The value of $\int_0^1 dx\ \bar{F}_3^{cc}(x)$, computed from older BEBC-Gargamelle data and from more recent CCFRR data, is plotted as a function of $q^2$ in Fig. 13

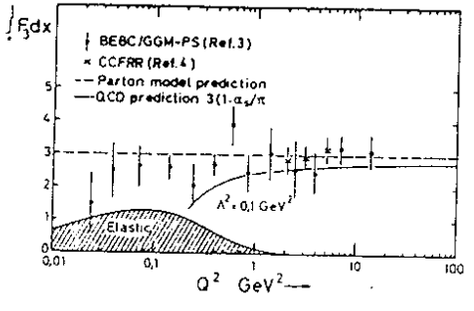


Fig. 13: Experimental status of the Gross-Llewellyn Smith sum rule. From Ref. 20



For large $q^2$ the sum rule appears to be reasonably well satisfied experimentally. The deviation for low $q^2$ could be a QCD effect. In fact, one can show /21/ that the Gross Llewellyn Smith sum rule is not exact in QCD but gets modified, to $O(\alpha_s)$, to

$$\int_0^1 dx\ \bar{F}_3^{cc}(x;q^2) = 3\left[1 - \frac{\alpha_s(q^2)}{\pi}\right] \quad (141)$$

The data is too uncertain - and the $q^2$ range probably too low - to test quantitatively this modification. However, qualitatively the corrections go in the right direction, suppressing the integral for smaller values of $q^2$.

For scattering off isoscalar targets the $F_2$ structure functions for neutrino and antineutrino scattering are the same. One finds, again for 4 flavors,

$$\left(F_2^{cc}(x)\right)_{\nu N} = \left(F_2^{cc}(x)\right)_{\bar{\nu} N} = x\left\{\left(d(x) + u(x) + s(x) + c(x)\right) + \left(\bar{d}(x) + \bar{u}(x) + s(x) + c(x)\right)\right\} \quad (142)$$

Thus the difference in cross section between neutrino and antineutrino cc scattering off isoscalar targets gives immediately $\bar{F}_3^{cc}$. Using Eq. (134) one has

$$x\bar{F}_3^{cc}(x) = \frac{\left(\frac{d\sigma}{dx\,dy}\right)_{\nu N}^{cc} - \left(\frac{d\sigma}{dx\,dy}\right)_{\bar{\nu} N}^{cc}}{\frac{G^2 M E_\nu}{\pi}\left[1 - (1-y)^2\right]} = x\left(u_v(x) + d_v(x)\right) \quad (143)$$

which is a direct measure of the valence quark distribution in nucleons. By considering a slightly different difference in cross sections one may also extract experimentally the distribution of the sea quarks. Using Eq. (134) and the results (138) and (142) one can write the difference

$$\frac{\left(\frac{d\sigma}{dxdy}\right)^{cc}_{\bar{\nu}N} - (1-y)^2\left(\frac{d\sigma}{dxdy}\right)^{cc}_{\nu N}}{\left(\frac{G_F^2 M E_\nu}{\pi}\right)} = \Big[ x\,(\bar{d}(x)+\bar{u}(x)+2s(x)) + (1-y)^2 x\,(2c(x)-2s(x)) - (1-y)^4\,(\bar{d}(x)+\bar{u}(x)+2c(x))\Big]$$

(144)

For large y, $y \gtrsim 1/2$, this expression allows a good experimental determination of the sea quark distribution

$$\bar{q}(x) = x\,(\bar{d}(x)+\bar{u}(x)+2s(x)) \qquad (145)$$

A plot of this distribution from the CDHS experiment along with that of $xF_3$ and $F_2$, taken from Eisele's rapporteur talk in Paris /22/, is shown in Fig. 14

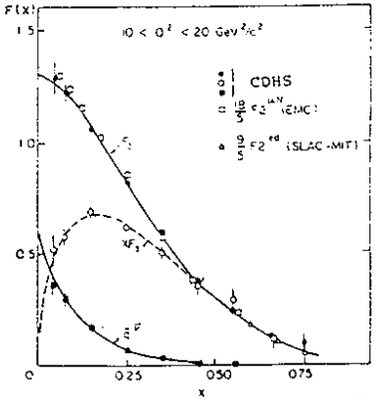


Fig. 14: $F_2$, $xF_3$ and $\bar{q}$ for fixed values of $q^2$. From Ref. 22

As can be seen the sea distribution is concentrated at small x.

A final comment is in order. The integral over $(F_2^{cc})_{\nu N}$ measures the momentum fraction of the charged constituents of the nucleon (quarks and antiquarks):



$$\int_0^1 dx\,(F_2^{cc}(x))_{\nu N} = \int_0^1 dx\,(F_2^{cc}(x))_{\bar{\nu}N} = \int_0^1 dx\; x\Big[(u(x)+d(x)+c(x)+s(x)) + (\bar{u}(x)+\bar{d}(x)+c(x)+s(x))\Big]$$

(146)

This integral, neglecting the small contribution of the strange and charm sea, is just given by

$$\int_0^1 dx\; F_2^{cc}(x) = \frac{3\pi}{4G_F^2 M}\left[\frac{\sigma^{cc}_{\nu N}+\sigma^{cc}_{\bar{\nu}N}}{E_\nu}\right] \simeq 0.44 \pm 0.02$$

(147)

The numerical result above follows from using for the average slope of the neutrino and antineutrino cross sections the value of Ref. 22

$$\frac{\sigma^{cc}_{\nu N}+\sigma^{cc}_{\bar{\nu}N}}{E_\nu} = (0.92 \pm 0.03)\times 10^{-38}\ \text{cm}^2/\text{GeV}$$

(148)

Eq. (147) implies that the gluons in the nucleon carry a substantial fraction of the constituent momentum ( $\sim$ 50 %). The direct influence of the gluonic component of the nucleon is not felt in the lowest order QCD calculations I discussed in this section. However, to $O(\alpha_s)$ one "sees" the gluon structure function and one can try to extract it from the data. Before discussing the subject of QCD corrections to deep inelastic scattering, however, I examine some further tests of the GSW model involving neutral current processes.

## SOME FURTHER TESTS OF THE GSW MODEL

In the previous section it was seen that deep inelastic neutral current scattering for neutrinos and antineutrinos gave the same value for $\sin^2\theta_W$. This is a first test of the validity of the GSW model in its fermion-gauge section. Deep inelastic charged lepton scattering, employing polarized leptons, provides further checks on the theory. In reality the process $\ell N \to \ell X$ has two contributions, as illustrated schematically in Fig. 15.


(1) (2)

Fig. 15: Electromagnetic (1) and weak (2) contributions to deep inelastic lepton scattering

In the previous section we neglected altogether the effects of the weak neutral current interactions, because for the total rate its contribution for moderate $q^2$ are small. One can easily estimate that

$$\frac{|\mathcal{M}_{weak}|^2}{|\mathcal{M}_{em}|^2} \sim \left(\frac{G_F q^2}{e^2}\right)^2 \sim 10^{-8}\left(\frac{q^2}{M^2}\right)^2 \qquad (149)$$

However, if one studies the interference between the weak and electromagnetic contributions the effects can be reasonable:

$$\frac{|T_{weak} \cdot T_{em}|}{|T_{em}|^2} \sim \frac{G_F q^2}{e^2} \sim 10^{-4}\,\frac{q^2}{M^2} \qquad (150)$$

Physically, the determination of such a weak-electromagnetic interference necessitates the measurement of some polarization asymmetry.

One can measure two types of asymmetries in polarized lepton deep inelastic scattering. Either one measures a cross section difference for scattering of leptons of different polarizations, but the same charge (A-asymmetry). Or one measures the difference in cross section between leptons and antileptons of a given polarization, or polarizations (B-asymmetry). Both effects are of order that estimated in Eq. (150). However, only the A-asymmetry is a purely parity violating effect. The A-asymmetry, defined by

$$A_{\ell^\pm;P_1,P_2} = \frac{d\sigma_{\ell^\pm;P_1} - d\sigma_{\ell^\pm;P_2}}{d\sigma_{\ell^\pm;P_1} + d\sigma_{\ell^\pm;P_2}} \qquad (151)$$

has been measured at SLAC by scattering polarized electrons on a Deuteron target. The B-asymmetry, defined by



$$B_{\ell;P_1,P_2} = \frac{d\sigma_{\ell^+;P_1} - d\sigma_{\ell^-;P_2}}{d\sigma_{\ell^+;P_1} + d\sigma_{\ell^-;P_2}} \qquad (152)$$

has been measured at CERN in deep inelastic scattering of polarized $\mu^+$ and $\mu^-$ on a Carbon target. I will now detail what one expects for these asymmetries in the GSW model, again neglecting possible QCD corrections.

Consider first the A-asymmetry, which involves the difference between right and left polarized electron deep inelastic scattering:

$$A \equiv A_{e^-;R,L} = \frac{d\sigma_{e^-;R} - d\sigma_{e^-;L}}{d\sigma_{e^-;R} + d\sigma_{e^-;L}} \qquad (153)$$

In a parton model to calculate A one must compute first the cross section for scattering $e_R$ and $e_L$ off quarks *. This is easily calculated from the T-matrix for e-q scattering, derived from the diagrams of Fig. 16 .

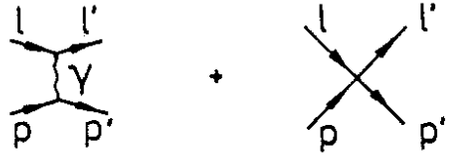


Fig. 16: e-q scattering, including weak NC effects

* In what follows I will compute in valence approximation and so will ignore antiquarks altogether.

$$T_{eq} = -\frac{4\pi\alpha e_q}{q^2}\,[\bar{u}(e')\gamma_\mu u(e)]\cdot[\bar{u}(q')\gamma^\mu u(q)]$$

$$+\frac{2G_F\rho}{\sqrt{2}}\,[\bar{u}(e')\gamma_\mu(Q^{NC}_{eR}(1+\gamma_5)+Q^{NC}_{eL}(1-\gamma_5))u(e)]$$

$$\cdot\,[\bar{u}(q')\gamma^\mu(Q^{NC}_{qR}(1+\gamma_5)+Q^{NC}_{qL}(1-\gamma_5))u(q)] \tag{154}$$

Here the charges $Q^{NC}_{fR}$, $Q^{NC}_{fL}$ are those of the GSW model

$$Q^{NC}_{fR} = -e_f \sin^2\theta_W \quad ; \quad Q^{NC}_{fL} = (\tau_3)_f - e_f \sin^2\theta_W \tag{155}$$

and the factor of 2 in the second line arises because there are two e-q interactions in the product of $J^\mu_{NC}\cdot J_\mu{}^{NC}$ of Fig. 16.

The calculation of the relevant cross sections is immediate once one decomposes also the electromagnetic contribution into right and left projections

$$\gamma^\mu = \tfrac{1}{2}\gamma^\mu(1+\gamma_5) + \tfrac{1}{2}\gamma^\mu(1-\gamma_5) \tag{156}$$

Then one has

$$T_{eq} = -\frac{\pi\alpha}{q^2}e_q\,[\bar{u}(e')(\gamma_\mu(1+\gamma_5)+\gamma_\mu(1-\gamma_5))u(e)]\cdot$$

$$\cdot\,[\bar{u}(q')(\gamma^\mu(1+\gamma_5)+\gamma^\mu(1-\gamma_5))u(q)]$$

$$+\sqrt{2}G_F\rho\,[\bar{u}(e')\gamma_\mu(Q^{NC}_{eR}(1+\gamma_5)+Q^{NC}_{eL}(1-\gamma_5))u(e)]$$

$$\cdot\,[\bar{u}(q')\gamma^\mu(Q^{NC}_{qR}(1+\gamma_5)+Q^{NC}_{qL}(1-\gamma_5))u(q)] \tag{157}$$

Recalling that (cf. Eqs. 115 and 116) $d\sigma_{LL} = d\sigma_{RR} \sim 1$, while $d\sigma_{LR} = d\sigma_{RL} \sim (1-y)^2$ it follows that



$$d\sigma_{e^-;R}(q_L) \sim \left|-\frac{\pi\alpha e_q}{q^2} + \sqrt{2}G_F\rho\,Q^{NC}_{eR}Q^{NC}_{qL}\right|^2(1-y)^2 \tag{158a}$$

$$d\sigma_{e^-;R}(q_R) \sim \left|-\frac{\pi\alpha e_q}{q^2} + \sqrt{2}G_F\rho\,Q^{NC}_{eR}Q^{NC}_{qR}\right|^2 \tag{158b}$$

$$d\sigma_{e^-;L}(q_L) \sim \left|-\frac{\pi\alpha e_q}{q^2} + \sqrt{2}G_F\rho\,Q^{NC}_{eL}Q^{NC}_{qL}\right|^2 \tag{158c}$$

$$d\sigma_{e^-;L}(q_R) \sim \left|-\frac{\pi\alpha e_q}{q^2} + \sqrt{2}G_F\rho\,Q^{NC}_{eL}Q^{NC}_{qR}\right|^2 (1-y)^2 \tag{158d}$$

The desired asymmetry A is just the sum of Eqs. (158a) and (158b) minus the sum of Eqs. (158c) and (158d), weighted by the appropriate parton distributions, all normalized by the sum of all four terms in Eqs. (158), weighted by the relevant parton distributions.

After a little algebra one finds, in the valence quark approximation we are working in and dropping terms of $O(G_F^2)$

$$A = \frac{q^2\left\{\sum_q e_q\,q(x)\left[a_{1q} + a_{2q}\frac{[1-(1-y)^2]}{[1+(1-y)^2]}\right]\right\}}{\left\{\sum_q e_q^2\,q(x)\right\}} \tag{159}$$

where

$$a_{1q} = -\frac{G_F\rho}{\sqrt{2}\pi\alpha}\,[Q^{NC}_{eR}-Q^{NC}_{eL}]\cdot[Q^{NC}_{qR}+Q^{NC}_{qL}] \tag{160a}$$

$$a_{2q} = -\frac{G_F\rho}{\sqrt{2}\pi\alpha}\,[Q^{NC}_{eR}+Q^{NC}_{eL}]\cdot[Q^{NC}_{qR}-Q^{NC}_{qL}] \tag{160b}$$

It is clear from the above that A is a purely parity violating asymmetry, since the coefficients $a_1$ and $a_2$ measure products of axial times vector couplings at the electron and quark vertices, respectively. For an isoscalar target like the Deuteron, employed in the SLAC experiments, one can easily check that the dependence on the structure functions in Eq. (159) cancels altogether. In this case the formula for the asymmetry reads, simply:

$$A = \left[ a_1 + a_2 \frac{(1-(1-y)^2)}{(1+(1-y)^2)} \right] q^2 \qquad (161)$$

where

$$a_1 = \frac{q}{5}\left[\frac{2}{3}a_{1u} - \frac{1}{3}a_{1d}\right] = -\frac{G_F \rho}{\sqrt{2}\pi\alpha}\left[\frac{q}{20} - \sin^2\theta_W\right] \qquad (162a)$$

$$a_2 = \frac{q}{5}\left[\frac{2}{3}a_{2u} - \frac{1}{3}a_{2d}\right] = -\frac{G_F \rho}{\sqrt{2}\pi\alpha}\left[\frac{q}{20} - \frac{q}{5}\sin^2\theta_W\right] \qquad (162b)$$

Note that $a_2$ vanishes for $\sin^2\theta_W = \frac{1}{4}$. Since as we have seen from our discussion of neutrino deep inelastic scattering $\sin^2\theta_W \simeq 0.23$, it is clear that little y-dependence is to be expected for the A-symmetry.

The results of the SLAC-YALE experiment /23/ on the A-symmetry are shown in Fig. 17

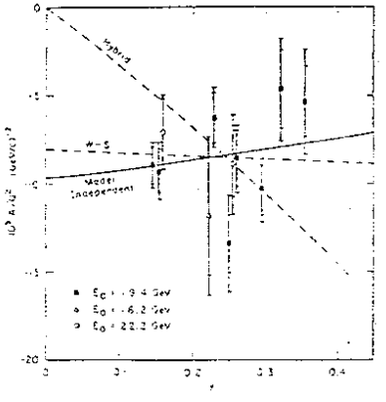


Fig. 17: Results of Ref. 23 on the A asymmetry in polarized eD deep inelastic scattering



The parameters $a_1$ and $a_2$ determined from the experiment are

$$a_1 = (-9.7 \pm 2.6) \times 10^{-5}\ \text{GeV}^{-2}$$

$$a_2 = (4.9 \pm 8.1) \times 10^{-5}\ \text{GeV}^{-2} \qquad (163)$$

A clear parity violation is seen and the y dependence of the data, within the large errors, is minimal as expected if $\sin^2\theta_W$ is near 1/4. Setting $\rho = 1$ this experiment yields a value for $\sin^2\theta_W$:

$$\sin^2\theta_W = 0.22 \pm 0.012 \pm 0.008 \qquad (164)$$

where the last error above is systematic. The agreement of this value with that obtained from deep inelastic neutrino scattering provides a further check on the GSW model. Note that this is a nontrivial check since different neutral current vertices are measured in the two different experiments.

Let me now discuss, with a little less detail, the B-asymmetry. The particular asymmetry measured in the CERN experiment on polarized $\mu$ -Carbon deep inelastic scattering /24/ is:

$$B \equiv B_{\mu;R,L} = \frac{d\sigma_{\mu^+;R} - d\sigma_{\mu^-;L}}{d\sigma_{\mu^+;R} + d\sigma_{\mu^-;L}} \qquad (165)$$

In a parton model and in the valence approximation therefore B is given by

$$B = \frac{\sum_q q(x)\left[d\sigma_{\mu^+;R}(q) - d\sigma_{\mu^-;L}(q)\right]}{\sum_q q(x)\left[d\sigma_{\mu^+;R}(q) + d\sigma_{\mu^-;L}(q)\right]} \qquad (166)$$

I computed already before the lepton-quark scattering cross sections (c.f. Eqs. (158))

$$d\sigma_{e^-;L}(q) = d\sigma_{e^-;L}(q_L) + d\sigma_{e^-;L}(q_R) \qquad (167a)$$

$$d\sigma_{e^-;R}(q) = d\sigma_{e^-;R}(q_L) + d\sigma_{e^-;R}(q_R) \qquad (167b)$$

and have remarked that the first terms in Eqs. (167) are proportional to 1 while the last terms in these equations are proportional to $(1-y)^2$. It is easy to convince oneself that the cross section $d\sigma_{\mu^+;R}(q)$ needed in Eq. (166) can be obtained from Eq. (167a) by the substitution

$$d\sigma_{e^+;R}(q) \longleftrightarrow d\sigma_{e^-;L}(q)$$
$$1 \longleftrightarrow (1-y)^2 \tag{168}$$

One now has all the elements for computing $B$ and I just quote the result:

$$B = \frac{q^2 \left\{ \sum_q e_q\, q(x)\, b_q \right\} \left( 1 - (1-y)^2 \right)}{\left\{ \sum_q e_q^2\, q(x) \right\} \left( 1 + (1-y)^2 \right)} \tag{169}$$

with

$$b_q = -\frac{\sqrt{2}\, G_F\, \rho}{\pi \alpha}\, Q_{eL}^{NC} \left( Q_{qR}^{NC} - Q_{qL}^{NC} \right) \tag{170}$$

Here again only terms of $O(G_F)$ are retained.

A few comments are in order on this result. First, it is clear from Eq. (170) that the asymmetry is no longer a purely parity violating effect. In fact writing

$$Q_{eL}^{NC} = \tfrac{1}{2}\left[ Q_{eL}^{NC} - Q_{eR}^{NC} \right] + \tfrac{1}{2}\left[ Q_{eL}^{NC} + Q_{eR}^{NC} \right] \tag{171}$$

one sees that the asymmetry is almost purely a parity conserving effect since $Q_{eL}^{NC} + Q_{eR}^{NC} \simeq 0$ for $\sin^2\theta_W \simeq \frac{1}{4}$. This means that in comparing experimental results with the above formula, one should also subtract away some purely $O(\alpha^1)$ electromagnetic contributions to the asymmetry, before one tries to extract a value for $\sin^2\theta_W$. For the CERN experiment this has been done. Furthermore, since this experiment is done on Carbon, which is an isoscalar target, one can further simplify Eq. (168) and all structure function dependence drops out. A simple calculation gives

$$B = b\, q^2 \left[ \frac{1 - (1-y)^2}{1 + (1-y)^2} \right] \tag{172}$$



with

$$b = \frac{9}{5}\left( \frac{2}{3} b_U - \frac{1}{3} b_d \right) = -\frac{\sqrt{2} G_F \rho}{\pi \alpha}\left( \tfrac{1}{2} - \tfrac{2}{3}\sin^2\theta_W \right)\left( \tfrac{1}{2} - \tfrac{4}{3}\sin^2\theta_W \right) \tag{173}$$

Numerically for $\sin^2\theta_W = 0.23$, $\rho = 1$ the coefficient b is

$$b = -1.51 \times 10^{-4}\ \text{GeV}^{-2} \tag{174}$$

The measured B asymmetry in the CERN experiment /24/, after radiative corrections have been subtracted, for runs at 120 GeV and 200 GeV are shown in Fig. 18

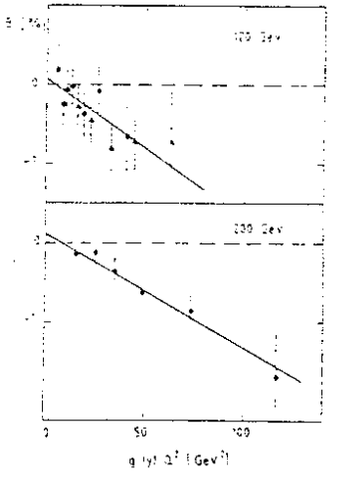


Fig. 18: $q^2$ dependence of the B asymmetry, with the kinematical factor $[1-(1-y)^2] / [1+(1-y)^2]$ removed, from ref. 24

The two slopes obtained

$$b(120\ \text{GeV}) = (-1.76 \pm 0.75) \times 10^{-4}\ \text{GeV}^{-2} \tag{175a}$$

$$b(200\text{GeV}) = (-1.47 \pm 0.37) \times 10^{-4}\ \text{GeV}^{-2} \tag{175b}$$

are in excellent agreement with the predictions of the GSW model, Eq.(174).

I would like to conclude this section with two further tests of the GSW model which involve purely leptonic process: $\nu_\ell e$ scattering and the measurement of forward-backward asymmetries in $e^+e^- \to \ell^+\ell^-$, with $\ell = \mu, \tau$. These processes need no parton model assumptions. However, the neutrino scattering experiments have somewhat limited statistics and the forward-backward asymmetry, although testing the GSW model, does not lead to a determination of $\sin^2\theta_W$. Nevertheless, these processes complement very nicely our discussion of deep inelastic scattering.

The reactions $\nu_\ell e \to \nu_\ell e$ and $\bar{\nu}_\ell e \to \bar{\nu}_\ell e$ are purely due to the weak neutral current, as shown in Fig. 19.

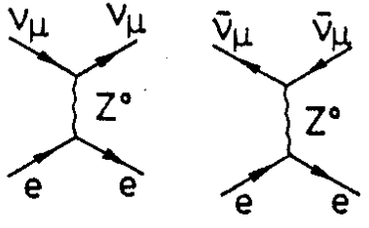


Fig. 19: $\nu_\ell e$ and $\bar{\nu}_\ell e$ reactions due to $Z^0$ exchange.

We have calculated analogous cross sections for neutrino nucleon deep inelastic scattering at the parton level ( $\nu_\ell q \to \nu_\ell q$ ; $\bar{\nu}_\ell q \to \bar{\nu}_\ell q$ ). To obtain the cross sections for the processes of Fig. 19 all we need to do is replace in the parton cross sections $Q^{NC}_{qL} \to Q^{\nu e}_{eL}$ ; $Q^{NC}_{qR} \to Q^{NC}_{eR}$. In this way one finds

$$\left(\frac{d\sigma}{dy}\right)^{\nu_\ell e} = \frac{2G_F^2 m E_\nu \rho^2}{\pi}\left[(Q^{NC}_{eL})^2 + (Q^{NC}_{eR})^2(1-y)^2\right] \tag{176a}$$

$$\left(\frac{d\sigma}{dy}\right)^{\bar{\nu}_\ell e} = \frac{2G_F^2 m E_\nu \rho^2}{\pi}\left[(Q^{NC}_{eR})^2 + (Q^{NC}_{eL})^2(1-y)^2\right] \tag{176b}$$

where, recall,

$$Q^{NC}_{eR} = \sin^2\theta_W \quad ; \quad Q^{NC}_{eL} = -\tfrac{1}{2} + \sin^2\theta_W \tag{177}$$



One should note that these cross sections are tiny, since here, in contrast to the scattering off nucleons, the electron mass $m$ appears. Typically one expects cross sections of the order of $10^{-42}\, E_\nu(\text{GeV})\ \text{cm}^2$ For high energy neutrino scattering ($E_\nu \approx 100$ GeV) the cross sections are thus around $10^{-40}\ \text{cm}^2$. For reactor experiments (where actually $\bar{\nu}_e$ are scattered) with $E_\nu$ of order of MeV the cross sections are vanishingly small ( $\sim 10^{-45}\ \text{cm}^2$) and signals can only be detected because of the very intense neutrino fluxes.

The CHARM collaboration at CERN has measured both* $\bar{\nu}_\ell e$ and $\nu_\ell e$ scattering /25/ at high energy with "high" statistics. Because both processes were observed their ratio can be determined, which gets rid of the unknown $\rho$ parameter. Furthermore, in this way also various systematic errors can be eliminated. Integrating Eqs. (176) over y and taking their ratio, one predicts for the standard model

$$R = \frac{\sigma_{\nu_\ell e}}{\sigma_{\bar{\nu}_\ell e}} = \frac{3 - 12\sin^2\theta_W + 16\sin^4\theta_W}{1 - 4\sin^2\theta_W + 16\sin^4\theta_W} \tag{178}$$

which is a pure function of the Weinberg angle. The CHARM collaboration finds /25/

$$R = 1.37 \,^{+\,0.65}_{-\,0.44} \tag{179}$$

which implies a value for $\sin^2\theta_W$,

$$\sin^2\theta_W = 0.215 \pm 0.032 \pm 0.012, \tag{180}$$

which is in very good agreement with that determined in deep inelastic scattering. I should remark that, even though the errors in R are large, because the function in Eq. (178) is rapidly changing near $\sin^2\theta_W \simeq 1/4$ the errors for $\sin^2\theta_W$ are rather small. This is shown graphically in Fig. 20.

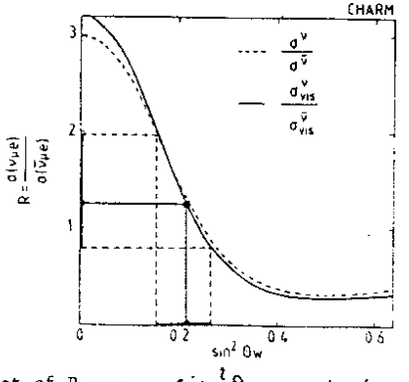


Fig. 20: Plot of R versus $\sin^2\theta_W$, showing the range measured by the CHARM experiment.

* "High" statistics in the field means of the order of 100 events!

The CHARM collaboration gives also values for the slope of the cross section rise with energy, for both $\nu_\mu$ and $\bar{\nu}_\mu$ scattering /25/:

$$\sigma(\nu_\mu e)/E_\nu = (1.9 \pm 0.4 \pm 0.4) \times 10^{-42}\ \mathrm{cm}^2/\mathrm{GeV}$$

$$\sigma(\bar{\nu}_\mu e)/E_\nu = (1.5 \pm 0.3 \pm 0.4) \times 10^{-42}\ \mathrm{cm}^2/\mathrm{GeV} \qquad (181)$$

From these numbers one can extract a value for the $\rho$ parameter, and they find:

$$\rho = 1.09 \pm 0.09 \pm 0.11 \qquad (182)$$

This value agrees within errors with the prediction of the standard model, with doublet Higgs breaking, $\rho = 1$. Very recently the CHARM results have been corroborated by a Brookhaven experiment /26/. They find

$$\sigma(\nu_\mu e)/E_\nu = (1.60 \pm 0.29 \pm 0.26) \times 10^{-42}\ \mathrm{cm}^2/\mathrm{GeV}$$

$$\sigma(\bar{\nu}_\mu e)/E_\nu = (1.16 \pm 0.20 \pm 0.16) \times 10^{-42}\ \mathrm{cm}^2/\mathrm{GeV} \qquad (183)$$

The last test of NC phenomena which I want to discuss concerns the process $e^+e^- \to \ell^+\ell^-$. As shown in Fig. 21, besides the usual electromagnetic contribution one expects also a $Z^0$ contribution. For the values of $s = -q^2 = -(e+\bar{e})^2$ relevant to PETRA and PEP

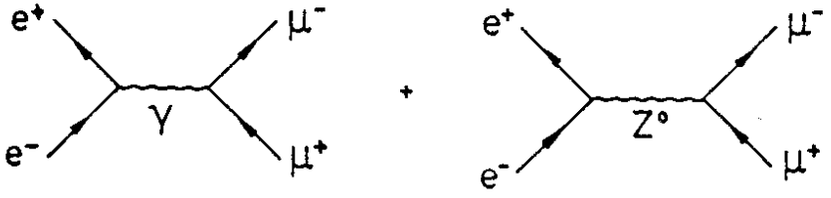


Fig. 21: Electroweak contributions to $e^+e^- \to \ell^+\ell^-$

it is still reasonable to approximate the second term in Fig. 21 by its current x current form. Hence, the relevant T-matrix for the process



can be written as

$$T = i\left\{ \frac{e^2}{q^2}\left[\bar{u}(p)\gamma^\mu v(\bar{p})\right]\cdot\left[\bar{v}(\bar{e})\gamma_\mu u(e)\right] + \frac{2G_F}{\sqrt{2}}\rho\left[\bar{u}(p)\left(\gamma^\mu g_{ev} + \gamma^\mu\gamma_5 g_{eA}\right)v(\bar{p})\right]\cdot \left[\bar{v}(\bar{e})\left(\gamma_\mu g_{ev} + \gamma_\mu\gamma_5 g_{eA}\right)u(e)\right] \right. \qquad (184)$$

where the vector and axial leptonic coupling constants $g_{ev}$ and $g_{eA}$ are given by

$$g_{ev} = 2\sin^2\theta_W - \tfrac{1}{2} \quad ; \quad g_{eA} = \tfrac{1}{2} \qquad (185)$$

with $g_{ev} \ll g_{eA}$ for $\sin^2\theta_W = 0.23$. Since one is interested in the corrections only to $O(G_F)$ due to the weak neutral current one can write the spin averaged T-matrix as

$$\langle|T|^2\rangle \simeq \langle|T_{em}|^2\rangle + \langle T_{em}\cdot T^*_{weak} + T^*_{em}\cdot T_{weak}\rangle \qquad (186)$$

It is not difficult to convince oneself that in the interference contributions only terms proportional to $g_{ev}^2$ or $g_{eA}^2$, but not terms proportional to $g_{ev}\,g_{eA}$, appear. Furthermore the term proportional to $g_{ev}^2$ gives only a correction to the total rate and is numerically small *. Hence I shall neglect it altogether. Focussing on the $g_{eA}^2$ term only, it is easy to see that its contribution is

$$\langle|T|^2\rangle\Big|_{g_{eA}^2} = \frac{e^2}{q^2}\frac{G_F}{\sqrt{2}}\rho\, g_{eA}^2\, \mathrm{Tr}\,\gamma^\mu\gamma_5\, r\cdot\ell\,\gamma^\nu\gamma\cdot\bar{e}\cdot\mathrm{Tr}\,\gamma_\mu\gamma_5\,\bar{r}\cdot\bar{p}\,\gamma_\nu\gamma\cdot p$$

$$= -\frac{4\sqrt{2}\,e^2G_F\rho}{s}\left((\ell\cdot\bar{p})(\bar{e}\cdot p) - (\ell\cdot p)(\bar{e}\cdot\bar{p})\right)$$

$$= -\sqrt{2}\,e^2G_F\rho\cos\theta \qquad (187)$$

* It is for this reason that these asymmetries at PETRA/PEP energies do not provide very useful information on $\sin^2\theta_W$.

where the last line applies in the $e^+e^-$ CM-system and $\theta$ is the angle of the outgoing lepton with respect to the electron's direction.

From the above one sees that the effect of the weak neutral current is to produce a term linear in $\cos\theta$ in the angular distribution. Since the, lowest order, electromagnetic distribution is symmetric in $\cos\theta$, it is clear that the interference term can be selected by measuring the forward-backward asymmetry:

$$A_{F-B} = \frac{\int_0^1 d\cos\theta \left(\frac{d\sigma}{d\cos\theta}\right) - \int_{-1}^0 d\cos\theta \left(\frac{d\sigma}{d\cos\theta}\right)}{\sigma(e^+e^- \to \ell^+\ell^-)} \qquad (188)$$

Using that

$$\frac{d\sigma}{d\cos\theta} = \frac{1}{32\pi s} \langle |T|^2 \rangle \qquad (189)$$

and the standard result

$$\sigma(e^+e^- \to \ell^+\ell^-) = \frac{4\pi\alpha^2}{3s} \qquad (190)$$

it is now immediate to obtain the coefficient $A_{F-B}$ predicted by the GSW model, for $\sqrt{s} << M_Z$

$$A_{F-B} = -\left[\frac{3 G_F \rho}{16\pi\sqrt{2}\,\alpha}\right] s \qquad (191)$$

I end this section with a few remarks on Eq. (191):

(1) The coefficient of s in the above equation is of order $7 \times 10^{-5}$ GeV$^{-2}$. Hence at the upper ranges of PEP and of PETRA ($s \sim 10^3$ GeV$^2$) the asymmetry should be a sizable effect.

2) Because $A_{F-B}$ is not a parity violating effect - recall it was proportional to $g_{eA}^2$ - before comparing Eq. (191) with experiment one must subtract purely electromagnetic $O(\alpha^3)$ corrections to the asymmetry.

(3) At the highest PETRA energies the $Z^0$ propagator begins to be felt. Including the propagator corresponds to the change



$$s \to \frac{s M_Z^2}{M_Z^2 - s} \qquad (192)$$

in Eq. (191), which increases the asymmetry.

(4) The asymmetry is clearly seen in the data of $e^+e^- \to \mu^+\mu^-$ shown in Fig. 22. This figure is taken from Naroska's talk /27/ at the 1983 Cornell conference. Essentially the same result /2/ obtains for $e^+e^- \to \tau^+\tau^-$, but the errors are naturally somewhat bigger.

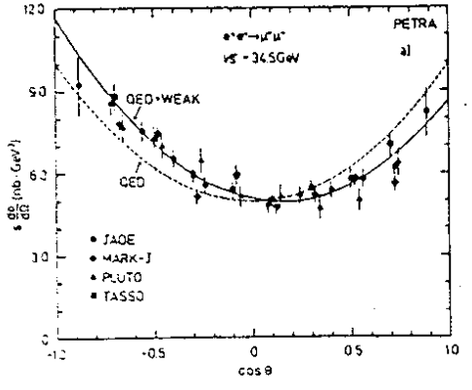


Fig. 22: $A_{F-B}$ in $e^+e^- \to \mu^+\mu^-$ corrected for QED effects to $O(\alpha^3)$. From Ref. 27.

(5) There is good agreement of experiment with the GSW prediction. For the data at PETRA, taken at an average energy of $\sqrt{s}$ = 34.5 GeV the results are /27/:

$$(A_{F-B})_{\mu^+\mu^-} = -10.8 \pm 1.1\ \%$$
$$(A_{F-B})_{\tau^+\tau^-} = -7.6 \pm 1.9\ \% \qquad (193a)$$

to be compared with the GSW prediction of - 9.4 %. Data taken at the highest PETRA energies is beginning to show the effect of the substitution (192) although, because of lower statistics, the errors are somewhat bigger. The average value of the $\mu^+\mu^-$ asymmetry for all four experiments at $\sqrt{s}$ = 41.6 GeV is /28/

$$(A_{F-B})_{\mu^+\mu^-} = -14.7 \pm 3.1\ \% \qquad (193b)$$

while the expected asymmetry with (without) the substitution of Eq. (192) is 14.5 % (11.7 %).

## W AND Z PRODUCTION: REFINED GSW TESTS AND BASIC QCD TEST

The most far reaching prediction of the GSW model, when it was proposed as a model of the weak interactions, was that these interactions are mediated by heavy vector bosons. Furthermore, given a measurement of $\sin^2\theta_W$ and of $\rho$, the masses of these bosons are predicted (cf Eqs. (55) and (56)). The observation at the CERN collider of both W /29/ and Z /30/ bosons, with masses in the predicted range, is thus a significant triumph of the model. I would like in this section to discuss these results first as a QCD test and then as a more refined test of the GSW model.

In lowest order QCD (parton model) one can compute the production of the W and Z bosons in pp annihilation from the diagram schematically shown in Fig. 23.

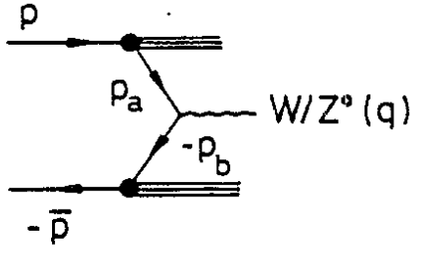


Fig. 23: Parton model diagram for W and Z boson production in $p\bar{p}$ annihilation

Essentially the same diagram applies, with trivial changes, for the Drell-Yan process $pp \to \mu^+\mu^- X$. If one writes

$$p_a = \xi_a P \quad ; \quad p_b = \xi_b \bar{P} \tag{194}$$

kinematics fixes the product of the parton momentum fractions to be:

$$\xi_a \xi_b = \frac{M_V^2}{s} \tag{195}$$

The parton model production cross section for W or Z then is simply



$$\sigma(p\bar{p} \to W/Z\, X) = \sum_{a,b} \int d\xi_a\, d\xi_b\; f_{q_a}(\xi_a)\, f_{q_b}(\xi_b) \cdot \frac{1}{3}\, \sigma_{\text{Parton}}(q_a q_b \to W/Z) \tag{196}$$

The factor of $\frac{1}{3}$ above appears since for the quarks $q_a$, $q_b$ to be able to annihilate into a W or a Z they must have the same color.

I shall compute Eq. (196) in valence approximation. For $W^-$ production, for instance, this means that

$$f_{q_a}(\xi_a) = d_v(\xi_a) \quad ; \quad f_{q_b}(\xi_b) = u_v(\xi_b) \tag{197}$$

That is the $W^-$ is produced by annihilation of the valence d quark in the proton with the valence $\bar{u}$ quark in the antiproton (whose distribution is the same as that of the valence u quark in the proton). The elementary cross section $d + \bar{u} \to W^-$ is readily computed from Eq. (50), taking into account of Cabibbo mixing. The T-matrix is given by:

$$T = \frac{i e \cos\theta_c}{2\sqrt{2}\sin\theta_W}\, \bar{v}(p_b)\, \gamma^\mu (1-\gamma_5)\, u(p_a)\, \epsilon_\mu(q;\lambda) \tag{198}$$

where $\epsilon_\mu(q;\lambda)$ is the W-polarization tensor. Using that

$$\sum_\lambda \epsilon_\mu(q;\lambda)\, \epsilon_\nu(q;\lambda) = \eta_{\mu\nu} + \frac{q_\mu q_\nu}{M_W^2} \tag{199}$$

a simple calculation gives

$$\langle |T|^2 \rangle = \frac{1}{4} \sum_{s_a} \sum_{s_b} |T|^2 = \sqrt{2}\, G_F\, M_W^4 \cos^2\theta_c \tag{200}$$

The elementary cross section then follows from the standard formula

$$\sigma_{\text{Parton}}(d + \bar{u} \to W^-) = \frac{1}{(-4\, p_a \cdot p_b)} \int \frac{d^3q}{(2\pi)^3 2q^0} (2\pi)^4 \delta^4(q - p_a - p_b)\, \langle |T|^2 \rangle \tag{201}$$

which gives

$$\sigma_{\text{parton}}(d+\bar{u}\to W^-) = \sqrt{2}\,\pi\, G_F M_W^2 \cos^2\theta_c\, \delta(\xi_a\xi_b s - M_W^2) \tag{202}$$

Using Eq. (196), finally, this gives for the $W^-$ production cross section

$$\sigma(p\bar{p}\to W^- X) = \frac{\sqrt{2}\pi}{3} G_F \cos^2\theta_c \left(\frac{M_W^2}{s}\right) \int_{\frac{M_W^2}{s}}^1 \frac{d\xi}{\xi}\, d_V(\xi)\, U_V\left(\frac{M_W^2}{3}/s\right) \tag{203}$$

By charge symmetry exactly the same formula follows for $W^+$ production. For $Z^0$ production a simple calculation gives

$$\sigma(p\bar{p}\to Z^0 X) = \frac{\sqrt{2}\pi}{3} G_F \cos^2\theta_c \left(\frac{M_Z^2}{s}\right) \int_{\frac{M_Z^2}{s}}^1 \frac{d\xi}{\xi}\, \mathcal{L}^0(\xi; M_Z^2/s) \tag{204}$$

where the luminosity function $\mathcal{L}^0$ is given by

$$\mathcal{L}^0(\xi; M_Z^2/s) = \left[\tfrac{1}{4} - \tfrac{2}{3}\sin^2\theta_W + \tfrac{8}{9}\sin^4\theta_W\right] U_V(\xi)\, d_V\left(\frac{M_Z^2/s}{3}\right)$$
$$+ \left[\tfrac{1}{4} - \tfrac{1}{3}\sin^2\theta_W + \tfrac{2}{9}\sin^4\theta_W\right] d_V(\xi)\, U_V\left(\frac{M_Z^2/s}{3}\right) \tag{205}$$

The above formulas predict the cross section for W and Z production at the collider, directly from a knowledge of the valence quark distribution functions obtained in deep inelastic scattering. In Fig. 24 I display some curves, obtained some time ago by Paige /31/, which illustrate the expected range of W and Z production at colliders. These cross sections include possible scale breaking effects typical of QCD,



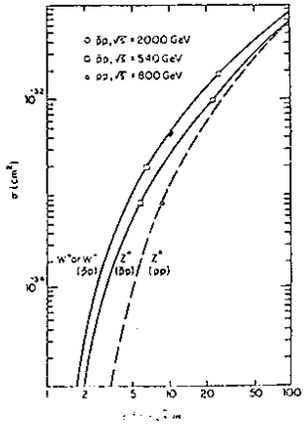


Fig. 24: Production cross sections for W and Z, from Ref. 31

in which the structure functions "evolve" with $q^2$, but do not include effects of the, so called, K-factor. I will, in the next section, discuss these matters in more detail. Here I comment only that the curves in Fig. 25 probably underestimate the cross section by a factor of 1.5 - 2.

From Fig. 24 one sees that for the CERN collider ($\sqrt{s}$ = 540 GeV) one expects

$$\sigma(W^+) + \sigma(W^-) \approx 4 \text{ nb} \tag{206}$$

Experimentally the UA1 and UA2 collaborations have observed the W's decaying in the $e\nu$ mode and UA1 has also seen the $\mu\nu$ decay mode. For the cross section times branching ratio the collaborations give the values, /32/ /33/

$$\begin{aligned}
(\sigma\cdot B)_{e\nu}\ (\text{UA2}) &= 0.53 \pm 0.10 \pm 0.10 \text{ nb} \\
(\sigma\cdot B)_{e\nu}\ (\text{UA1}) &= 0.53 \pm 0.008 \pm 0.09 \text{nb} \\
(\sigma\cdot B)_{\mu\nu}\ (\text{UA1}) &= 0.67 \pm 0.17 \pm 0.15 \text{ nb}
\end{aligned} \tag{207}$$

The width for W's to decay into $\ell\nu$ is easily calculated

$$\Gamma(W\to \ell\nu) = \frac{G_F M_W^3}{6\sqrt{2}\,\pi} \tag{208}$$

This number can readily be seen to correspond to about 8 % of the total expected width. Thus, using Eq. (206), one would expect

$$(\sigma \cdot B)^{Th}_{ev} \simeq 0.32 \text{ nb} \tag{209}$$

This number is a little low, but as I have indicated above, the estimate (206) probably underestimates the W production cross section. At any rate, it is still remarkable that information from deep inelastic scattering can, via QCD, predict the production of heavy weak bosons in pp annihilation to within a factor of 2. This, if nothing else, attest to the validity of the perturbative QCD approach.

Although W/Z production gives a nice test of perturbative QCD, of course their discovery is of fundamental importance for the GSW model for it allows a precise test of their properties. Eq. (55) relates the Fermi constant to the W-mass and the Weinberg angle. It predicts for the W mass

$$M_W = \left[ \frac{\pi \alpha}{\sqrt{2} G_F \sin^2\theta_W} \right]^{1/2} = \frac{37.28}{\sin\theta_W} \text{ GeV} \tag{210}$$

Using $\sin^2\theta_W = 0.23$ this gives for $M_W$:

$$M_W = 77.8 \text{ GeV} \tag{211a}$$

From the fact that $\rho \simeq 1$, the Z mass also follows

$$M_Z = \frac{M_W}{\cos\theta_W} = 88.7 \text{ GeV} \tag{211b}$$

These values for $M_W$ and $M_Z$ are somewhat below the average values obtained by the UA1 and UA2 collaborations /34/:

$$M_W = 82.1 \pm 1.7 \text{ GeV}$$
$$M_Z = 93.0 \pm 1.8 \text{ GeV} \tag{212}$$

This circumstance is actually expected since the values obtained in Eqs. (211) are computed without taking into account of radiative corrections. As I will show below, including radiative effects brings the theoretical and experimental values of the weak boson masses in complete quantitative agreement.

In lowest order the Weinberg angle was defined (cf Eq. (49)) in terms of the ratio of two coupling constants:

$$\sin\theta_W = \frac{e}{g} \tag{213}$$

However, radiative effects produce infinite corrections to the above formula, which must be removed by renormalization. After renormalization one is left with a $(\sin^2\theta_W)_{ren}$ which is perfectly finite and related to some physically measured parameters. In fact, one can define a variety of such $(\sin^2\theta_W)_{ren}$, all connected to one another by finite power series in $\alpha$. Of course, also cross sections get modified to higher order and they contain various infinities that must be renormalized. The removal of these infinities must be done consistently and the radiative corrected formulas will differ depending on which way one has chosen to define certain parameters, including $(\sin^2\theta_W)_{ren}$.

The above is best illustrated by a concrete example. Consider again the ratio R of the $\nu_\mu e$ and $\bar{\nu}_\mu e$ cross sections. According to the lowest order calculation of the last section one had:

$$R = \frac{\sigma(\nu_\mu e)}{\sigma(\bar{\nu}_\mu e)} = \frac{3 - 12\sin^2\theta_W + 16\sin^4\theta_W}{1 - 4\sin^2\theta_W + 16\sin^4\theta_W} \tag{214}$$

which is a pure function of the (lowest order) Weinberg angle. Radiative corrections, an example of which is shown in Fig. 25, will modify our expectation for R. However, one expects that R will again be expressible in terms of a renormalized Weinberg angle by a formula analogous to Eq. (214), with coefficients that differ from those of Eq. (214) by $O(\alpha)$.



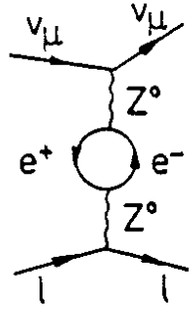


Fig. 25: A radiative contribution to $\nu_\mu e$ scattering

Including radiative corrections (to $O(\alpha)$) one has

$$R = \frac{(3+q_i\alpha) - (12+b_i\alpha)(\sin^2\theta_W)^i_{Ren} + (16+c_i\alpha)(\sin^2\theta_W)^i_{Ren}}{(1+d_i\alpha) - (4+e_i\alpha)(\sin^2\theta_W)^i_{Ren} + (16+f_i\alpha)(\sin^2\theta_W)^i_{Ren}} \quad (215)$$

The various coefficients $a_i, b_i, \ldots, f_i$ above are calculable but their precise value depends on which definition for $(\sin^2\theta_W)^i_{Ren}$ one has chosen. In particular, one could define $(\sin^2\theta_W)^i_{Ren}$ by demanding that all the coefficients $a_i, \ldots, f_i$ vanish. However, such a definition is not particularly convenient if one wants to study what radiative shifts the theory predicts for the W and Z masses.

The most convenient choice for $(\sin^2\theta_W)_{Ren}$ is to define this parameter via the physical W and Z masses, by the relation

$$(\sin^2\theta_W)_{Ren} \equiv 1 - \frac{M_W^2}{M_Z^2} \quad (216)$$

Radiative corrections to neutrino neutral current deep inelastic scattering and polarized electron-deuteron scattering have been computed /35/ /36/ using this renormalization prescription and a value for $(\sin^2\theta_W)_{Ren}$ has been extracted. Before including radiative corrections the "best fit" value of Kim et al. /16/ for the combined NC neutrino data and the polarized e D data was (assuming $\rho = 1$)

$$\sin^2\theta_W = 0.229 \pm 0.009 \quad (217)$$

After including radiative corrections, these experiments imply for $(\sin^2\theta)_{Ren}$ of Eq. (216)

$$(\sin^2\theta_W)_{Ren} = 0.217 \pm 0.014 \quad (218)$$

Note that the effect of radiative corrections is not small, for this definition of $(\sin^2\theta_W)_{Ren}$, causing about a 6 % decrease in $\sin^2\theta_W$.

The formula for $M_W$ which we previously used, Eq. (210), also gets modified by radiative corrections using the same definition of $(\sin^2\theta_W)$ one has /37/



$$M_W = \left[\frac{\pi\alpha}{\sqrt{2}\, G_\mu\, (\sin^2\theta_W)_{Ren}\, [1-\Delta r]}\right]^{1/2} \quad (219)$$

Here $G_\mu = (1.16637 \pm 0.00002) \times 10^{-5}$ GeV$^{-2}$ is the Fermi constant extracted from radiatively corrected $\mu$-decay /38/ and $\Delta r$ is a further radiative correction which can be computed /37/. Indeed, and this is what makes using the definition of $(\sin^2\theta_W)_{Ren}$ of (216) particularly useful, the correction $\Delta r$ is essentially absorbed if one changes $\alpha$ in Eq. (219) to the running coupling constant evaluated at $M_W^2$; $\alpha(M_W^2)$. Marciano /37/ gives

$$(\Delta r)_{theory} = 0.0696 \pm 0.0020 \quad (220)$$

The change of $\alpha$ to $\alpha(M_W)$, on the other hand, already is equivalent to a 7.3 % change, so this is clearly the dominant effect.

Using Eqs. (220) and (218) in the formula (219) predicts for the W-mass, the radiatively corrected value

$$M_W = 83 \pm 2.5 \text{ GeV} \quad (221a)$$

The $Z^0$ radiatively corrected mass follows from

$$M_Z = \frac{M_W}{(\cos\theta_W)_{Ren}} = 93.8 \pm 2.5 \text{ GeV} \quad (221b)$$

These values are in excellent agreement with the UA1 and UA2 averages of Eq. (212) and constitute an impressive success for the GSW model. One can, conversely, use the value of the W mass (or of the Z mass) and Eqs. (219) and (220) to extract $(\sin^2\theta_W)_{Ren}$. One obtains in this way

$$(\sin^2\theta_W)_{Ren} = 0.221 \pm 0.007 \quad (222)$$

This value of the Weinberg angle, extracted from properties of the W boson determined by the UA1 and UA2 collaborations is in excellent agreement with that of Eq. (218), which comes from the "low energy" $\nu N$ and eD experiments.

PERTURBATIVE QCD-EVOLUTION EQUATIONS AND TESTS

Up to now I have discussed "hard scattering" processes only at the parton model level ($0^{th}$ order QCD). It is now time to discuss what corrections QCD gives to these parton model predictions. As I have mentioned earlier, QCD causes basically two different modifications:

(i) It makes the parton structure and fragmentation functions "run". That is, these functions now depend on $q^2$:

$$f_q(x) \rightarrow f_q(x;q^2)$$
$$D_q^H(z) \rightarrow D_q^H(z;q^2) \qquad (223)$$

(ii) It changes $d\sigma_{parton}$ in a well defined way, which can be computed in a power series in $\alpha_s(q^2)$:

$$d\sigma_{parton} \rightarrow d\sigma_{parton}\,[\,1 + c\,\alpha_s(q^2) + \ldots\,] \qquad (224)$$

with c a calculable coefficient.

The $q^2$-dependence of the structure and fragmentation functions is not calculable per se, since it arises from the "soft" processes by which hadrons get transmuted into partons and vice versa. However, one may compute the evolution in $q^2$ of these functions. Given, for instance, $f_q(x,q_o^2)$ one can compute $f_q(x,q^2)$ for $q^2 > q_o^2$. The evolution of the structure and fragmentation functions can be computed by means of the, so called, Altarelli-Parisi equations /39/. This evolution is somewhat analogous to what happens with the running coupling constant. Given $\alpha_s(q_o^2)$ and the $\beta$-function one can compute $\alpha_s(q^2)$.

To derive the Altarelli-Parisi equations it proves useful to examine deep inelastic scattering processes again, to understand the physical reason for the running of the parton structure functions. I want to focus in particular on the quark + $V^*$ scattering subprocess, shown in Fig. 26, where $V^* = \{\gamma, Z^0, W\}$ depending on what particular deep inelastic process one is considering

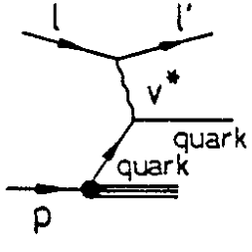


Fig. 26: Schematic depiction of a deep inelastic scattering process

The process $q + V^* \rightarrow q$ gets modified when one takes into account of QCD. There are both virtual modifications, which occur because quarks can emit and reabsorb gluons, and real modifications corresponding to the case when additional gluons are involved in the process. The relevant graphs for both contributions, to $O(\alpha_s)$, are shown in Fig. 27.



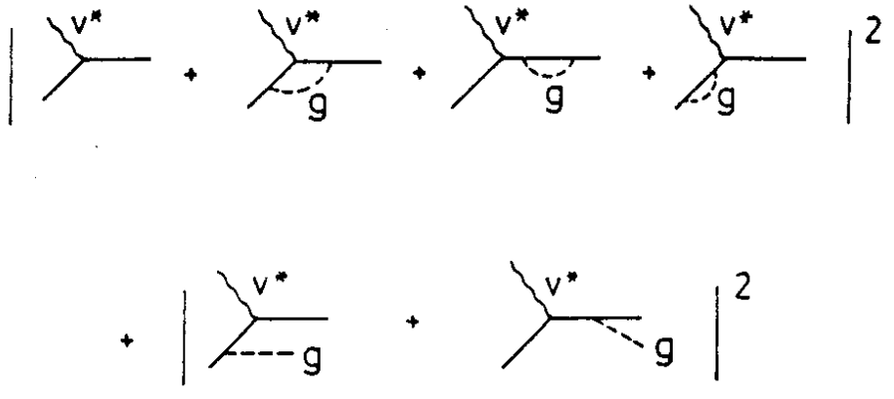


Fig. 27: Virtual and real QCD corrections to the process $q + V^* \rightarrow q$

Generically let me write the hadronic structure function corresponding to the unmodified process $q + V^* \rightarrow q$ as

$$F^o(x) = \int_x^1 \frac{d\xi}{\xi}\, f_q(\xi)\, \sigma^o_{parton}(x_p = \tfrac{x}{\xi})$$
$$= \int_x^1 \frac{d\xi}{\xi}\, f_q(\xi)\, \delta(\tfrac{x}{\xi} - 1) = f_q(x) \qquad (225)$$

To lowest order, the parton cross section is just a $\delta$-function, so that the hadronic structure function $F^o(x)$ is just the same as the quark distribution function, $f_q(x)$. If one takes into account of the QCD corrections of Fig. 27, the structure function $F^o(x)$ gets an additional $q^2$ dependent contribution. One can write the corrected structure function as

$$F(x;q^2) = \int_x^1 \frac{d\xi}{\xi}\, f_q(\xi)\,[\,\delta(\tfrac{x}{\xi} - 1) + \sigma^1_{parton}(\tfrac{x}{\xi};q^2)\,] \qquad (226)$$

As I will show below, Eq. (226) can be rewritten in terms of a running quark distribution function $f_q(x;q^2)$ plus a calculable correction of $O(\alpha_s(q^2))$:

$$F(x;q^2) = f_q(x;q^2) + O(\alpha_s(q^2)) \tag{227}$$

This separation, which may appear trivial at this stage, is important. Only by making the parton distribution functions run are the corrections in Eq. (227) controllable.

To understand this crucial point one needs to examine what are the sources of $q^2$-dependence in the parton cross section $\sigma^1_{parton}$. There are actually two distinct sources of $q^2$ dependence. The first is that the coupling constant $\alpha_s$ - associated with gluonic corrections - should really always be replaced by the running coupling constant $\alpha_s(q^2)$. This procedure sums up the large logarithms associated with the effective quark-gluon coupling and is what allows one to calculate perturbatively at large $q^2$, where $\alpha_s(q^2)$ is small. The second source of $q^2$ dependence in $\sigma_{parton}$ arises because the process $V + q \to q + g$ contains an explicit logarithmic dependence on $q^2$. This logarithmic dependence is a typical results of the hard gluon bremsstrahlung spectrum, which is cut off by $q^2$: $\int^{q^2} dk_\perp^2/k_\perp^2 \to \ln q^2$ *. Schematically, therefore one expects for $\sigma^1_{parton}$ the structure

$$\sigma^1_{parton}(x_p;q^2) = \frac{\alpha_s(q^2)}{2\pi}\left[P(x_p)\ln q^2 + R(x_p)\right] \tag{228}$$

where the functions $P(x_p)$ and $R(x_p)$ are calculable.

Eq. (228) shows that contrary to what one might have naively expected $\sigma^1_{parton}$ is not small for large $q^2$! Even though $\alpha_s(q^2)$ vanishes, as $(\ln q^2)^{-1}$, in this limit, the hard gluon $\ln q^2$ factor compensates entirely this behaviour. To make sense of the parton model calculations I discussed in the previous sections, it is necessary that a reasonable perturbative contribution should emerge from $\sigma^1_{parton}$. Such a contribution indeed ensues once one factorizes some of the $\ln q^2$ factors in (228) into the parton structure function $f_q(\xi)$, thereby making this structure function run. Only by this factorization procedure does one obtain then a perturbative expansion in $\alpha_s(q^2)$.

To see what is involved, let me rewrite Eq. (226), using the expression (228) for $\sigma^1_{parton}$, in a suggestive way

* This result can also be understood in terms of mass singularities of the virtual quark exchanged in the process.



$$F(x;q^2) = \int_x^1 \frac{d\xi}{\xi} f_q(\xi)\left\{\delta\left(\frac{x}{\xi}-1\right) + \frac{\alpha_s(q^2)}{2\pi}\left[P\left(\frac{x}{\xi}\right)\ln q^2 + R\left(\frac{x}{\xi}\right)\right]\right\}$$

$$= \int_x^1 \frac{d\xi}{\xi}\left\{f_q(\xi) + \frac{\alpha_s(q^2)}{2\pi}\int_\xi^1 \frac{d\xi'}{\xi'} P\left(\frac{\xi}{\xi'}\right) f_q(\xi') \ln q^2\right\} \cdot$$

$$\cdot\left\{\delta\left(\frac{x}{\xi}-1\right) + \frac{\alpha_s(q^2)}{2\pi} R\left(\frac{x}{\xi}\right)\right\} \tag{229}$$

The factorized expression in the second line above is correct to $O(\alpha_s)$. Note that by this procedure I have split the contributions in $\sigma^1_{parton}$ into a modification of the parton structure function $f_q(\xi)$ (first curly bracket) plus a true $O(\alpha_s(q^2))$ modification to $\sigma^0_{parton}$ (second curly bracket). Let me define a running parton structure function $f_q(\xi;q^2)$, to this order in $\alpha_s(q^2)$, by

$$f_q(\xi;q^2) = f_q(\xi) + \frac{\alpha_s(q^2)}{2\pi}\ln q^2 \int_\xi^1 \frac{d\xi'}{\xi'} P\left(\frac{\xi}{\xi'}\right) f_q(\xi') + \ldots \tag{230}$$

Further let me define a perturbative parton cross section by

$$\sigma_{parton}(x_p;q^2) = \delta(x_p-1) + \frac{\alpha_s(q^2)}{2\pi} R(x_p) + \ldots \tag{231}$$

Then the structure function $F(x;q^2)$ reads simply

$$F(x;q^2) = \int_x^1 \frac{d\xi}{\xi} f_q(\xi;q^2)\,\sigma_{parton}\left(\frac{x}{\xi},q^2\right)$$

$$= f_q(\xi;q^2) + O(\alpha_s(q^2)) \tag{232}$$

which is precisely the result I anticipated in Eq. (227). Crucial to obtaining this result is the factorization property which allows one to remove the unwanted $\ln q^2$ factors into a modified parton distribution function. One can show that this factorization is possible to all orders in $\alpha_s$ and furthermore that it is process independent /40/. That is, the transformation of parton distribution functions into running parton distribution functions is independent of the process in question. Of course the remaining perturbative parton cross section will in general depend on the process at hand.

The expression for $f_q(\xi;q^2)$ obtained in Eq. (230) is equivalent, to the order in $\alpha_s$ that I am working in, to the integro-differential equation.

$$\frac{df_q(\xi;q^2)}{d\ln q^2} = \frac{\alpha_s(q^2)}{2\pi}\int_\xi^1 \frac{d\xi'}{\xi'} f_q(\xi';q^2) P(\xi/\xi') \tag{233}$$

This is the Altarelli-Parisi equation /39/, which describes how the structure function $f_q(\xi;q^2)$ evolves with $q^2$. I have arrived at it by factorizing away the $\ln q^2$ pieces from $\sigma^2_{\text{parton}}$ into a running structure function. There is a more physical way of obtaining this equation, which is the one originally followed by Altarelli and Parisi /39/. They argued that the distribution function of quarks, besides having an intrinsic component, has an additional contribution coming from the fact that partons of higher fractional momentum can always degrade their momentum by gluon (or quark) emission. That is, probing with higher $q^2$, one should always be able to "resolve" the quark density for instance into that of a quark plus a gluon. The "splitting function" $P(\xi/\xi')$ in Eq. (233) is precisely the probability function of finding within a quark of fractional momentum $\xi'$ another quark of fractional momentum $\xi < \xi'$. As $q^2$ increases the physical effect which Eq. (233) portrays is a depopulation of the structure functions for large values of $\xi$ and an increase of $f(\xi;q^2)$ for small values of $\xi$. This is shown schematically in Fig. 28

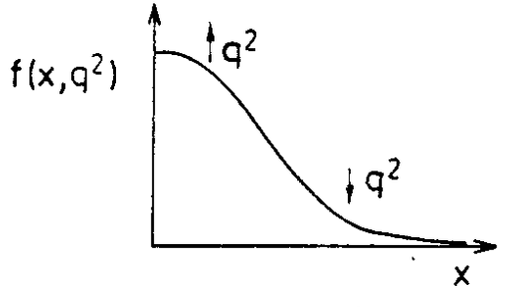


Fig. 28: Qualitative behaviour of $f(x;q^2)$ as a function of $q^2$



The physical effects of the running of the parton structure functions are most easily seen by focussing directly on the Altarelli-Parisi equations. Because the splitting function $P$ is a function only of $\xi/\xi'$, it is clear that the Altarelli-Parisi equation becomes simple if one considers not $f_q(\xi;q^2)$ directly but its moments:

$$M_n(q^2) = \int_0^1 d\xi\, \xi^{n-1} f_q(\xi;q^2) \tag{234}$$

Using Eq. (233) it follows immediately that the moments obey the differential equations

$$\frac{dM_n(q^2)}{d\ln q^2} = \frac{\alpha_s(q^2)}{2\pi} A_n M_n(q^2) \tag{235}$$

where

$$A_n = \int_0^1 d\xi\, \xi^{n-1} P(\xi) \tag{236}$$

These equations can be solved readily since the behaviour of the QCD coupling constant $\alpha_s(q^2)$ is known. Using the lowest order formula for the $\beta$-function, given in Eq. (93), one has

$$\frac{d\alpha_s(q^2)}{d\ln q^2} = \beta(\alpha_s) = -\frac{(33-2n_f)}{12\pi}\alpha_s^2(q^2) \tag{237}$$

which implies

$$\alpha_s(q^2) = \frac{[12\pi/33-2n_f]}{\ln q^2/\Lambda^2} \tag{238}$$

where $\Lambda$ is a free parameter, which will be determined eventually from experiment.

Using Eq. (238), the $q^2$ behaviour of the moments $M_n(q^2)$ is easily computed from Eq. (235). One finds

$$M_n(q^2) \sim (\ln q^2)^{\frac{6A_n}{33-2n_f}} \tag{239}$$

Recalling Eq. (227), which related the behaviour of the hadronic structure functions to that of the parton structure functions, apart from corrections of $O(\alpha_s(q^2))$, it is clear that the main effect of QCD is to give logarithmic variations with $q^2$ to the moments of the experimentally measured structure functions. That is, QCD implies scaling violations in deep inelastic scattering. The moments of the structure functions will vary with $\ln q^2$ in a well defined way, $(\ln q^2)^{d_n}$, with the exponents $d_n$ being calculable numbers.

Before going on to examine whether data in deep inelastic scattering really shows the scaling violations implied by QCD, I need to remedy a bit the above discussion, which contained some simplifications. To $O(\alpha_s)$ it is really not sufficient only to consider modifications of the process $q + V^* \to q$ in which gluons are emitted (e.g. $q + V^* \to q + g$). The graph of Fig. 2a, in which a gluon in the hadron pair produces a $q\bar{q}$ pair in the presence of the virtual vector boson $V^*$ ($g + V^* \to q\bar{q}$) is of the same order in $\alpha_s$ and should be included in the, QCD corrected, computation of deep inelastic scattering.

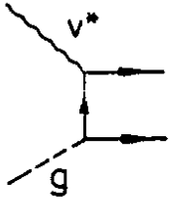


Fig. 29: Gluon pair production by $V^*$

The inclusion of gluons is rather easily done at the level of the Altarelli-Parisi equation. The point is that the quark structure function as $q^2$ increases gets really two kind of additional contributions. One of these we already discussed. A quark of higher fractional momentum $\xi'$ degrades, by emitting a gluon, into a quark of lower fractional momentum $\xi$. The splitting function $P(\xi/\xi') \equiv P_{qq}(\xi/\xi')$ basically is computed by calculating the probability of this transition - shown schematically by Fig. 30a. On the other hand, a quark of fractional momentum $\xi$ can also ensue by pair production from a gluon. The splitting function for this process $P_{qg}(\xi/\xi')$ basically measures the probability for the process in Fig. 30b to happen. This additional contribution to the quark structure function obviously must be proportional to the distribution functions for gluons of fractional momentum $\xi'$.




Fig. 30: Processes giving rise to the splitting functions $P \equiv P_{qq}$ (a) and $P_{qg}$ (b)

Thus the correct Altarelli-Parisi equation is not that of Eq. (233) but rather

$$\frac{d f_q(\xi;q^2)}{d\ln q^2} = \frac{\alpha_s(q^2)}{2\pi} \int_\xi^1 \frac{d\xi'}{\xi'} \left[ P_{qq}(\xi/\xi') f_q(\xi';q^2) + P_{qg}(\xi/\xi') g(\xi';q^2) \right] \tag{240}$$

where $g(\xi';q^2)$ is the gluon distribution function. Because this equation involves also $g(\xi';q^2)$ it is not complete in itself. The gluon distribution function has an evolution equation which is similar to (240), except that it involves the splitting functions for a quark to become a gluon, $P_{gq}$, and for a gluon to become a gluon, $P_{gg}$. One has

$$\frac{d g(\xi;q^2)}{d\ln q^2} = \frac{\alpha_s(q^2)}{2\pi} \int_\xi^1 \frac{d\xi'}{\xi'} \left[ \sum_q P_{gq}(\xi/\xi') f_q(\xi';q^2) + P_{gg}(\xi/\xi') g(\xi';q^2) \right] \tag{241}$$

The splitting functions $P_{qq}$, $P_{qg}$, $P_{gq}$ and $P_{gg}$ can be extracted by picking out the coefficient of the $\ln q^2$ terms in appropriate parton scattering processes. For future use, I record here the form for $P_{qq}(x_p)$ and give a very brief discussion of how this splitting function can be calculated. The result for $P_{qq}(x_p)$ one finds is that

$$P_{qq}(x_p) = \frac{4}{3}\left\{ \frac{1+x_p^2}{(1-x_p)_+} + \frac{3}{2}\delta(1-x_p)\right\} \qquad (242)$$

The form for $P_{qq}(x_p)$, for $x_p \neq 1$, is quite easily obtained by remarking that the $\log q^2$ term in the cross section for the process $q + V^* \to q + g$ arises essentially from an angle singularity in the differential cross section, in the limit in which all masses are set to zero. If $\theta$ is the angle, in the $q - V^*$ CM system, between the outgoing gluon and the incident quark direction, a simple calculation gives

$$\frac{d\sigma}{d\cos\theta}(q+V^* \to q+g) = \frac{1}{(1-\cos\theta)}\,\frac{\alpha_s}{2\pi}\left[\frac{4}{3}\,\frac{1+x_p^2}{1-x_p}\right] + \text{non singular terms} \qquad (243)$$

thereby identifying $P_{qq}(x_p)$ for $x_p \neq 1$.

For $x_p = 1$ one has to proceed with some care /39/, /41/. The virtual gluon diagrams of Fig. 27 will give a contribution to the parton cross section which is proportional to $\delta(1 - x_p)$. The exact value of the coefficient of this $\delta$-function depends on how one regulates the potentially divergent piece arising from soft gluon bremsstrahlung ( $x_p \to 1$) /39/. The prescription adopted in Eq. (242) is to replace $(1 - x_p)^{-1}$ by $(1 - x_p)_+^{-1}$, which is really a principal value prescription. Basically it means that for any function $f(x_p)$ one has by definition

$$\int dx_p \frac{f(x_p)}{(1-x_p)_+} \equiv \int dx_p \frac{f(x_p)-f(1)}{1-x_p} \qquad (244)$$

Given this definition, then it is not difficult to convince oneself that indeed the coefficient of $\delta(1 - x_p)$ in Eq. (244) must be 3/2. This follows since the first moment of $P_{qq}(x_p)$ is easily shown to vanish. The proof of this statement is left as an exercise,

$$\int_0^1 dx_p\, P_{qq}(x_p) = 0 \qquad (245)$$

Although in general both quark and gluon structure functions enter in the Altarelli-Parisi equations (240) and (241), one may construct combinations of quark structure functions in which all dependence on the gluon structure functions vanishes. Basically one needs to construct <u>non-singlet</u> structure functions in which, obviously, the gluons contributions are missing. For instance, the valence quark distribution



$$V(x;q^2) = U_V(x;q^2) + d_V(x;q^2) \qquad (246)$$

obeys the simple Altarelli-Parisi equation (233):

$$\frac{dV(x;q^2)}{d\ln q^2} = \frac{\alpha_s(q^2)}{2\pi}\int_x^1 \frac{d\xi}{\xi} P_{qq}\left(\frac{x}{\xi}\right) V(\xi;q^2) \qquad (247)$$

Recalling Eq. (139) one sees that for the structure function $\overline{F}_3^{cc}(x;q^2) = \frac{1}{2}\left[(F_3^{cc}(x;q^2))_{\nu N} + (F_3^{cc}(x;q^2))_{\bar\nu N}\right]$ QCD predicts a simple behaviour for its moments. Since to leading order in $\alpha_s(q^2)$ (cf Eq. (227))

$$\overline{F}_3^{cc}(x;q^2) = V(x;q^2) + O(\alpha_s(q^2)) \qquad (248)$$

it follows that

$$M_n^V(q^2) = \int_0^1 dx\, x^{n-1}\overline{F}_3^{cc}(x;q^2) \simeq \int_0^1 dx\, x^{n-1} V(x;q^2)$$

$$= C_n\left(\ln q^2/\Lambda^2\right)^{d_n} \qquad (249)$$

Here the coefficient $d_n$ is calculable in terms of the moments of $P_{qq}$, precisely as detailed in Eq. (239):

$$d_n = \frac{6}{[33-2n_f]}\int_0^1 d\xi\, \xi^{n-1} P_{qq}(\xi) \qquad (250)$$

Using the explicit form of $P_{qq}(\xi)$ of Eq. (242) one finds readily that

$$d_n = \frac{8}{[33-2n_f]}\left[-\frac{1}{2} + \frac{1}{n(n+1)} - 2\sum_{j=2}^{n}\frac{1}{j}\right] \qquad (251)$$

This result was obtained first, in quite a different fashion, by Georgi and Politzer /42/ and Gross and Wilczek /43/.

Singlet structure functions, like $F_2(x;q^2)$, have a somewhat more complicated behaviour with $q^2$ than non singlet structure functions. Because in these cases both the quark and gluon structure functions contribute, the moments of $F_2$ behave as the sum of two distinct $(\ln q^2)^{d_{NS}^{\pm}}$ terms - with again the $d_{NS}^{\pm}$ coefficients calculable. This makes the direct comparison of the QCD prediction with data more complicated and therefore I shall not further pursue this matter here. A useful discussion of how to proceed in these cases is provided by Buras /44/.

For the nonsinglet case a direct check of QCD, in principle, is provided by the, so-called, moment plot. Clearly a graph of $\ln M_n^{\nu}$ versus $\ln M_m^{\nu}$ will have, according to Eq. (249), a slope of $\frac{d_n}{d_m}$. Such a moment plot, taken from Altarelli's review /45/ is shown in Fig. 31 and, as can be seen, appears to be in excellent agreement with the QCD predictions

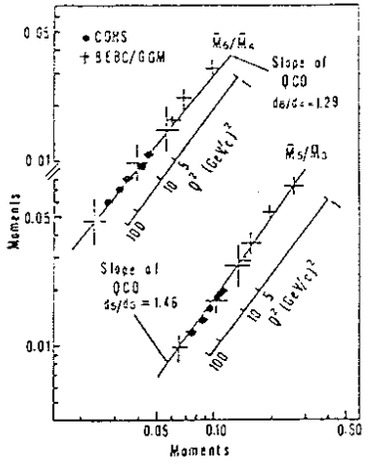


Fig. 31: Moment plot for the nonsinglet structure functions $\bar{F}_3^{cc}$, from Ref. 45

I should caution, however, that even though the agreement is impressive, there is really quite a bit of theory input that is included in this plot. In practice to compute the moments, since the measurements of $F_3^{cc}$ do not cover all the range in x and $q^2$, one has to extrapolate the measured structure functions into the unmeasured regions. These extrapolations bias the ratios shown in Fig. 31.

A better approach to test QCD has been pursued lately. This consists of starting with a given set of structure functions at a fixed $q^2 = q_o^2$ and then using the Altarelli-Parisi equations directly to predict the behaviour of these structure functions for larger values of



$q^2$ ($q^2 > q_o^2$). The advantage of this approach over the moment plot is that, while the moments require a knowledge of $f_q(x;q^2)$ for all values of x, to compute the evolution of a structure function to $f_q(x;q^2)$ requires knowledge of $f_q(x_o;q_o^2)$ only for values of $x_o > x$.

In Fig. 32 I show a compilation of data on $x F_3^{\nu N}$, taken from the Cornell report of Dydak /46/. One sees clearly a nice qualitative agreement with the expectation of QCD. The structure function grows with $q^2$ for small values of x and decreases with $q^2$ for large values of x

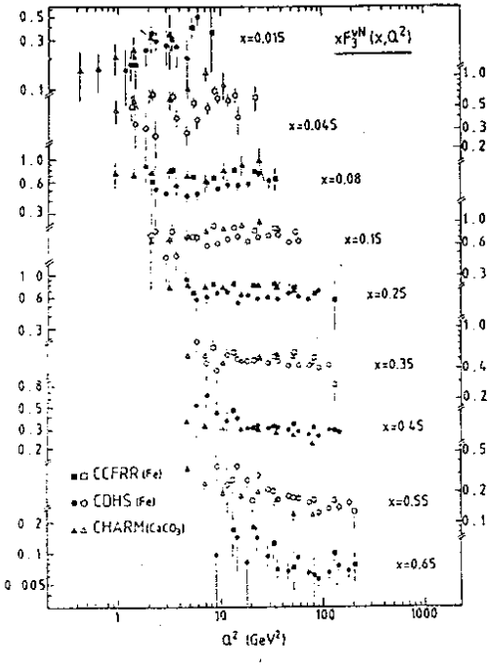


Fig. 32: Behaviour of $x F_3^{\nu N}$ as a function of $q^2$, from Ref. 46

This data can be used for a quantitative test of QCD by fitting it using the Altarelli Parisi equation. Such a fit determines the value for the only free parameter in the theory, the scale $\Lambda$ of the QCD coupling constant (cf Eq. (238)). In practice, in performing these fits, also some higher order effects in $\alpha_s(q^2)$ are included and one determines a slightly different scale $\Lambda_{\overline{MS}}$, which is prescription dependent. I will discuss this, somewhat confusing, point below. However, let me first give the results. The best fit value for $\Lambda_{\overline{MS}}$ given by Dydak /46/ in his report is

$$\Lambda_{\overline{MS}} = (250 \pm 150)\ \text{MeV} \qquad (252)$$

This value is consistent with, although somewhat larger than, the pre-

vious best global fit value for $\Lambda_{\overline{MS}}$ of Buras /47/

$$\Lambda_{\overline{MS}} = (160 \pm {}^{100}_{80})\ \text{MeV} \tag{253}$$

I end this section by commenting on the distinction between various QCD scale parameters. I will phrase my discussion in terms of moments of structure functions /44/ although an analogous discussion can be carried through in terms of Altarelli-Parisi equations, appropriately modified to include higher order QCD corrections /45/. Recall again our result (227) for the hadronic structure function

$$F(x;q^2) = f_q(x,q^2) + O(\alpha_s(q^2))$$

In the discussion up to now I have consistently forgotten the $O(\alpha_s(q^2))$ correction and equated the running of the hadronic structure function with that of the parton structure function. To include the $O(\alpha_s(q^2))$ terms necessitates specifying a way of renormalization and of calculating the evolution of $f_q(x;q^2)$ beyond the leading order. The evolution of $f_q(x;q^2)$ depends, in general, on the prescription adopted, although how $F(x;q^2)$ evolves obviously should not, since this latter quantity is measurable.

I detail the structure of the results for the non singlet $\bar{F}_3^{cc}$ structure function. Let me define the moment of $\bar{F}_3^{cc}(x;q^2)$ and of the valence parton density $V(x;q^2)$ by

$$M_n^V(q^2) = \int_0^1 dx\, x^{n-1}\, \bar{F}_3^{cc}(x;q^2) \tag{254}$$

$$\mathcal{M}_n(q^2) = \int_0^1 dx\, x^{n-1}\, V(x;q^2) \tag{255}$$

Neglecting corrections of $O(\alpha_s(q^2))$ these two moments are identical (c.f. Eq. (249)). Including these corrections, however, one has /44/:

$$M_n^V(q^2) = \mathcal{M}_n(q^2)\left[1 + \alpha_s(q^2) B_n\right] \tag{256}$$

where

$$\mathcal{M}_n(q^2) = \mathcal{M}_n(q_0^2)\left[\frac{\alpha_s(q^2)}{\alpha_s(q_0^2)}\right]^{d_n}\left\{1 + \left[\alpha_s(q^2) - \alpha_s(q_0^2)\right] Z_n\right\} \tag{257}$$



The coefficients $B_n$ and $Z_n$ depend on the renormalization scheme. However this scheme dependence cancels in Eq. (256), so that the physical moments are scheme independent.

Although the final formula is independent of the scheme, it does depend on the definition adopted for $\alpha_s(q^2)$ (i.e. on the $\Lambda$ parameter used). Using the $\beta$-function computation to $O(\alpha_s^4)$, Eq. (93), one finds for $\alpha_s(q^2)$ the formula /44/:

$$\alpha_s(q^2) = \frac{12\pi}{[33-2n_f]}\,\frac{1}{\ln q^2/\Lambda^2} - \frac{72\pi(153-19n_f)}{[33-2n_f]^2}\,\frac{\ln(\ln q^2/\Lambda^2)}{\ln^2 q^2/\Lambda^2} \tag{258}$$

which contains corrections of $O\left(\frac{1}{\ln q^2}\right)$ to the lowest order formula, Eq. (238). Using this formula one may rewrite Eq. (256) as

$$M_n^V(q^2) = C_n\left[1 + \frac{R_n(q^2)}{(11-\frac{2}{3}n_f)\ln q^2/\Lambda^2}\right]\left(\ln q^2/\Lambda^2\right)^{d_n} \tag{259}$$

where

$$R_n(q^2) = B_n + Z_n - 2\frac{(153-19n_f)}{(33-2n_f)}\, d_n \ln(\ln q^2/\Lambda^2) \tag{260}$$

Obviously, neglecting any $O(\alpha_s)$ corrections to the moments ($B_n, Z_n \to 0$) and dropping $(\ln q^2)^{-1}$ corrections to $\alpha_s(q^2)$, reduces Eq. (259) to the lowest order result, detailed in Eq. (249). Retaining the $R_n(q^2)$ corrections one must, however, specify which $\Lambda$ one is dealing with. For if one changes $\Lambda$ by

$$\Lambda \to e^K \bar{\Lambda} \tag{261}$$

in Eq. (259), one can reabsorb the change in a redefinition of $R_n$. To wit

$$R_n \to \bar{R}_n = R_n + \frac{2}{3}(33 - 2n_f) d_n K \tag{262}$$

To fit data using the corrected moment formula (259), one must specify which $\Lambda$ one is dealing with. That is, what coefficients $R_n$ one is really using. The $\Lambda_{\overline{MS}}$ scale which is now traditionally used is one for which certain constants, like $(\ln 4\pi - \gamma_E)$, which normally arise in $R_n$, when one calculates using dimensional regularization, are removed. Obviously, there is nothing particularly sacred in this procedure. One should only take care that, if different physical quantities are analyzed, the same $\Lambda$ scale is consistently used.

## THE K-FACTOR IN DRELL-YAN PROCESSES

Higher order QCD corrections can be studied in other processes besides deep inelastic scattering. The factorization property discussed in the last section allows one to absorb uncontrollable $\ln q^2$ factors into running parton distribution functions, leaving over an, in principle, well defined perturbation expansion in $\alpha_s(q^2)$. I want to examine in this section the effects of QCD for Drell-Yan processes ($\mu^+\mu^-$ production or $W/Z$ production in hadronic processes) since, as I have already mentioned, the QCD corrections for these processes appear to be significant. These effects are what lead to the $K$ -factor ambiguity on the overall size of the production cross section.

The lowest order process $q + \bar{q}' \to V^*$ gets modified to $O(\alpha_s)$ by processes in which the vector boson $V^*$ is accompanied in the final state either by a gluon ($q + \bar{q}' \to V^* + g$) or by a quark ($q + g \to V^* + q'$), as shown in Fig. 33. In addition there are virtual gluon corrections.


Fig. 33: $O(\alpha_s)$ real corrections to Drell-Yan processes

The effect of these additional contributions is two-fold: i) the original quark and antiquark distribution functions get replaced by running distribution functions. This is the leading QCD modification, totally analogous to what happened in deep inelastic scattering and is what is expected by the factorization property. (ii) Two different types of $O(\alpha_s(q^2))$ corrections ensue. One of these, subdominant, corrections basically arises from the second diagram of Fig. 33, and involves $V^*$ production by quark-gluon fusion. This is a pure $\alpha_s(q^2)$ effect and is proportional to the gluon structure function. For the collider data this contribution is not particularly important and can be safely neglected. The second $O(\alpha_s(q^2))$ correction is directly a correction to the original parton process and, although formally of order $\alpha_s$ , turns out to be large. This correction is responsible for the K-factor ambiguity.

Let me specifically discuss $W^-$ production, since I have already given the lowest order prediction for it in Eq. (203). Including QCD corrections, but neglecting the contribution of quark-gluon fusion, this formula is modified to



$$\sigma(p\bar{p}\to W^- X) = \frac{\sqrt{2}\pi}{3} G_F \cos^2\theta_c \frac{M_W^2}{s} \int d\xi\, d\xi'\, d_V(\xi;M_W^2)\, U_{\bar{V}}(\xi';M_W^2)$$

$$\cdot \left\{ \delta\left(\xi\xi' - \frac{M_W^2}{s}\right) + \theta\left(\xi\xi' - \frac{M_W^2}{s}\right) \frac{\alpha_s(M_W^2)}{2\pi} R\left(\frac{M_W^2}{\xi\xi' s}\right) \right\} \tag{263}$$

The parton distribution functions are running functions now, which are evaluated at $M_W^2$ which is the scale of the process. The explicit $O(\alpha_s)$ correction, denoted by R, has been calculated in the literature /45/ and is found to be very large. The origin of this unexpectedly large contribution can be traced to the fact that one is comparing space-like processes to time like processes. Let me try to explain this point.

The running parton distributions which enter in (263) are defined with respect to the space-like, deep inelastic scattering. In factorizing away potentially dangerous $\ln q^2$ terms (or even $(\ln q^2)^2$ terms, which actually eventually cancel entirely between virtual and real contributions) $q^2$ is always positive. In the Drell-Yan process, on the other hand $q^2 < 0$. If one wants to reconstruct the running parton distribution of deep inelastic scattering, it is necessary to change the sign of $q^2$ and so some additional terms containing $\ln(-1)$, or even $(\ln(-1))^2$ are left over. The dominant term in R in Eq. (263) arises precisely in this way. The virtual correction for the vertex $V^* + q \to q$ and that for the vertex $q + q \to V^*$, shown in fig. 34, both have a leading term proportional to $(\ln q^2)^2$, except that $q^2$ is positive in one case and negative in the other.

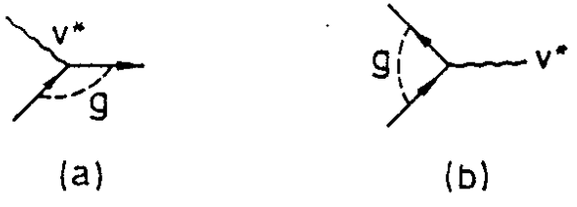


Fig. 34: Virtual gluonic corrections for deep inelastic (a) and Drell-Yan (b)

This leads to a contribution to R:

$$R_{\text{continuation}} = -\frac{\alpha_s}{2\pi}\left[\frac{4}{3}\left(\ln(-1)\right)^2\right]\delta(\xi\xi' - M_W^2/s)$$

$$= \frac{2\pi}{3}\alpha_s\,\delta(\xi\xi' - M_W^2/s) \qquad (264)$$

which is of the same order of magnitude as the leading term in Eq. (263). Note that this contribution just changes the value of the 0th order rate.

Because the $O(\alpha_s)$ corrections in R in Eq. (263) are so large, one cannot really trust the perturbative calculation. However, because these corrections come, mainly, from virtual effects one has at least a qualitative understanding of what QCD does. Basically, one expects that the usual parton model predictions obtain - including effects of the running of the structure functions - modified by some over all factor (the K-factor) which should be of the order of 1-2. For a fixed $M_V^2$ process - like W/Z production - this prediction is not terribly helpful, except that it allows one to understand why pure parton model predictions can be off by a factor of 2 or so. For $\mu^+\mu^-$ production, however, one has a stronger prediction. Namely that the parton model prediction for the shape of the differential cross section $d\sigma/dM^2$ should be manifest in the data. Fig. 35 shows data for the $\mu^+\mu^-$ mass distribution in the process $\bar{p}N \to \mu^+\mu^- X$, measured at Fermilab and CERN, compared to a Drell-Yan calculation using the CDHS parton structure functions, scaled by a K-factor of 2.3 /48/. It is clear that the agreement of the shape of the data with the parton model prediction is quite satisfactory.

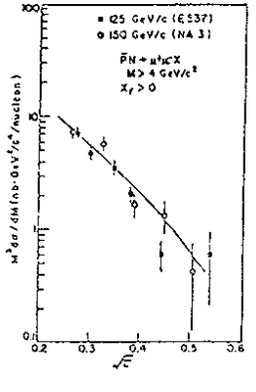


Fig. 35: Comparison of Drell-Yan data with the prediction of the parton model, scaled by a factor of 2.3. From ref. 48



JETS IN $e^+e^-$ PHYSICS

The last item of QCD phenomenology that I want to discuss is hadronic jet production in $e^+e^-$ annihilation *. Qualitatively one expects 2 jet production to dominate in $e^+e^-$ collisions, with the jets following the direction of the qq pairs produced by the virtual photon. That is, the lowest order QCD diagram of Fig. 36 in the CM system should give rise to back to back hadronic jets, as illustrated in Fig. 37.


Fig. 36: Lowest order QCD diagram in $e^+e^-$ annihilation

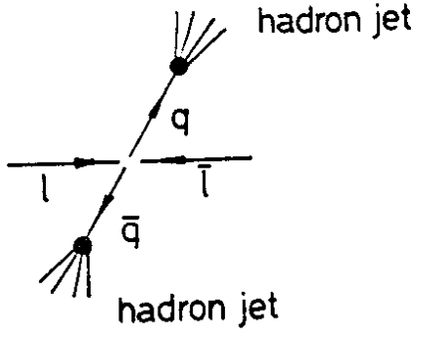


Fig. 37: Two jet production in $e^+e^-$ annihilation

Occasionally (i.e. to $O(\alpha_s(q^2))$) a third, gluon, jet should also be produced corresponding to the process shown in Fig. 38.

* I will not discuss jet physics in hadronic collisions, since this item is very well covered in Astbury's lectures in these proceedings.

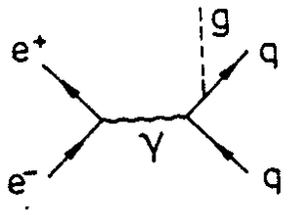


Fig. 38: $O(\alpha_s(q^2))$ QCD diagram in $e^+e^-$ collisions, which gives rise to a third hadronic jet

Both of these qualitative features are present in the SLAC and DESY data on $e^+e^- \to$ hadrons. However, to quantify these observations and compare to QCD is not so simple at present energies, because one cannot really neglect the process of hadronization by which quarks transmute themselves into hadrons. In particular, one would really like to study quantities which do not depend on the fragmentation functions $D_q^H(z)$, since these functions essentially parametrize our ignorance of the hadronization process. There are two general types of observables in $e^+e^-$ processes where one can proceed, in principle, without a knowledge of the fragmentation functions. (I say, in principle, because in practice in most cases some mild information on hadronization remains necessary). Type I quantities consist of appropriately weighted cross sections, for which one can show that the $D_q^H$ functions disappear. Type II quantities are appropriate averages which, because they are free of infrared singularities, should also be independent of the $D_q^H$ functions.

For a type I quantity, the fragmentation functions do not enter because one is looking sufficiently inclusively, and with an appropriate weight, so that the energy momentum sum rule, Eq. (101), for the $D_q^H$ functions can be used:

$$\sum_H \int d\xi'\, \xi'\, D_q^H(\xi';q^2) = 1$$

Furthermore, because there are no hadrons in the initial state, obviously no structure functions appear in $e^+e^-$ processes. Hence, type I quantities should be calculable directly in a perturbation series in $\alpha_s(q^2)$.

The best known example of a type I quantity is the total hadronic cross section, $\sigma_{tot}(e^+e^- \to \text{hadrons})$. Although it is intuitively obvious that no fragmentation functions should be necessary in calculating $\sigma_{tot}$, it may prove worthwhile demonstrating how the sum rule (101) eliminates the $D_q^H$ functions. For this purpose it is convenient to write $\sigma_{tot}$ formally as a sum of inclusive cross sections

$$\sigma_{tot} = \sum_H \int dz\, z\, \frac{d\sigma^H}{dz} \qquad (265)$$



Here z is the energy fraction carried by the hadron H in the final state. Note that the z weighing above is necessary; if not one would obtain, instead of $\sigma_{tot}$, the total cross section multiplied by the average hadron multiplicity. The inclusive cross section can be written in terms of the usual parton convolution

$$\frac{d\sigma^H}{dz} = \sum_{parton} \int_z^1 \frac{d\xi'}{\xi'} \left( \frac{d\sigma_{parton}}{dz_p} \right) D^H_{parton}(\xi';q^2)$$

$$= \sum_{parton} \int d\xi'\, dz_p\, \delta(z-\xi' z_p) \left( \frac{d\sigma_{parton}}{dz_p} \right) D^H_{parton}(\xi';q^2)$$

(266)

Inserting (266) into (265) and using Eq. (101) immediately gives

$$\sigma_{tot} = \sum_{parton} \int dz_p\, z_p\, \frac{d\sigma_{parton}}{dz_p} \qquad (267)$$

which shows that the total hadronic cross section can be calculated at the parton level, without any need of fragmentation functions.

It is usual to define instead of $\sigma_{tot}$ the quantity R which is the ratio of $\sigma_{tot}$ to the $\mu$-pair cross section

$$R = \frac{\sigma_{tot}(e^+e^- \to \text{hadrons})}{\sigma(e^+e^- \to \mu^+\mu^-)} \qquad (268)$$

To lowest order on QCD, since the graph in Fig. 36 differs from that for $\mu$-pair production only because quarks have different charges and a given color multiplicity, it is obvious that

$$R = 3 \sum_q e_q^2 \qquad (269)$$

This equation receives QCD corrections and the result of a rather straightforward calculation gives /49/

$$R = 3 \sum_q e_q^2 \left\{ 1 + \frac{\alpha_s(q^2)}{\pi} + \dots \right\} \qquad (270)$$

Clearly R with increasing energy approaches the parton model value from above. However, the correction is small and it is quite difficult to measure this effect given the errors in the data, shown in Fig. 39. Obviously, however, the parton model prediction, which says that R is essentially a constant, appears to be valid up to the highest measured energies. One should not forget that this is a non trivial consequence of QCD also!

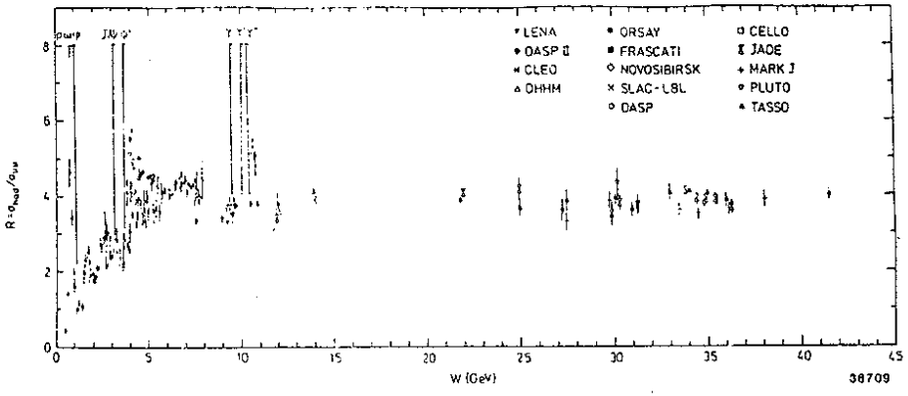


Fig. 39: Behaviour of R versus energy $W = \sqrt{-q^2}$, from Ref. 50

A less inclusive quantity than $\sigma_{tot}$, which is again of Type I, is the angular energy flow /51/ of hadrons in $e^+e^-$ annihilation. It is not hard to convince one self that

$$\frac{d\Sigma}{d\Omega} = \sum_H \int dz\, z \frac{d\sigma^H}{d\Omega\, dz} = \sum_{partons} \int dz_p\, z_p \frac{d\sigma_{parton}}{d\Omega_p\, dz_p} = \frac{d\Sigma}{d\Omega_{parton}} \tag{271}$$

so that also $d\Sigma/d\Omega$ does not need any fragmentation function information and is calculable in a power series in $\alpha_s(q^2)$. Unfortunately, this quantity, as well as more complicated energy-energy correlation functions /52/, contains an implicit assumption which makes it necessary to use some hadronization information before it can be compared to data. Namely in (271) one assumed that the hadronic energy flow follows precisely that of the partons : $d\Omega = d\Omega_{parton}$ . This is obviously an approximation. When the partons hadronize, in general the resulting hadrons will be produced with some fixed average spread in $p_\perp$ , $\langle p_\perp \rangle$, with respect to the parton. This introduces uncertainties in the hadron direction of $\mathcal{O}(\langle p_\perp^2 \rangle / q^2)$ which tend to smear the resulting energy flow. With this caution in mind, I show in Fig. 40 some recent data on energy-energy correlations in $e^+e^-$ collisions compared to what is predicted by QCD (dashed curve) and including some hadronization corrections (solid curve).



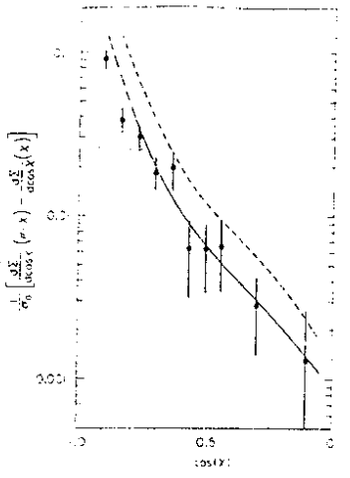


Fig. 40: Data on energy-energy correlations in $e^+e^-$, from Ref. 53

Type II quantities are averages of distributions in $e^+e^-$ collisions which are well defined at the parton level. More precisely, they are quantities without any infrared singularities produced by collinear or soft gluon radiation. Because these quantities are calculable directly at the parton level they should give information on hadronic properties, which do not require introducing fragmentation functions. Roughly speaking, the fragmentation functions are put in, in a QCD calculation, to absorb the uncalculable soft processes by which partons turn into hadrons. The presence of infrared singularities at the parton level, which are then incorporated into the fragmentation functions, is precisely what makes these functions "run". If no infrared singularities are present, there should be no need to introduce fragmentation functions to absorb them!

Obviously all Type I quantities are also Type II, since they are calculable directly at the parton level. However, some Type II quantities sometimes prove to be more convenient to analyze. A good example, and the only one which I shall discuss, is Thrust. The Thrust variable is defined by

$$T = \frac{\sum_i |\vec{p}_i \cdot \hat{e}|}{\sum_i |\vec{p}_i|} \tag{272}$$

where $p_i$ are the momenta of the outgoing hadrons and the vector $\hat{e}$ is varied until the maximum value for T is found. This is then the Thrust axis. The lowest order process $e^+e^- \to q\bar{q}$ obviously gives a Thrust distribution which is a $\delta$ -function at T = 1. Gluon radiation will give events which are not back to back and so, at the parton level, one has a spreading of this $\delta$ -function. The actual thrust distribution is, how-

ever, infrared singular at $T = 1$, reflecting the fact that gluons like to be soft and collinear. Thus, this parton model calculation cannot be translated directly into a hadronic prediction without introducing fragmentation functions. As $T \to 1$ one finds /54/

$$\frac{1}{\sigma_{tot}} \frac{d\sigma}{dT} \simeq \frac{8}{3} \frac{\alpha_s(q^2)}{\pi} \frac{1}{1-T} \ln \frac{1}{1-T} \qquad (273)$$

Although (273) is not well behaved as $T \to 1$, the average $\langle 1-T \rangle$ is perfectly well defined. Thus $\langle 1-T \rangle$ is an infrared safe quantity and in principle the parton model calculation for it should reflect directly what is happening at the hadronic level.

Of course also for $\langle 1-T \rangle$, as for the energy flow, not all effects of hadronization can be neglected. These effects will tend to smear the 0th order QCD $\delta(1-T)$ distribution and give a non zero value for $\langle 1-T \rangle$. However, these hadronization corrections will vanish as $\langle n_h \rangle^2/q^2$. What QCD predicts for $\langle 1-T \rangle$ is a much softer fall off with $q^2$, namely $\langle 1-T \rangle \sim \alpha_s(q^2) \sim (\ln q^2)^{-1}$. In Fig. 41 I show some recent TASSO data /55/ on the behaviour of $\langle 1-T \rangle$ versus $W = \sqrt{-q^2}$. The fit shown is the QCD prediction, in which hadronization is incorporated, using the independent jet model of Hoyer et al. /57/. The effect of hadronization can be clearly seen by focusing on the dotted line in the figure which represents just $e^+e^- \to q\bar{q}$. However, it is obvious that the expected QCD effect is clearly distinguishable, especially at higher W values. This is a nice way to demonstrate the existence of gluon radiation.

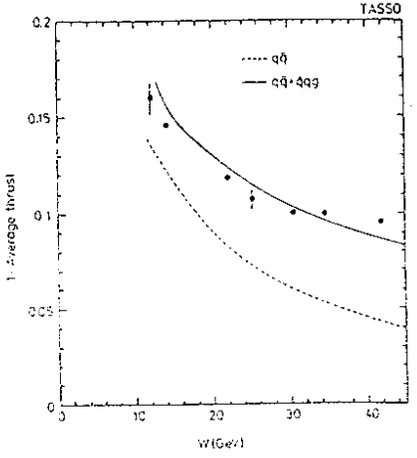


Fig. 41: Behaviour of $\langle 1-T \rangle$ versus $W = \sqrt{-q^2}$, from Ref. 55



## WHERE ARE WE NOW: COMMENTS AND SPECULATIONS

I would like to end these lectures by discussing some of the open issues in the standard model. I hope that the discussion up to now has made it clear that the standard model does provide an excellent phenomenological description for the interactions of leptons and for hadronic, hard scattering processes. Nevertheless, there are some open questions that need to be resolved, and whose answers may point to a deeper synthesis. I begin by discussing QCD, since here there are fewer questions of principle left open.

QCD, in some sense, is better established than the GSW model. The success of the parton model are really QCD successes. Quantum chromodynamics passes all qualitative tests, with flying colors* : there is approximate scaling in R and in deep inelastic scattering; 2 jet and 3 jet phenomena are seen; color counting rules work; etc. In addition, QCD passes at least some semiquantitative tests: the structure functions evolve in the predicted way with $q^2$, growing for small $x$ and decreasing at large x; there is evidence for gluon radiation in $e^+e^-$ collisions, of the magnitude predicted; the data for R lies above the parton model predictions, as expected; there is a K-factor in Drell-Yan processes and the shape of the mass distribution of the lepton pairs agrees with the parton model; in addition, lattice calculations of the hadronic spectra are beginning to give encouraging results /57/.

It is clear that really quantitative tests of QCD will have to wait until a better understanding of how to calculate long distance properties is achieved. Although the lattice approach to QCD is beginning to tackle with success some of the static aspects of hadrons (masses, magnetic moments, charge radii), it is very difficult to see how it could provide, in the near future, some more complicated dynamical information, like the $q^2$ behaviour of structure functions. The hope is, however, that lattice calculations may give some insight on how to better tackle analytically some of the long distance aspects of QCD.

To my knowledge, there are really two open problems in QCD. One of these is why is there no strong CP violation /58/? This problem is somewhat technical and it would take me too far afield to discuss it properly here. Suffice it to say that the vacuum structure of QCD suggests than an additional term $\theta F\tilde{F}$, where $\tilde{F}$ is the dual of the color field strength, should be present in the QCD Lagrangian. This term induces a large electric dipole moment for the neutron, not seen experimentally, and thus $\theta$ must be very small ($\theta \lesssim 10^{-8} - 10^{-9}$). This is a mystery, unless one can find some plausible dynamical reason for $\theta$ to be so small. Very probably, at some deep level, the protective chiral symmetry suggested by H. Quinn and I long ago /59/ is the correct solution to this problem, although technically one runs into problems with axions.

The second and main problem of QCD is one of calculation. There are so many things one would like to calculate, but as of yet our theoretical tools are too primitive to achieve much success. I list below

* Sorry, I could not resist this pun.

some of the things that it would be nice to be able to compute, from first principles, from QCD. This list is ordered in a (probable) order of difficulty:

(i) Spectrum of hadrons: mesons, glueballs, baryons and exotic states ($(q\bar{q})^2$, etc.)

(ii) Structure functions and fragmentation functions

(iii) Soft processes, like elastic $\pi$ p scattering and multiparticle production

(iv) Nuclear physics

Clearly the theoretical task ahead is immense and there will be little additional experimental input which can serve as illumination.

The open problems of the GSW model are of a different nature. As should have been clear from these lectures, the GSW model agrees beautifully with experiment. However, what is really tested is essentially only the gauge-fermion sector of the model. Radiative corrections do, in principle, depend on the Higgs sector; but for reasonable Higgs masses, the dependence in practice is well within the errors in $\sin^2\theta_W$. The principal information that we have on $\mathcal{L}_{\text{Higgs-gauge}}$ is that $\rho = 1$, which means that the symmetry breaking is done by an SU(2) doublet object. Of $\mathcal{L}_{\text{Higgs-fermion}}$ we know even less, except that with three families the Cabibbo matrix can have a complex phase, so that there is a natural origin for CP violation in the model. Because the pieces of the GSW Lagrangian connected with the Higgs sector are largely unknown, they constitute a natural open problem. Actually, as I will explain below there is some theoretical prejudice against having $\mathcal{L}_{\text{Higgs-gauge}}$ and $\mathcal{L}_{\text{Higgs-fermion}}$ as given in the standard model. So not only are these pieces an experimental open problem, they are a theoretical one too!

I begin by discussing some potential theoretical difficulties of the pure Higgs sector. Recall that the breakdown of the SU(2) x U(1) symmetry was caused by introducing the Higgs potential (61):

$$V = \lambda \left( \Phi^\dagger \Phi - \tfrac{1}{2} v^2 \right)^2$$

Although the parameter $\lambda$ is free, the scale v in the potential V is fixed by the scale of the Fermi constant. Indeed, from Eq. (72), one has

$$v = \left( \sqrt{2}\, G_F \right)^{-1/2} \simeq 250 \text{ GeV}$$

Wilson /60/, was the first to point out that fixing v this way was unnatural, if one imagined that there is some cut off in the theory. Since radiative corrections for scalar fields are quadratically divergent, the parameter v can only be maintained at 250 GeV by carefully tuning the original parameters of the theory. Otherwise the natural value it would take would be that of the cut off.

I illustrate this by considering what happens to the mass of the physical Higgs field. Recall that to lowest order, Eq. (72), we found



for the Higgs field mass

$$m_H^2 = 2\lambda v^2$$

This mass, however, gets shifted by radiative corrections, some examples of which are shown in Fig. 42

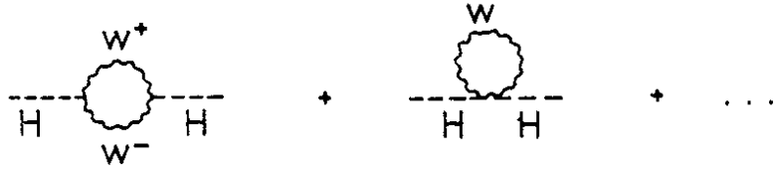


Fig. 42: Contributions to the radiative mass shift of the Higgs field

Since the graphs in Fig. 42 are quadratically divergent, evaluating them with a cut off, $\Lambda_c$, gives for the radiative corrected Higgs mass the formula

$$m_H^2 = 2\lambda v^2 + \alpha \Lambda_c^2 \qquad (274)$$

Clearly the Higgs mass gets driven to $\Lambda_c$, if $\Lambda_c \gg v$. To keep $m_H \ll \Lambda_c$, the original parameter v has to also be very big and a careful cancellation (fine tuning) has to occur.

If one lets the parameter $\Lambda_c \to \infty$, this discussion ceases to make sense. Since the GSW model is renormalizable, all that really happens is that the Higgs mass has to be put in as an undetermined parameter, to absorb the relevant infinities. The same thing happens to the Fermi scale v. It also has to be put in as an input in the theory. Therefore, strictly speaking there is no problem in the GSW model in isolation. However, gravity really introduces a scale, because for momenta above $M_{\text{Planck}} \simeq 10^{19}$ GeV it cannot be ignored. Therefore the naturalness problem is a real problem and one should look for possible ways to avoid it. I will return to this point shortly, but first I want to mention a second possible difficulty connected with the Higgs potential-triviality.

Triviality is a property proven by mathematical physicists /61/ for pure $\lambda \phi^4$ field theory, with $\phi$ a real field. What was shown is that the only consistant version of this theory is the one for which $\lambda_{\text{ren}} = 0$, i.e. a theory with no interactions. Such a result, of course, is a disaster if it was applicable in general, for it is precisely the self interactions of the Higgs fields which are needed for the spontaneous breakdown of SU(2) x U(1)! Of course, it is a long way from the simple $\lambda \phi 4$ theory to the GSW model, where there are besides scalar fields also gauge fields and fermions. In fact, it has been argued /62/ that perhaps

the presence of the gauge fields - at least the U(1) gauge field - may stabilize the Higgs sector and avoid the triviality argument. Roughly speaking, one can think of the triviality result as being due to the fact that $\lambda = 0$ is the only stable point of the theory. If $\lambda$ is positive*, it will be always driven with increasing $q^2$ to infinity since the $\beta$-function grows with $\lambda$. What was argued in Ref. 62, is that if there is a U(1) gauge field in the theory, this stabilizes the behaviour of $\lambda$ provided that $\lambda$ is small enough. Stability - at least in a perturbative sense - was found provided

$$\lambda \lesssim g'^2 \tag{275}$$

where g' is the U(1) coupling constant. With no U(1) interaction, it is clear that from (275) one recovers the triviality result, $\lambda \to 0$. Furthermore Eq. (275) implies a bound on $m_H$. Using Eq. (72) it follows that

$$m_H^2 \lesssim \frac{8}{\tan^2\theta_W} M_W^2 \tag{276}$$

which implies $m_H \lesssim 130$ GeV.

The triviality problem may be solved, therefore, if the coupling is small enough. A "perturbative" solution can also be found for the naturalness problem, but it involves a rather large speculative step. Namely, that nature is approximately supersymmetric. If all the particles in the standard model had supersymmetric partners then the mass shift in Eq. (274) would no longer be quadratically divergent. The W exchange graph, for example, would be accompanied by a Wino exchange graph (which is the spin 1/2 partner of the W), as shown in Fig. 43. These two contributions would cancel each other off, since the fermionic graph has a (-1) factor from Fermi statistics. This cancellation would be incomplete if supersymmetry were broken by having the W and Wino have different masses. Nevertheless, the radiative corrections to $m_H^2$ would depend only on $\ln \Lambda_c$ and not any more on $\Lambda_c^2$ and they would be therefore naturally under control, if $\alpha$ is small.

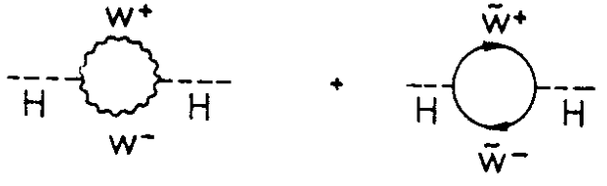


Fig. 43: Radiative corrections to the Higgs mass in a supersymmetric theory

* $\lambda$ must be positive for the positivity of the potential V



If supersymmetry is the solution to the naturalness problem of the Higgs potential, there is an extraordinarily rich phenomenology of superpartners wanting to be discovered. These superpartners cannot be pushed too far away in mass from the Fermi scale v, since it is their existence which is supposed to render this parameter natural. However, there may be a different solution to naturalness than the "perturbative" supersymmetric one. Clearly there is no problem with naturalness in Eq. (274) if the cut off $\Lambda_c \sim v$, because the radiative corrections then are small. However, having a physical cut off of the order of v means really that the Higgs particle cannot be elementary! It must be a bound state of some underlying strongly interacting theory. This scenario is the Technicolor scenario /63/.

Technicolor is a non perturbative solution to the naturalness problem. One basically replaces the whole Higgs sector by an underlying Technicolor theory. What causes the breakdown of SU(2) x U(1) is the existence of SU(2) x U(1) breaking condensates in this theory, $\langle \bar{T}T \rangle \neq 0$. The scale of these condensates is related to the dynamical scale of the Technicolor theory $\Lambda_{TC}$ - the analogue of $\Lambda$ for QCD. Hence, the Fermi scale is also related to $\Lambda_{TC}$ and its value is a purely dynamical issue. Obviously, if a Technicolor theory really exists and it replaces the Higgs potential, also the triviality problem is irrelevant.

There are, therefore, two possible options for removing from the Higgs sector of the GSW model the stigmas of unnaturalness and triviality. A "perturbative" option, in which one has a light Higgs boson and a doubling of all degrees of freedom, through supersymmetry*. Or a "non perturbative" solution, in which there is no Higgs potential at all but a dynamical breakdown of SU(2) x U(1) occurs due to condensate formation in some new underlying theory. In both cases there is considerable additional physics beyond the standard GSW model. If either of these options obtains, spectacular phenomena await discovery in the next generation of experiments, which will be probing the energies of the Fermi scale.

This is clearly not the place to discuss the phenomenology expected from these speculative extensions of the standard model. Nevertheless, let me give at least one example of the way in which the physics of the GSW model will change if one of these scenarios is true. If the Higgs sector is replaced by a strongly interacting theory, one predicts that at sufficient high energies the W-bosons will scatter strongly. This remarkable result can be understood as follows. The formation of technicolor condensates $\langle \bar{T}T \rangle \neq 0$, being a manifestation of spontaneous symmetry breakdown, causes the appearance of Goldstone excitations in the spectrum of the underlying technicolor theory. (An analogous phenomena actually happens in QCD. There one knows that quark condensates form ($\langle \bar{u}u \rangle \neq 0$) In the limit of zero quark masses these condensates break an exact global symmetry and Goldstone pions emerge. Restoring the quark masses gives the pions a small mass). The W-bosons get a mass precisely by absorbing these excitations, since the $\langle \bar{T}T \rangle$ condensates are assumed to break SU(2) x U(1). Thus, roughly speaking, the longitudinal component of the W fields is made up by the Technicolor Goldstone excitations - Technipions. At scales of the order of the dynamical scale of Technicolor

* Supersymmetric extensions of the GSW model, in fact, require two Higgs multiplets. In general one of the five physical Higgs of these extended theories is light.

$\Lambda_{TC}$, these Technipions will scatter strongly, just as pions scatter strongly. More precisely, one can argue for pions that the strong scattering should occur at energies of the order $\sqrt{s} \simeq \sqrt{16\pi}\, f_\pi$ where $f_\pi \simeq 95$ MeV is the pion decay constant, which characterizes the breakdown which made pions, (approximate) Goldstone bosons in QCD. For the Technipions, the appropriate breakdown scale is just the Fermi scale $v \simeq 250$ GeV. Hence, one predicts that W should scatter strongly at energies of the order $\sqrt{s} \simeq \sqrt{16\pi}\, v \simeq 1.5$ TeV.

Up to now, I discussed potential problems associated with the Higgs potential. The Fermion-Higgs sector is also unsatisfactory theoretically. The introduction of Yukawa couplings between fermions and the Higgs doublet causes the appearance of both fermion masses and Cabibbo mixing angles. However, because these couplings are arbitrary, the masses and mixing angles are uncalculable. This is the price one must pay if one retains the quarks and leptons as elementary and introduces no other interactions. It is difficult to conceive that all the fermion masses and mixing angles are really free parameters. The known quarks and leptons now span a range in mass of almost five orders of magnitude and have certain characteristic patterns which cry out to be explained. For instance the mixing angles among quarks which are very well separated in mass is extremely small. Why is this so?

If there is no elementary Higgs boson as in the Technicolor option then one must also find a way to generate the masses of quarks and leptons. The most "reasonable" supposition in this case is that really - despite the evidence for elementarity proved by the incredible successes of QED - quarks and leptons are composite objects. Composite models of quarks and leptons /64/ offer the hope of providing an understanding of the quark and lepton mass patterns, since in principle these parameters are now calculable. However, these models are still in a very primitive state and face extremely difficult dynamical challenges. My own view, nevertheless, is that this is the correct way to go beyond the standard model. I speculate that the underlying theory that provides for the spontaneous breakdown of SU(2) x U(1) is also the same theory whose "light" bound states are the quarks and leptons.

Having discussed some of the open theoretical problems of the standard model, let me close these lectures by making some comments also on some recent experimental challenges to the standard model. I want to touch upon three subjects, very briefly.

(i) The EMC effect
(ii) The long B lifetime and CP violation
(iii) Exotic events at the collider

I do not believe that any of this new data necessarily puts the standard model in trouble. However, the CP violation data and some of the collider data could well be the first indication that some non standard physics is emerging.

The EMC effect /65/, named after the collaboration that found it, is the surprising observation that the x-dependence of structure functions seems to depend on the nucleon number A of the target. This is illustrated in Fig. 44.



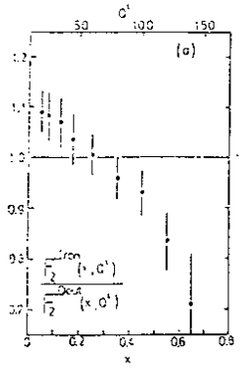


Fig. 44: Illustration of the EMC effect, from Ref. /65/

Obviously if deep inelastic scattering in nuclear targets is off quarks, then there should be no A dependence. Fermi motion effects alter things slightly, but go the other way. So the behaviour shown in Fig. 44 is really a challenge to QCD.

Because one is dealing with nuclei, a variety of "nuclear" explanations for the EMC effects have been proposed /66/. I am really not terribly competent in judging the reasonableness of these suggestions. However, I believe that a QCD inspired qualitative explanation by Jaffe /67/, and a more quantitative analysis by Close, Jaffe, Roberts and Ross /68/, are probably closer to the truth. The idea is very simple to grasp. The plot in Fig. 44 has the qualitative behaviour of what one expects in QCD if one plots the ratio of two structure functions taken at different $q^2$ values. For higher $q^2$ there is an increase at small x and a decrease at large x. The data of Fig. 44 looks precisely as if the x distribution in large A nuclei has been degraded to lower x. Such a circumstance could happen if quarks in nuclei are partially deconfined. That is, one has the beginning of a quark-gluon plasma in the presence of many nucleons, which means that the effective QCD scale $\Lambda$ is slightly decreased in nuclei.

Specifically, Close et al. /68/ in their analysis showed that if the effective nucleon size $R \sim \frac{1}{\Lambda}$ in a nucleus becomes $R' \sim \frac{1}{\Lambda'}$, then one would expect for the nuclear structure function the relations:

$$F_2'(x;q^2) = F_2(x;\xi q^2) \tag{277}$$

where

$$\xi = \left[ \left( \frac{R'^2}{R^2} \right) \right]^{\alpha_s(q_0^2)/\alpha_s(q^2)} \tag{278}$$

For reasonable range of parameters ($q_0^2 = 1$ GeV$^2$, $q^2 = 50$ GeV$^2$, $R'/R = 1.15$) one finds that $\xi \simeq 2$. As can be seen from Fig. 45, in the

ratio of $F_2^{Iron}(x,q^2)$ to $F_2^{Deut.}(x,q^2/2)$, essentially the EMC effect has disappeared. Thus, even though I find the EMC effect interesting, I

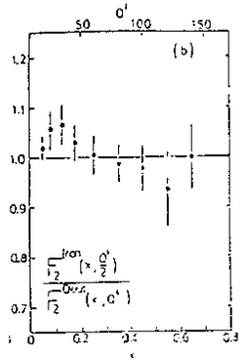


Fig. 45: Compensation of the EMC effect by degradation. From Ref. 68

believe it does not constitute a dangerous problem for QCD. The effective rescaling of the nuclear structure functions, given in Eq. (277), probably is a true reflection of what is really happening.

The standard model is perhaps slightly more challenged by recent measurements bearing on CP violation. The dominant source of CP violation in the kaon system is due to the mass mixing parameter $\epsilon$ in the $K-\bar{K}$ mass matrix. In the standard model, the major contribution to $\epsilon$ /69/ arises from the imaginary part of the box graph diagram of Fig. 46.

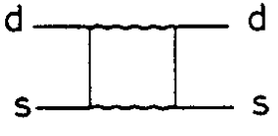


Fig. 46: Dominant graph contributing to $\epsilon$

Since for two generations of quarks and leptons the Cabibbo mixing matrix is real, there is no CP violation unless all three generations of quarks participate in the diagram of Fig. 46. It follows therefore that, in the standard model, the parameter $\epsilon$ must be proportional to the product of the sines of all the real angles in C, times the sine of the CP violating phase $\delta$ :



$$\epsilon \sim \sin\theta_1 \sin\theta_2 \sin\theta_3 \sin\delta \qquad (279)$$

where $\theta_1 = \theta_c$ is the Cabibbo angle.

Recent measurements on the lifetime of B mesons have shown /70/ that these states are surprisingly long lived. This can be understood only if the weak transitions $b \to c$ and $b \to u$, which depend on the values of $\theta_2$ and $\theta_3$, are very suppressed. In turn, small values of $\theta_2$ and $\theta_3$ force $\epsilon$ to be very small. In fact for $\theta_2$ and $\theta_3$ sufficiently small the parameter $\epsilon$, calculated in the standard model, may in fact be smaller than the observed $\epsilon_{exp} \simeq 2.3 \times 10^{-3}$. This circumstance would necessitate introducing physics beyond the GSW model to explain CP violation.

The present situation is a little uncertain. To calculate $\epsilon$ one needs besides the product of angles of Eq. (279) also values for the top and charm quark masses. In addition one needs an estimate for the matrix element of $\bar{d}\gamma_\mu(1-\gamma_5)s\,\bar{d}\gamma_\mu(1-\gamma_5)s$ between K and $\bar{K}$. If $m_t \simeq 40$ GeV, as has been suggested recently by the UA1 collaboration /71/, probably the calculated value of $\epsilon$ can be made to agree with $\epsilon_{exp}$, if $\delta$ is near $90^0$ and the value of the $(\bar{d}s)^2$ matrix element is near that given by the vacuum insertion approximation /72/. However, the situation needs further clarification and could become worse if the B lifetime is shown to be even longer, or $m_t$ is smaller than 40 GeV.

Besides $\epsilon$, there is a further parameter, $\epsilon'$, which measures CP violation in the kaon system. $\epsilon'$ essentially measures how much CP violation is there in the $\Delta S = 1$ part of the weak Lagrangian. The ratio $\epsilon'/\epsilon$ is calculable in the standard model and is considerably less dependent on the Cabibbo mixing angles, since these disappear in the ratio. New data on $\epsilon'/\epsilon$ has become available this year, from two different experimente /72/ /73/. This ratio is still consistent with zero:

Ref. 72: $$\frac{\epsilon'}{\epsilon} = (-4.6 \pm 5.3 \pm 2.4) \times 10^{-3} \qquad (280)$$

Ref. 73: $$\frac{\epsilon'}{\epsilon} = (4.5 \pm 8) \times 10^{-3} \qquad (281)$$

The magnitude of this effect predicted by the standard model has a large uncertainty, in part due to the estimation of another hadronic matrix element. However, the predictions /74/ which are in the range $\epsilon'/\epsilon \sim (5-10) \times 10^{-3}$ are beginning to be seriously challenged by experiment. It will be interesting to see how this situation develops in the future.

The last, and perhaps most interesting, experimental anomalies are connected with data obtained at the CERN collider. A variety of unusual phenomena have been reported by the UA1 and UA2 collaborations in the last year, ranging from anomalous radiative decays /75/ to the productions of jets accompanied by large missing energy /76/, or by a lepton and large missing energy /77/. Because one is dealing with a very small sample of events, it is quite possible that all these indications of "new phenomena" may eventually just prove to be statistical fluctuations.

At any rate, this collider exotica has generated an enormous amount of theoretical activity. I shall not try here to review all the possible suggestions of new physics beyond the standard model, which have been adduced to explain this data /78/. Rather, I will just give one example to give a flavor of the possible physics which may be emerging from the collider.

If low energy supersymmetry is a reality, both quarks and gluons should have superpartners (squarks and gluinos). If these states are not too massive they should be abundantly produced at the collider. For instance, gluino pair production $q\bar{q} \to \tilde{g}\tilde{g}$ would follow from graphs which are analogous to the ones for gluon production. An example of this is illustrated in Fig. 47:

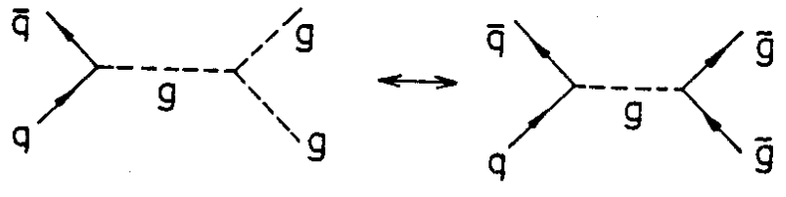


Fig. 47: Correspondence between gluon and gluino production graphs

Both squarks and gluinos can be the source of the jet plus missing energy events. Basically these particles in general must decay to the lightest supersymmetric particle, which in most models is the photino - the supersymmetric partner of the photon. The presumption is that the missing energy "seen" at the collider is due to photino production coming from squark or gluino decay. This scenario has been analyzed in detail by a number of authors /79/. The consensus is that if gluinos or squarks exist in the 30-40 GeV mass range then one would expect about the number of monojet events reported by the UA1 collaboration. Lighter gluinos or squarks would produce too much exotica. Again, more data forthcoming from the collider, should shed light on these speculations.

Let me conclude my lectures on the status of gauge theories of the strong, weak and electromagnetic interactions by emphasizing three main points:

(1) There is impressive evidence supporting certain pieces of the standard model ($\mathcal{L}_{\text{fermion-gauge}}$ and the short distance aspects of QCD).

(2) There are grey or unknown areas in the standard model ($\mathcal{L}_{\text{Higgs}}$ and the long distance aspects of QCD).

(3) Some of the tantalizing hints emerging from experiments now are bound to be reinforced with the advent of the new generation of colliders operating at or near the Fermi scale. Hopefully, new insights into gauge theories will emerge experimentally in the not too distant future, which should help us clarify the deeper open questions of the standard model.



ACKNOWLEDGEMENTS

I am extremely grateful to Tom Ferbel for giving me the opportunity to lecture in such pleasant surroundings and to all the students of the school for their unbounded enthusiasm. I should also thank Sherwin Love for his assistance with some of the material discussed in these notes.

Exercises

1. Verify the transformation law, Eq. (12), for the covariant derivative $D_\mu \phi(x)$

2. Check that under local U(1) transformations

$$\mathcal{L}_{mass} = -\tfrac{1}{2} m_A^2 A^\mu(x) A_\mu(x) \not\to \mathcal{L}_{mass}$$

Is $\mathcal{L}_{\text{mass}}$ invariant under global transformations?

3. Check that the adjoint matrices for SU(2) $(g_i)_{jk} = -i\epsilon_{ijk}$ obey the SU(2) algebra $[g_i, g_j] = i\epsilon_{ijk} g_k$

4. Verify Eq. (23) for $\delta(D_\mu q_a(x))$

5. Prove that the field strengths $F_i^{\mu\nu}$ of Eq. (25) transform under infinitesimal transformations as

$$\delta F_j^{\mu\nu}(x) = \delta\omega_i(x) f_{ijk} F_k^{\mu\nu}(x)$$

6. Prove Eq. (32)

7. Show that for the U(1) model the shifted Lagrangian written in terms of the $\rho$ and $B_\mu$ fields reads

$$\mathcal{L} = -\tfrac{1}{4} F^{\mu\nu} F_{\mu\nu} - \tfrac{1}{2} m_A^2 B^\mu B_\mu - \tfrac{1}{2} \partial^\mu \rho \, \partial_\mu \rho - \tfrac{1}{2} m_\rho^2 \rho^2$$

$$- \lambda v \rho^3 + \tfrac{1}{4}\rho^4) - \tfrac{1}{2} g^2 B^\mu B_\mu (\rho^2 + 2\rho v)$$

where $m_A^2 = (gv)^2$ and $m_\rho^2 = 2\lambda v^2$

8. An exotic triplet of leptons $\ell_L \sim 3$, $\ell_R \sim 1$ are discovered. What are the appropriate covariant derivatives for these states, under SU(2) x U(1), if their charges are +1, 0 and -1

9. Verify Eq. (40)

10. Verify Eq. (47)

11. Show that Eq. (53) arises in second order perturbation theory. Pay

particular attention to factors of 2 and 1/2 and i

12. Derive Eq. (64)

13. Convince yourself that a factor of $\frac{1}{2} M^2$ is necessary for the mass term of a real field, but a factor of $M^2$ is correct for the mass term of a complex field

14. Check that for $\vec{\xi}/v$ infinitesimal, Eq. (69) reduces to the infinitesimal transformation law for the $W_i^\mu$ fields under SU(2) local transformations

15. Derive Eq. (70)

16. Show that the charge conjugate field

$$\tilde{\Phi} = i\tau_2 \Phi^* = \begin{pmatrix} \phi^+ \\ -\phi^{0*} \end{pmatrix}$$

transforms as an SU(2) doublet

17. Show that the basis change analogous to (84)

$$(\psi_f)_L \to U^f_L (\psi_f)_L \quad ; \quad (\psi_f)_R \to U^f_R (\psi_f)_R$$

has no effect on leptonic charged currents, if neutrinos are massless. Show further that such a change cannot affect weak neutral currents

18. Consider the Cabibbo matrix C for the case of two families of quarks and leptons, for the special case in which the up and down quark matrices have the form

$$M^u = \begin{pmatrix} 0 & \alpha \\ \alpha^* & \beta \end{pmatrix} \quad ; \quad M^d = \begin{pmatrix} 0 & \gamma \\ \gamma^* & \delta \end{pmatrix}$$

Can you say something special about the Cabibbo angle's relation to the quark masses in general. What about if $\alpha, \beta, \gamma, \delta$ are real

19. Show that even for the case of many families the coupling of the physical Higgs boson to fermion is diagonal. That is, it is given by Eq. (83)

20. Using the QED result for the $\beta$-function, show that in QCD the fermionic contribution to the $\beta$-function, for each fermion flavor, is

$$\beta_f^{QCD} = \frac{1}{6\pi} \alpha_s^2$$

21. Prove Eq. (98)



22. The deep inelastic cross section $\frac{d\sigma}{dx\,dy}$ obeys the, so called, energy momentum sum rule

$$\frac{d\sigma}{dx\,dy} = \sum_H \int_0^1 dz\; z \left( \frac{d\sigma^H}{dx\,dy} \right)$$

Use this result and the fact that no fragmentation functions enter in $d\sigma/dy\,dx$ to show that the fragmentation functions $D^H_{parton}(z^2; q^2)$ obey Eq. (101)

23. Neglecting all masses, but starting from first principles derive Eq. (104)

24. By using the relations

$$\sum_{spin} u_\alpha(p)\, \bar{u}_\beta(p) = \sum_{spin} v_\alpha(p)\, \bar{v}_\beta(p) = -(\not{p})_{\alpha\beta}$$

$$\mathrm{Tr}\, \gamma_\mu \gamma_\alpha \gamma_\nu \gamma_\beta = 4 (\eta_{\mu\alpha}\eta_{\nu\beta} - \eta_{\mu\nu}\eta_{\alpha\beta} + \eta_{\mu\beta}\eta_{\nu\alpha})$$

$$\mathrm{Tr}\, \gamma_\mu \gamma_\alpha \gamma_\nu \gamma_\beta \gamma_5 = 4i\, \epsilon_{\mu\nu\alpha\beta}$$

derive Eqs. (111)

25. Prove the kinematical relations (113). Note $\epsilon^{0123} = 1$ while $\epsilon_{0123} = -1$

26. Show that the Paschos-Wolfenstein ratio (Phys. Rev. D7 (1973) 91)

$$R_{PW} = \frac{\sigma_{NC}(\nu N) - \sigma_{NC}(\bar{\nu} N)}{\sigma_{NC}(\nu N) + \sigma_{NC}(\bar{\nu} N)}$$

in the GSW model is given by

$$R_{PW} = \rho^2 \left( \frac{1}{2} - \sin^2\theta_W \right)$$

27. Prove Eq. (138)

28. Show that the difference

$$\frac{1}{2x} \left[ (F_2^{cc}(x))_{\bar{\nu}_p} - (F_2^{cc}(x))_{\nu_p} \right] = (u(x) + \bar{u}(x)) - (d(x) + \bar{d}(x))$$

Then show that because protons (neutrons) have charge 1(0), it follows that

$$\int_0^1 \frac{dx}{2x} \left[ (F_2^{cc}(x))_{\bar{\nu}p} - (F_2^{cc}(x))_{\nu p} \right] = 1$$

This is the Adler sum rule (Phys. Rev. 143 (1966) 1144)

29. Derive Eq. (144)

30. Derive Eqs. (160)

31. Verify that $d\sigma_{e^+;R}(q)$ can be gotten from $d\sigma_{e^-;L}(q)$ by the substitution of Eq. (168)

32. For $\nu_e e \to \nu_e e$ scattering also charged currents contribute. By making use of the Fierz identity

$$(\bar{\nu}_e \gamma^\lambda (1-\gamma_5) e)(\bar{e} \gamma_\lambda (1-\gamma_5) \nu_e) = (\bar{\nu}_e \gamma^\lambda (1-\gamma_5) \nu_e)(\bar{e} \gamma_\lambda (1-\gamma_5) e)$$

show that

$$\left(\frac{d\sigma}{dy}\right)^{\nu_e e} = \frac{2 G_F^2 m E_\nu \rho^2}{\pi} \left[ \left( Q_{eL}^{Nc} + \frac{1}{\rho} \right)^2 + (Q_{eR}^{Nc})^2 (1-y)^2 \right]$$

33. (Not for Greek students) Cross sections of $10^{-33}$ cm$^2$, $10^{-36}$ cm$^2$ and $10^{-39}$ cm$^2$ are in nanobarns, picobarns and fentobarns, respectively. What do $10^{-42}$ cm$^2$ and $10^{-45}$ cm$^2$ correspond to?

34. Show that because Tr $\gamma_\lambda \gamma \cdot p \gamma_\nu \gamma \cdot \bar{p}$ is symmetric in $\lambda$ and $\nu$, while Tr $\gamma_\lambda \gamma \cdot p \gamma_\nu \gamma \cdot \bar{p} \gamma_5$ is antisymmetric in $\lambda$ and $\nu$, then the interference term in $e^+e^- \to \ell^+\ell^-$ is proportional to $g_{eV}$ and $g_{eA}$ but not $g_{eV}\, g_{eA}$

35. Derive Eq. (187)

36. Derive Eq. (200)

37. Derive the expression for the $Z^0$ luminosity function of Eq. (205)

38. Derive Eq. (208) and show that the branching ratio $B(W \to e\nu) \simeq 8\,\%$ follows directly by counting possible decay channels of the W

39. Derive Eq. (235) for the moments of the running parton distribution function

40. Using Eq. (238) show that the solution of Eq. (235) is Eq. (239)

41. Interpret the splitting functions $P_{gq}$ and $P_{gg}$ diagramatically

42. Show that the valence quark sum rule



$$\int_0^1 d\xi \left[ f_q(\xi;q^2) - f_{\bar{q}}(\xi;q^2) \right] = \nu_q$$

where $\nu_q$ is the number of valence quarks of type q, implies that

$$\int_0^1 d\xi\, P_{qq}(\xi) = 0$$

43. Derive Eq. (251) by using the explicit form of $P_{qq}$ of Eq. (242)

44. Show that for the energy flow $\frac{d\Sigma}{d\bar{R}} = \frac{d\Sigma}{d\bar{R}_{parton}}$

45. Show that the kinematical limits for the Thrust variable T are $1/2 \leq T \leq 1$, where $T = 1/2$ is achieved for totally isotropic events.

REFERENCES


1. For a review, see for example W.J. Marciano and H. Pagels, Phys. Rept. 36C (1978) 137 or the monograph by Quigg; C. Quigg , Gauge Theories of the Strong Weak and Electromagnetic Interactions (Benjamin, Reading Mass, 1983)

2. S.L. Glashow, Nucl. Phys. 22 (1961) 579;
A. Salam, in Elementary Particle Theory, ed. by N. Svartholm (Almquist and Wiksells, Stockholm 1969);
S. Weinberg, Phys. Rev. Lett. 19 (1967) 1264

3. P.W. Higgs, Phys. Rev. Lett. 12 (1964) 132;
F. Englert and R. Brout, Phys. Rev. Lett. 13 (1964) 321;
G.S. Guralnik, C.R. Hagen and T.W. Kibble, Phys. Rev. Lett. 13 (1964) 585

4. S.L. Glashow, J. Iliopoulos and L. Maiani, Phys. Rev. D2 (1970) 1285

5. N. Cabibbo, Phys. Rev. Lett. 10 (1963) 531

6. M. Kobayashi and T. Maskawa, Prog. Theor. Phys. 49 (1973) 652

7. E.A. Uehling, Phys. Rev. 48 (1935) 55

8. H.D. Politzer, Phys. Rev. Lett. 30 (1973) 1346;
D.J. Gross and F. Wilczek, Phys. Rev. Lett. 30 (1973) 1343;
Phys. Rev. D8 (1973) 3633

9. W.E. Caswell, Phys. Rev. Lett. 33 (1974) 244;
D.R.T. Jones, Nucl. Phys. B75 (1974) 531

10. For a general discussion see the monograph of Feynman;
R.P. Feynman, Photon Hadron Interactions (Benjamin, Reading, Mass. 1972)

11. D.H. Perkins, Proceedings of the 1981 CERN-JINR School of Physics, Hanko, Finland, June 1981

12. M. Jonker et al., Phys. Lett. 99B (1931) 265

13. D.C. Cundy, Proceedings of the XVII International Conference on High Energy Physics, London 1974

14. C. Geweniger, Proceedings of the International Europhysics Conference on High Energy Physics, Brighton, July 1983

15. M. Jonker et al., Phys. Lett. 102B (1981) 67

16. J.E. Kim et al., Rev. Mod. Phys. 53 (1980) 211

17. C.H. Llewellyn Smith, Phys. Rept. 3C (1972) 163

18. C. Callan and D.J. Gross, Phys. Rev. Lett. 22 (1969) 156

19. D.J. Gross and C.H. Llewellyn Smith, Mod. Phys. B14 (1969) 337

20. D. Haidt, Proceedings of the XXI International Conference on High Energy Physics, Paris 1982

21. W.A. Bardeen, A.J. Buras, W. Duke and T. Muta, Phys. Rev. D18 (1978) 3998;
G. Altarelli, R.K. Ellis and G. Martinelli, Nucl. Phys. B143 (1978) 521; ibid., B146 (1978) 544 (E)

22. F. Eisele, Proceedings of the XXI International Conference on High Energy Physics, Paris, 1982

23. C. Prescott et al., Phys. Lett. 77B (1978) 347; ibid, 84B (1979) 524

24. A. Argento et al., Phys. Lett. 140B (1984) 142

25. F. Bergsma et al., Phys. Lett. 147B (1984) 481

26. L. A. Ahrens et al., Phys. Rev. Lett. 51 (1983) 1516; 54 (1984) 18

27. B. Naroska, Proceedings of the 1983 International Symposium on Lepton-Photon Interactions, Ithaca, N.Y.

28. H.U. Martyn, Proceedings of the Symposium on High Energy $e^+e^-$ Interactions, Vanderbilt Univ., Nashville, April 1984

29. G.Arnison et al., Phys. Lett. 122B (1983) 103;
M. Banner et al., Phys. Lett. 122B (1983) 496

30. G. Arnison et al., Phys. Lett. 126B (1983) 393;
P. Bagnaia et al., Phys. Lett. 129B (1983) 130

31. F.E. Paige, Brookhaven report BNL-27066 (1979). For a more up to date calculation see G. Altarelli et al., Nucl. Phys. B246 (1984) 12 and CERN preprint CERN-TH-4015

32. G. Arnison et al., Phys. Lett. 129B (1983) 273



33. P. Bagnaia et al., Zeit. für Physik C24 (1984) 1

34. H.D. Wahl, Proceedings of the 15th International Symposium on Multiparticle Dynamics, Lund, June 1984

35. C.H. Llewellyn Smith and J. Wheater, Phys. Lett. 105B (1981) 486

36. A. Sirlin and W. Marciano, Nucl. Phys. B189 (1981) 442

37. For a review see W. Marciano in Proceedings of the Fourth Topical Workshop on Proton Antiproton Collider Physics, Berne, March 1984

38. A. Sirlin, Phys. Rev. D29 (1984) 89

39. G. Altarelli and G. Parisi, Nucl. Phys. B126 (1977) 298;

40. A.H. Mueller, Phys. Rev. D18 (1978) 3705;
R.K. Ellis, H. Georgi, M. Machacek, H.D. Politzer and G.G. Ross, Nucl. Phys. B156 (1979) 285; Yu Dokshitser, D.I. Dyakonov and S.I. Troyan, Phys. Rept. 58C (1970) 270

41. See Dokshitser et al., Ref. 40

42. H. Georgi and H.D. Politzer, Phys. Rev. D9 (1974) 416

43. D.J. Gross and F. Wilczek, Phys. Rev. D9 (1974) 980

44. A.J. Buras, Rev. Mod. Phys. 52 (1980) 199

45. G. Altarelli, Phys. Rept. 81 (1982) 1

46. F. Dydak, Proceedings of the 1983 International Symposium on Lepton-Photon Interactions, Ithaca, N.Y.

47. A.J. Buras, Proceedings of the 1981 International Symposium on Lepton-Photon Interactions, Bonn

48. B. Cox, Proceedings of the XXI International Conference on High Energy Physics, Paris, 1982

49. T. Appelquist and H. Georgi, Phys. Rev. D8 (1973) 4000;
A. Zee, Phys. Rev. D8 (1973) 4038

50. S.L. Wu, DESY 84-020, to appear in Physics Reports

51. C.L. Basham, L.S. Brown, S.D. Ellis and S.T. Love, Phys. Rev. D17 (1978) 2298

52. C.L. Basham, L.S. Brown, S.D. Ellis and S.T. Love, Phys. Rev. D19 (1979) 2018

53. D. Schlatter et al., Phys. Rev. Lett. 59 (1982) 521

54. E. Fahri, Phys. Rev. Lett. 39 (1977) 1587;
A. De Rujula, J. Ellis, E.G. Floratos and M.K. Gaillard, Nucl. Phys. B138 (1978) 387

55. M. Althoff et al., Zeit. für Phys. C22 (1984) 307

56. P. Hoyer et al., Nucl. Phys. B161 (1979) 349

57. For a review, see for example I. Halliday, Proceedings of the International Europhysics Conference on High Energy Physics, Brighton, July 1983

58. For a review, see for example R.D. Peccei, Proceedings of the Fourth Kyoto Summer Institute on Grand Unified Theories and Related Topics, Kyoto, Japan 1981

59. R.D. Peccei and H.R. Quinn, Phys. Rev. Lett. 38 (1977) 1440; Phys. Rev. D16 (1977) 1795

60. K. Wilson as quoted in L. Susskind, Phys. Rev. D20 (1979) 2619

61. M. Aizenmann, Phys. Rev. Lett. 47 (1981) 1; J. Fröhlich, Nucl. Phys. B200 [FS4] (1984) 281

62. M. Beg, C. Panagiotakopoulos and A. Sirlin, Phys. Rev. Lett. 52 (1984) 883; D.J. Callaway, Nucl. Phys. B233 (1984) 189

63. L. Susskind, Phys. Rev. D20 (1979); S. Weinberg, Phys. Rev. D16 (1976) 974; Phys. Rev. D19 (1979) 1277

64. For a recent review, see for example R.D. Peccei, Proceedings of the International Europhysics Conference on High Energy Physics, Brighton, July 1983

65. J.J. Aubert et al., Phys. Lett. 123B (1983) 275

66. For a review, see C.H. Llewellyn Smith in the Proceedings of the Workshop on Experimentation at HERA, Amsterdam, June 1983

67. R. Jaffe, Phys. Rev. Lett. 50 (1983) 228; F.E. Close, R.G. Roberts and G.G. Ross, Phys. Lett. 129B (1983) 346

68. F.E. Close, R. Jaffe, R.G. Roberts and G.G. Ross, Phys. Lett. 134B (1984) 449

69. C.T. Hill, Phys. Lett. 97B (1980) 275; J.S. Hagelin, Nucl. Phys. B193 (1981) 123

70. N.S. Lockeyer et al., Phys. Rev. Lett. 51 (1983) 1316; E. Fernandez et al., Phys. Rev. Lett. 51 (1983) 1022

71. G. Arnison et al., Phys. Lett. 147B (1984) 493

72. B. Winstein, Proceedings of the XI International Conference on Neutrino Physics and Astrophysics, Nordkirchen, Germany, June 1984

73. R.K. Adair, Proceedings of the XXII International Conference of High Energy Physics, Leipzig 1984



74. For a review, see A.J. Buras, Proceedings of the Workshop on the Future of Medium Energy Physics in Europe, Freiburg, April 1984

75. G. Arnison et al., Phys. Lett. 126B (1983) 398; ibid. 135B (1984) 250; P. Bagnaia et al., Phys. Lett. 129B (1983) 130

76. G. Arnison et al., Phys. Lett. 139B (1984) 115

77. P. Bagnaia et al., Phys. Lett. 139B (1984) 105

78. R.D. Peccei, Proceedings of the VII European Symposium of Antiproton Interactions, Durham, U.K., July 1984

79. J. Ellis and H. Kowalski, Phys. Lett. 142B (1984) 441 and DESY 84-045; V. Barger, K. Hagiwara, J. Woodside and W.Y. Keung, Phys. Rev. Lett. 53 (1984) 641; E. Reya and D.P. Roy, Phys. Rev. Lett. 53 (1984) 881